COMPREHENSIVE MODEL FOR EFFECT OF DUAL STRING INTERACTION ON BUCKLING IN VERTICAL WELLS

A Thesis

Presented to

the Faculty of the Department of Petroleum Engineering

University of Houston

In Partial Fulfillment

of the Requirements for the Degree

Master of Science

By

CHANGNING LI

AUGUST 2016

COMPREHENSIVE MODEL FOR EFFECT OF DUAL STRING INTERACTION ON BUCKLING IN VERTICAL WELLS

Changning Li

Approved:

Chair of Committee
Dr. Mohamed Y. Soliman,
Professor, Petroleum Engineering

Committee Members:

Dr. Robello Samuel, Ajunct
Professor, Petroleum Engineering

Dr. Thomas K. Holley,
Professor, Petroleum Engineering

Dr. Suresh K. Khator,
Associate Dean,
Cullen College of Engineering

Dr. Mohamed Y. Soliman,
Professor and Chair,
Petroleum Engineering Department

ACKNOWLEDGEMENTS

Foremost, I would like to express my sincere gratitude to my advisor Dr. Robello Samuel, for his continuous support and guidance throughout this research. His guidance helped me in all the time of research and I could not have imagined having a better advisor and mentor for my research study.

Besides my advisor, I would like to thank the rest of my thesis committee: Dr. Soliman and Dr. Holley for their encouragement, advices and questions on this research. My sincere thanks also go to Ms.Sturm and Ms.Johnson, who gave me continuous guidance and help throughout my program at University of Houston. I would like to thank all my friends who bring happiness and stories to my life.

Last but not the least, I would like to thank my parents for giving birth to me and always supporting me throughout my life.

COMPREHENSIVE MODEL FOR EFFECT OF DUAL STRING INTERACTION ON BUCKLING IN VERTICAL WELLS

An Abstract

of a

Thesis

Presented to

the Faculty of the Department of Petroleum Engineering

University of Houston

In Partial Fulfillment

of the Requirements for the Degree

Master of Science

By

CHANGNING LI

AUGUST 2016

ABSTRACT

Drill string buckling has always been an important subject in a well completion design. Oil wells typically have multiple concentric casing strings. In common practice the outer string is assumed to be rigid, while in reality the outer string can displace when induced by contact force of inner buckled pipe. Interaction between dual strings has significant influence on buckling behavior. Better understanding of dual string buckling behavior helps to give reliable reference for completion design.

An analytical mathematical model has been brought up to describe the post buckling behavior of dual string. The newly derived model has been verified with previous literature. Effect of contact interaction has been considered in this model and evaluated in analysis. Case study has been conducted to further explore the buckling mechanism of dual string system. The influence of different parameters on final buckling configuration has been investigated.

TABLE OF CONTENTS

LIST OF FIGURES

LIST OF TABLES

NOMENCLATURE

A	Cross section area of tubular, in^2
A_i	Area corresponding to inner radius of tubing, in^2
Ao	Area corresponding to outer radius of tubing, in^2
Ap	Area corresponding to the packer bore, in^2
C	Helix curvature, dimensionless
E	Young's modulus, psi^4
F	Buckling force, lbf
F_a	Axial compressive loads, lbf
$\bar{F}$	Summed buckling force of individual pipes, lbf
I	Moment of inertia, in^4
$\bar{I}$	Summed moment of inertia, in^4 o
i	Bending moment coefficient
L	Length of unstressed pipe
$l_{i-(i+1)}$	Length of segment of interval $[x_i, x_{i+1}]$
L_h	Length of buckled pipe system along the helix axis, in.
M	Bending moment, lbf·ft
M_t	Maximum bending moment in tubing, lbf·ft,
M_c	Maximum bending moment in casing, lbf·ft
m	Length in feet of one dimensionless unit
N_{Pal}	Paslay number, dimensionless
p	Pitch, in.

P_i	Inner pressure of tubing at bottom hole, psi
P_o	Outer pressure of tubing at bottom hole, psi
p_i	Inner pressure of tubing at surface, psi
p_o	Outer pressure of tubing at surface, psi
q	Kelly displacement coefficient, dimensionless
r	Radial clearance with respect to wellbore, in.
r_{cc}	Radial clearance between casing and wellbore, in.
r_{ce}	External radius of casing, in.
r_{ci}	Inner radius of casing, in.
r_{tc}	Radial clearance between tubing and casing, in.
r_{te}	External radius of tubing, in.
r_w	Inner radius of wellbore, in.
U	Total potential energy
U_b	Bending strain energy
U_c	Compressive strain energy
U_f	Potential energy of external force
v	Radial displacement, in.
W_n	Contact force, inch
Wtc	Contact force between casing and tubing, lbf
Wwc	Contact force between wellbore and tubing, lbf
w	Weight per length with buoyancy effect, lbf/in.
w_c	Casing length per unit length, lbf/in.
w_i	Weight of liquid in the tubing per unit length, lbf/in.

w_o	Weight of outside liquid displaced per unit length, lbf/in.
w_s	Weight per length in air, lbf/in.
w_t	Tubing length per unit length, lbf/in.
α	Inclination angle of well with respect to vertical direction
β	Parameter related with helix geometry
θ	Helix angle, as shown in Figure 51
φ_ι	Initial phase of helix
σ_m	Maximum stress at cross section, psi
σ_t	Maximum bending stress in tubing, psi
σ_c	Maximum bending stress in casing, psi

CHAPTER 1
INTRODUCTION

1.1 Overview

Drilling operations is believed to be one of the most complex, dangerous, critical and costly operations in the oil and gas industry. Drilling operations accounts for a large portion of initial investment on reservoir development. Drilling technology has gone through a rapid development in the past twenty years. Drilling of super deep, highly deviated, horizontal and extended reach wells helps us with further access to reservoir that used to out of exploration. However, increased complexity of drilling programs always comes with new challenges and problems that have not been encountered before. Research on drilling design contributes to safe and efficient drilling and completion operations with full use of material, thus optimize the economic profits. The stability analysis of downhole tubulars has always been one of the most important part in drilling design and the hottest topic in oil and gas industry. Knowledge of the buckling configuration of tubulars is important to prevent costly failures and provides references to solve problems in operations.

Buckling of drilling tubulars is almost inevitable during drilling and completion operations. When a tubular (casing or drill string) buckles, it may cause a lot of problems, like breaking the string and conducting time consuming fishing operations and costly repairs etc. As drilling techniques and tools are getting more and more sophisticated and complicated, it is more significant than ever to have a safe dill tubular design to protect highly expensive high-tech logging equipment and directional drilling tools, because losing the BHA (bottom hole assembly) is literally throwing tens of thousands of dollars downhole. Although numerous study has been conducted on buckling analysis of drill tubulars in the past 50 years, rapid developing drilling technology has always been bring up new challenges and the buckling problems have still not been thoroughly understood now.

1.2 Problem Background

During drilling operations, drilling tubulars usually can go through several stages in configuration when it is subject to increasing compressive buckling loads. In vertical wells, stability critical force of drill string is usually so small that it can buckle very easily and goes directly to lateral buckling stage. However, for inclined or even horizontal wells, due to the stabilizing effect of gravity the drill string can hold straight to a certain point when the buckling force on drill string reaches the critical force. The next stage is usually referred to as lateral buckling or sinusoidal buckling, as it assumes a two dimensional sine wave form along the wellbore.

At the contact point drill string rubs against the wall of the hole, and this can cause cavity in certain soft formations. The rubbing effect becomes more and more severe as contact force increases, which may cause wellbore stability problems. When the buckled drill string is rotating, the compressive and tensile stress distribution over string cross section will reverse frequently. These reversing stresses will increase with radial clearance of the wellbore and may even lead to fatigue failure of drill string.

When compressive loads are increased further, the drill string usually undergoes an unstable stage, during which it can either takes the sinusoidal buckling form or helical buckling form. After that as the buckling force reaches another certain critical force, the helical buckling configuration occurs. This causes the drill string rides up the wellbore as a helix. In this helical buckling stage, the drill string is continuously in contact with wellbore, so the wall contact area increases dramatically. The induced axial drag will largely increase and thus a larger axial load is required to maintain a same weight on bit. The added axial load causes higher well contact force, which further increase drag.

As compressive loads continue to increase, the wall contact force will eventually increase to such a critical value that the induced drag can't be balanced by slacking off operations and the drill string can no longer be moved downward. In the sliding mode, this stage is usually referred to as lockup. At this point, a change in drilling string design or drilling program is required for drilling to continue. One option is to rotate the drill string, in which way the axial drag in a sliding mode will be converted to rotational drag thus decrease the axial drag. This is the reason why critical force for helical buckling mode is unchanged, while a higher weight on bit can be applied in rotary mode.

Numerous torque and drag software has been developed nowadays. From operational perspective, the real time torque and drag should be always be calculated to determine how much weight on bit is applied and thus control the penetration rate of drill bit. From safety design perspective, the torque and drag analysis gives reference for determining tubular dimensions and grade. Drill string buckling analysis is one of the most important and fundamental part of torque and drag analysis. The analysis should not only calculate the critical force at the onset of buckling (either sinusoidal or helical), but also calculate the post-buckle normal force and predict buckling space configuration. All these parameters are important features in predicting lock up. As the buckled drill string can develop a significant bending stress, the buckling analysis is also important in well drilling and completion safety design.

In common practice, oil wells typically have multiple concentric casing strings. In the design of oil and gas wells, it is often necessary to consider the stability of casing and tubing. Previously lots of study has been conducted to determine the stability of a single string under complex loadings, the resulting geometry and the stresses of a pipe that buckled inside of rigid outer pipe. In reality the outer pipe is also elastic and when outer pipe is not cemented, the outer pipe can have radial displacement due to the contact force applied by inner buckled pipe. Another scenario is that different compressive axial force is applied on outer pipe and inner pipe simultaneously and both the two pipes buckle individually, then the buckling configurations of two pipes have to fit together due to contact interaction between two pipes. If the dual pipe system is constrained to wellbore, the dual pipe buckling configuration has to conform to the wellbore dimension. Besides, as long as outer pipe and inner pipe, or outer pipe and wellbore are in contact, the contact force should be positive to make the result reasonable. Previous study (Mitchell) showed that interaction between tubing and casing has a large impact on final buckling behavior. However, the effect of this dual string interaction on post buckling behavior, bending stress and length change has not been very well studied yet.

This study aims to present a comprehensive analytical model to describe the post buckling behavior, including bending stress and length change when different axial loads are applied on dual pipes. The contact force between dual string and with wellbore can be explicitly calculated. It also aims to provide a better understanding of the effect of drill tubular dimensions on final buckling configuration to provide as a reference in drill tubular design and prevent undesired conditions. The proposed model should then be compared with other existing dual string buckling models in literature and potential application in practice should be numerated. Several examples from previous research are collected and recalculated with newly derived model to illustrate how this model is applied in real case.

1.3 Objective

- Propose an analytical comprehensive model to predict the post buckling behavior, bending stress and length change of dual string system.
- Apply previous existing models and this model to real cases to illustrate the advantages of new model.
- Study the effect of drill string parameters like dimensions etc. on the dual string buckling configuration. Analyze the possible mechanism of how dual string interaction impact final dual string buckling configuration.

CHAPTER 2
REVIEW OF PREVIOUS WORK

This section will highlight on a number of papers that are most closely related to the subject of dual tubulars buckling inside of wellbore. Although not all available literature are mentioned here, the majority of those that made important contributions, in the author's view, to this subject are referred in this section.

Buckling behavior of tubulars constrained to wellbore is the major subject of many articles in oil and gas industry. Furthermore, drilling of highly deviated, horizontal and extended wells bring up new demand to understand the buckling behavior in these new scenarios. This section will categorize previous research by well scenarios and review their work in time sequence.

2.1 Vertical Well Scenario

Lubinski (1950) conducted the first pioneering work in developing mathematical approach for sinusoidal buckling behavior of drill pipes in vertical wells. He used power series to solve the governing differential equations and achieved very accurate approximation result for practical purpose. Lubinski proposed that the critical load for the first mode of sinusoidal buckling should be calculated as

$$F = 1.94(EI)^{1/3}w^{2/3}. \tag{1}$$

Besides, the space shape of first to second mode of sinusoidal buckling is investigated. When the string goes very long, the power series solution may give inaccurate results after a certain length. The extension of this result to higher buckling orders would be of considerable interest. This is a static study on model in one plane, so another approach should be used to investigate high orders of buckling of drill strings. Lastly, the buckling induced drill string bending moment, wall contact force, inclination of the bit and force on the bit are all calculated and presented in that research. Engineering recommendation methods for minimizing its effects are given. These methods are applying proper weight on bit or use of special drilling methods.

Wang (1986) analytically studied the buckling on a long hanging column with a bottom compressive force. The buckling configuration is illustrated in Figure 1. If the bottom is free to move laterally, he proposed that the exact expression to produce critical load of buckling for an infinite pipe inside wellbore should be in the form of

$$F = 1.018793(EI)^{1/3}w^{2/3}. \tag{2}$$

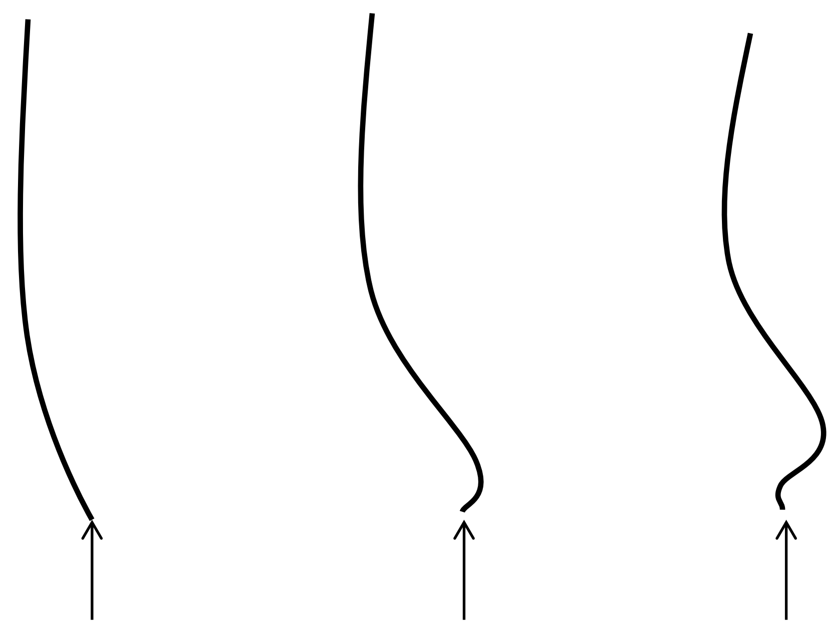

(a) (b) (c)

Figure 1 Post-buckling of Long Hanging Column by a Bottom Load, Wang (1986)

Lubinski (1962) made another great contribution by further developing the first mathematical model to describe helical buckling in vertical wells. This research first included the effect of fluid on buckling. Based on this model, analytical solution to drill pipe length change, strain energy and bending moment are all thoroughly discussed. The force and pitch relationship of helical buckling in this model is derived as

$$F = \frac{8\pi^2 EI}{p^2}. \tag{3}$$

Results of this study can be applied to many field applications. For example, this model addressed the problems of required seal length for packer after pressure and temperature are changed. For scenarios where wireline tools are to be run through the tubing, this model provides methods to prevent tubing from buckling, thus allowing free passage of wireline tools. All such calculations fully take into account the fact that lower part of the drill string is subject to elastic helical buckling.

Hammerlindl (1977), using the same basic buckling model, extended its application to more complicated situations, where completions with varying tubing and casing sizes are included. In this research, he also stated the important impact of friction to drill string length change. A large portion of deviation of measured buckling length change from the model predicted length change is attributed to friction.

Mitchell (1982) proposed differential equilibrium equations for helically buckled weightless tubing based on slender beam theory. Besides, his research showed that the packer has a strong influence on the buckling of well tubing. Lubinski's helical buckling model doesn't agree with his model because the previous one didn't include the influence of packer on buckling configuration. Mitchell's model described the shape between the packer and fully developed helix, which helped to solve for problems of interaction of tubing, casing and packer in the near packer region. Also this model helps to determine stress and deformation in near packer region so tubing and packer response can be assessed properly. The tubing motion at packer caused by helical buckling using conventional helix method and using helix with packer method is studied and shown in Figure 2. It concluded that the length change caused by buckling near packer is about one third of the length change due to conventional buckling. This model allows direct evaluation of the effects of friction and packer design on the buckling behavior of well tubing.

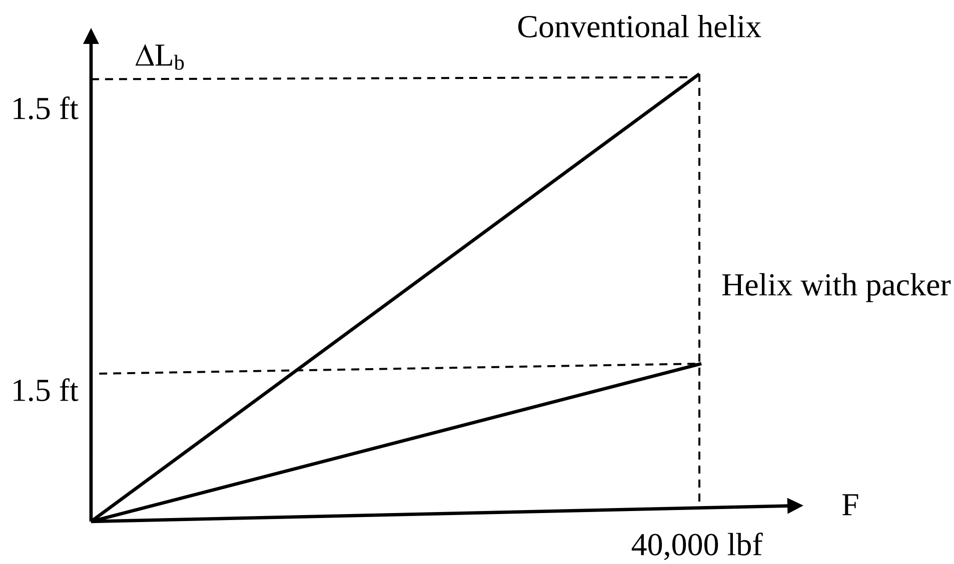

Figure 2 Tubing Motion at the Packer Caused by Helical Buckling, Mitchell (1982)

Cheatham and Patillo (1984), using virtual work principle, derived a different force pitch relationship model from Lubinski's model for helical buckling string inside wellbore. The model contains a numerical coefficient that highly depends on the history of loading and the presence of radial constraint. Based on simple laboratory experiments and stability analysis, they concluded that the myriad load histories to which a tubular string may be subjected can influence the response of a tubular string to applied loads. It is important, especially in tubular designing, to outline the anticipated loading history of a tubular string and design the string for the worst combination of force and pitch.

O'Brien (1984) used cases to illustrate how buckling directly or indirectly contributed to casing failures. Also discussed were important cementing considerations that helped to achieve casing stability and alleviate buckling problem. Also discussed were some suggestions on repair procedures when casing went buckling and failed.

Mitchell (1986) derived differential equations based on slender beam theory and for the first time took effect of frictional forces on helical buckling behavior into account. In this study he didn't give general solutions to helical buckling with friction but thoroughly discussed two simplified cases of interest: downward motion of tubing-e.g, during the landing of the tubing- and upward motion of tubing-e.g, during a slacking off operation. This study also confirmed that the loading history determines the final state of system with friction. Expressions for buckling forces along drill string were derived. It was shown in case study that the buckling force decreased more rapidly near the packer. This corresponded to the fact that friction is more important where the buckling force is large-e.g. near the packer. This phenomenon can be clearly shown in the Figure 3. Another interesting finding of friction analysis was that the buckling force was coupled to the actual tubing force through the friction. Friction was proved to have a significant impact on string length change due to buckling. Mitchell also gave engineering recommendations for these two conditions to safely evaluate the effect of friction on helical buckling in design.

Cheatham and Chen (1988) conducted lab experiments on how loading history will impact the helical buckling behavior. The result confirmed the previous study by Cheatham and Patillo (1984) that the force-pitch relationship for loading and unloading situations was significantly different. As is shown in Figure 4 from Cheatham and Chen's paper, the helically buckled rod followed different force-pitch relationship in the loading process and unloading process. During the unloading process, the coefficient of critical force is a half of the critical force in loading.

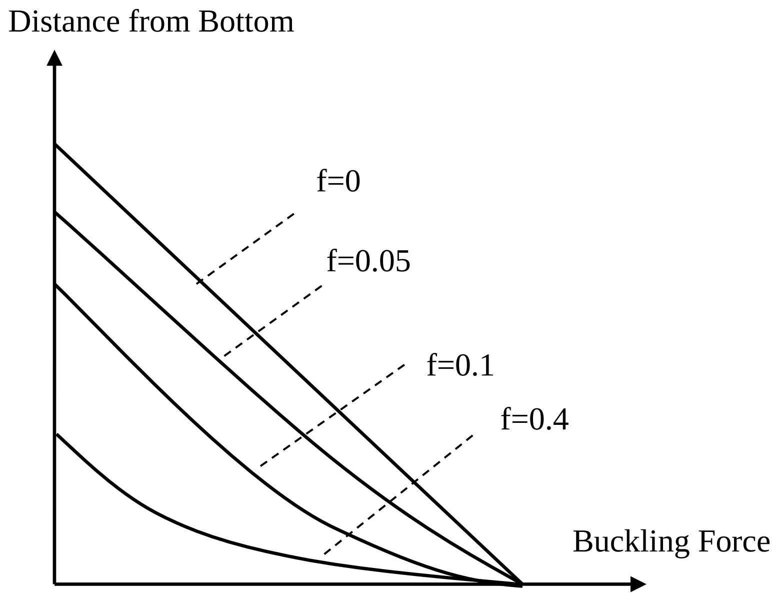

Figure 3 Buckling Force Distribution for Loading Case, Mitchell (1986)

Kwon (1988) conducted a semi-analytical analysis using virtual work on helical buckling with weight in vertical wells. The expression for helical shapes of buckled pipes was developer with varying pitch. In that study, equations for pipe length change, bending moment and lateral loads were developed.

Mitchell (1988) determined an approximate analytic solution for helical buckling of tubing with weight. This solution has very good accuracy expect near the neutral point. This study solved differential equations for helically buckled tubing with weight and directly determined the applicable range of Lubinski's helical buckling model. The generally accepted Lubinski's solution is proved to be a good approximation to the new generalized model under certain conditions. Mitchell also investigated on the initial conditions at the packer and tested the effects of boundary conditions on the solution.

Another contribution of this study is that Lubinski's solution was put in a technical context that provided a basis for further development as inclined wells and friction.

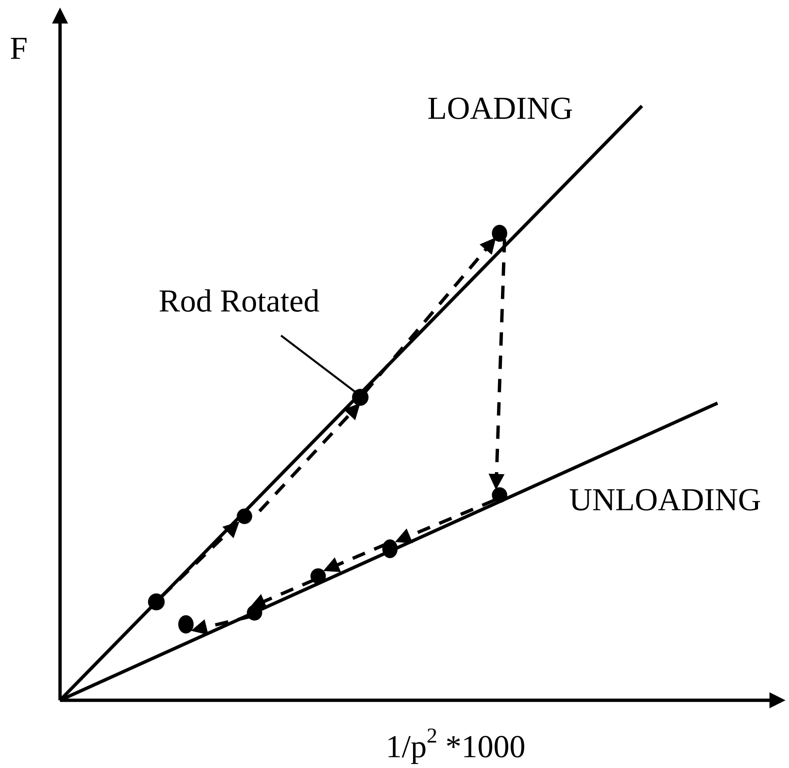

Figure 4 Lab Experiment on Effect of Loading History, Cheatham and Chen (1988).

Mitchell (1996) conducted comprehensive analysis on influence of friction on post buckling behavior by developing a numerical solution for helical buckling with friction. The stability of helical buckling is also researched and shown in Table 1. The Paslay Number is expressed as

$$N_{Pal} = \sqrt{\frac{4EIwsin\alpha/r}{F}}, \tag{4}$$

where N_{Pal} is Paslay Number, E is the Young's modulus, w is the weight per unit length, r is the radial clearance and F is the buckling force.

Table 1 Critical Limits for Buckling, Mitchell (1996)

${N_{Pal}}^{-1} < 1$	No Buckling
$1 < {N_{Pal}}^{-1} < \sqrt{2}$	Lateral Buckling
$\sqrt{2} < {N_{Pal}}^{-1} < 2\sqrt{2}$	Lateral or Helical Buckling
$2\sqrt{2} < {N_{Pal}}^{-1}$	Helical Buckling Only

2.2 Inclined Well Scenario

Paslay and Bogy (1964) analyzed the stability of a circular rod constrained to be in contact with an inclined circular cylinder. Energy method was used to obtain the stability criteria for the circular rod and determined the critical bucking conditions. Base on this research, Dawson and Paslay (1984) for the first time include the contribution of inclination angle to drill pipe stability and brought up the well- known critical force criteria for sinusoidal buckling of drill pipe in inclined wells, which is expressed as

$$F = 2\sqrt{\frac{EIwsin\alpha}{r}}. \quad (5)$$

Their research justified and showed that the drill string can tolerate significant levels of compression in small diameter high angle wells because of the support provided by the low side of well. The benefit of using drill string in compression is that the BHA weight will be reduced and kept low in high angle wells. This, in turn, helps to reduce the torque and drag, which are usually the critical limitations when operated in highly deviated or extended reach wells. Experiment data of stability loads has been attempted to reconstruct according to Figure 5.

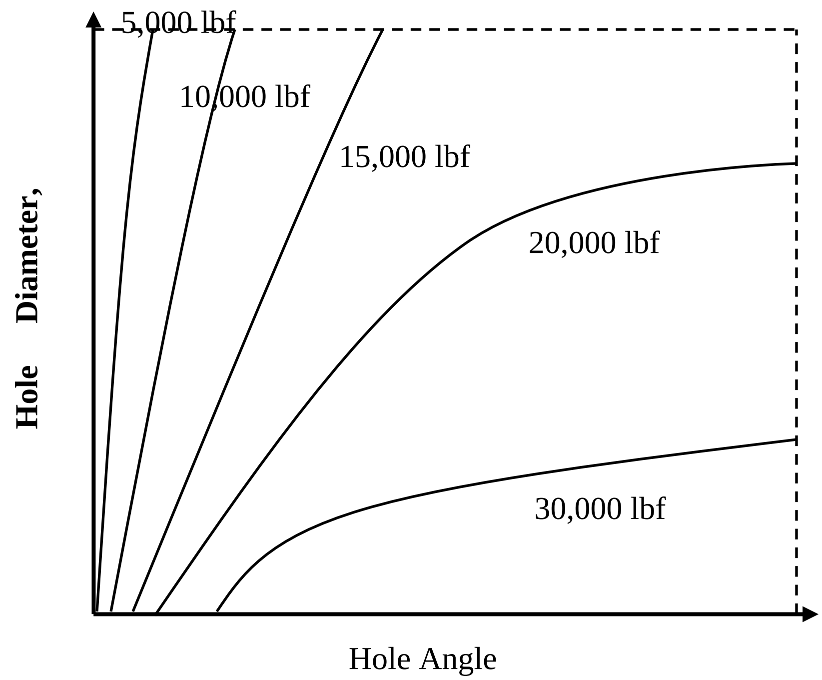

Figure 5 Critical Buckling Loads for 5-in Drillpipe, P.R. Paslay (1984).

Chen et al (1989) described theoretical results for predicting the buckling behavior of pipes in horizontal wells. They concluded that pipe buckling in horizontal wells occurs initially in a sinusoidal mode along the low side of the well. As the axial compression is increased, a helix will be formed. Equations were derived for computing the forces required to initiate these different buckling modes in horizontal wells. Besides, simple experiments were conducted to verify and confirm their theory. Results presented in this paper can be applied to friction modeling of buckled tubulars to predict if drill pipe can be further forced to move along a horizontal section. Equations for critical forces to initiate sinusoidal and helical buckling can be expressed by

$$F = 2\sqrt{\frac{EIw}{r}} \text{ and} \qquad (6)$$

$$F = 2\sqrt{\frac{2EIw}{r}}. \tag{7}$$

Chen and Cheatham (1990) derived expressions for wall contact forces on helically buckled tubulars in vertical and inclined wells. A method of analyzing the dependency of the wall contact force on axial force and wellbore inclination was presented. Also the research was categorized into two situations: loading and unloading respectively. The results of this study can be applied in friction modeling of buckled pipes in inclined or highly deviated wells. The post buckled configuration of pipe in a horizontal hole can be shown in.

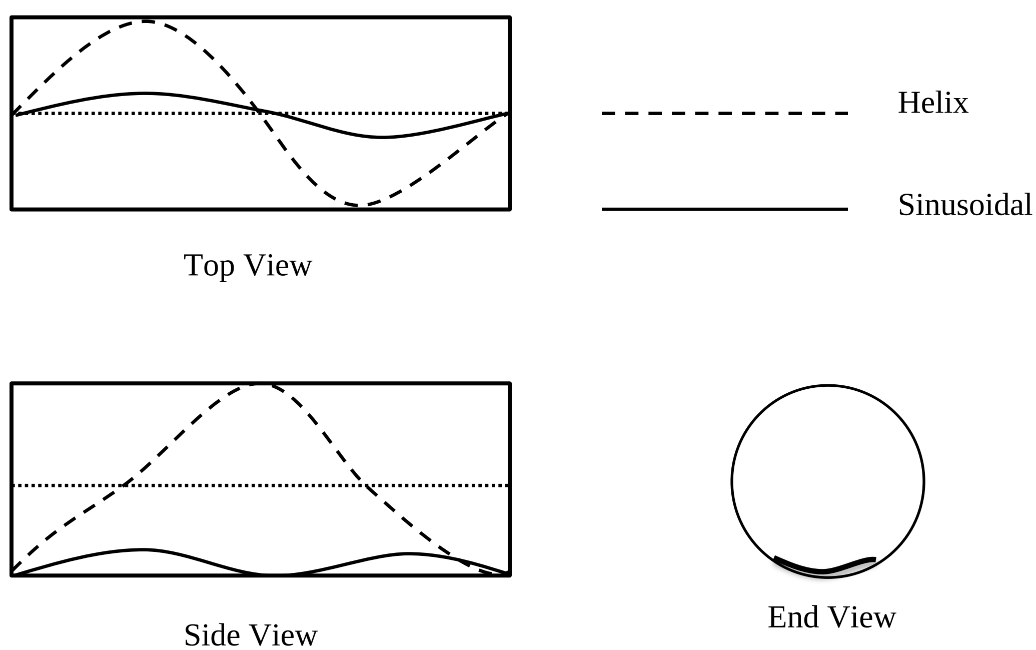

Figure 6 Post Buckled Configuration of Pipe in Horizontal Hole (Sinusoidal and Helical Buckling), Chen and Cheatham (1990)

Wu and Juvkam-Wold (1993) conducted study on helical buckling of pipes in horizontal wells. They concluded that the so-called helical buckling load in literature was actually the average axial load in the helical buckling development process. This study showed that a larger bit weight or packer load may be applied to increase the drilling rate or ensure a proper seal before helical buckling of pipes can occur. The frictional drag for helically buckled pipe war analyzed. The analysis showed that the drag would become much larger for helically buckled pipes in horizontal wellbore than unbuckled pipes. The pipe could even become "locked-up" so that the WOB can't be increased any more. The conditions that could result in "locked-up" were predicted in this study. Experiments were conducted to confirm the theoretical model. The expression for true helical buckling force is expressed as

$$F = 2(2\sqrt{2} - 1)\sqrt{\frac{EIw}{r}}. \tag{8}$$

The difference between this model and Cheatham and Chen's (1989) model is thoroughly discussed in this research. The major reason that leads to different critical force prediction is the assumption on loading process is different, as is shown in Figure 7.

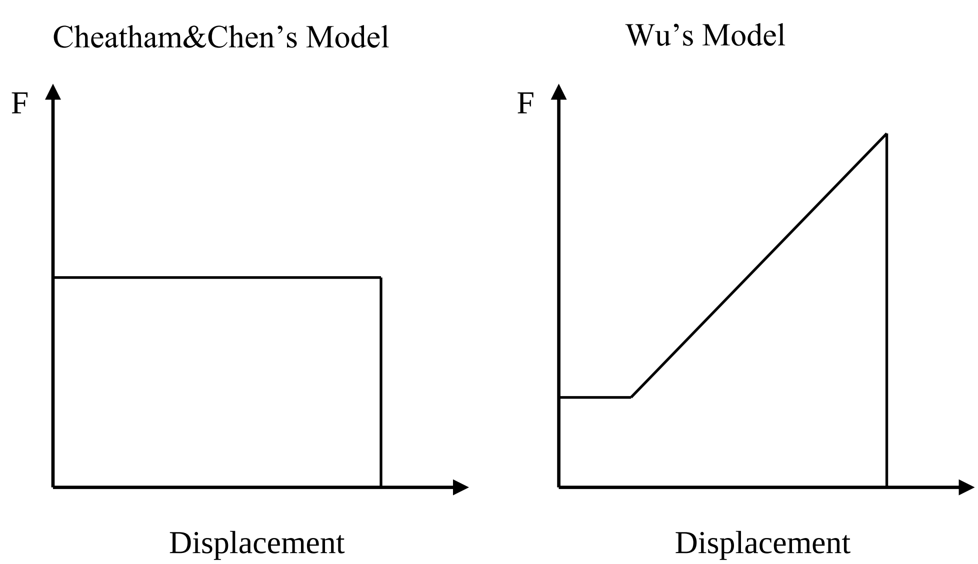

Figure 7 Force Application Process, Wu (1993)

McCann and Suryanarayana (1995) conducted attempt to study the helical buckling process experimentally. Their study described results from experiments on post-buckling behavior of rods laterally constrained in a cylindrical enclosure. This experiment paid particular emphasis on friction and curvature. Their experimental result showed that friction significantly delayed the onset of buckling (both sinusoidal and helical) and contributed to the noticeable hysteresis in post buckling behavior. They also noticed that for inclinations less than 15 degrees, the effects of friction were negligible for initiation of sinusoidal buckling, but when drill string went to helical buckling stage the friction had significant impact on space configuration of buckling.

He and Kyllingstad (1995) studied specifically towards the use of coiled tubing in curved wells. Their study showed that well curvature had a significant effect on the critical buckling force of coiled tubing. A positive inclination build rate or azimuth build rate would increase the critical buckling force. Their theoretically predicted effects had been confirmed in small scale experiments. Their study also showed that the critical buckling force can be substantially exceeded before lock-up or pipe failure. So the lock up and pipe failure should be used as the operation criteria.

Paslay (1994) conducted a study on stress analysis of drill string, in which torque was included in Lubinski's model for buckling of weightless string. His study concluded that the torques had little influence on the Lubinski's buckling model for most practical drill strings. Later Miska and Cunha (1995) presented a different solution, but their conclusion indicated that torque had small influence on buckling process.

Mitchell (1997) developed numerical solutions to nonlinear buckling differential equations in inclined wells. He established the stability criteria for sinusoidal and helical buckling. The equation is derived for critical helical buckling load in inclined wells. Mitchell used Galerkin technique and solved it numerically in his 1997 paper. In 1999, Mitchell tried to use correlation to get an approximation solution to this equation for practical application. In 2002, Mitchell happened to find two analytical solutions for above nonlinear differential equation. So it can be easily applied with spreadsheet or even hand calculation.

Miska and Qiu (1996) brought up axial force transfer model for buckling pipes in inclined well. Besides, analytical model for contact force are derived for sinusoidal and helical buckling configuration in inclined wells. In that research, they presented the critical limits for buckling as is shown in Table 2. In their paper (2000), they further developed software CTS-TUDRP simulator and simulate axial force transfer numerically.

Table 2 Critical Limits for Buckling, Miska and Qiu (1996)

Load	Configuration
$F_p < 2\sqrt{\frac{EIwsin\alpha}{r}}.$	Straight
$2\sqrt{\frac{EIwsin\alpha}{r}} < F_p < 3.75\sqrt{\frac{2EIwsin\alpha}{r}}.$	Sinusoidal
$3.75\sqrt{\frac{EIwsin\alpha}{r}} < F_p < 4\sqrt{\frac{2EIwsin\alpha}{r}}.$	Unstable Sinusoidal
$F_p > 4\sqrt{\frac{2EIwsin\alpha}{r}}.$	Helical

Samuel and Gao (2014) brought up a new concept of *Buckling Limit Factor*, which can be in short called BLF (Samuel). This factor includes the effect of wellbore tortuosity, borehole quality and shape and helps to calibrate the constants used in previous buckling equations. Besides, this factor helps to calibrate and use a standard value based on company policies. The suggested BLF with respective to the models is given in Table 3.

Table 3 BLF Values for Different Models, Samuel and Gao (2014)

Model	BLF
Chen and Cheatham (1990)	1
He and Kyllingstad (1995)	1
Lubinski and Woods (1953)	1.007
Lubinski and Logan (1962)	0.848
Qui, Miska and Volk (1998)	2
Qui, Miska and Volk (1998)	1.326
Wu and Juvkam Wold (1993)	1.295
Wu and Juvkam Wold (1995)	1.498

2.3 Dual String Buckling and Why This Study

There are only two known solutions to dual string buckling problem until now. Christman (1976) developed a technique to analyze the stability behavior of a system of concentric pipes. He stated that loads and property of individual pipes contributed to the overall stability of multiple pipe system. Specifically, the buckling force of concentric pipes system is the arithmetic sum of individual forces, and the overall system stiffness is the sum of individual moments of inertia. He also assumed that the radial clearances between pipes are negligible. This implicit statement is that the relative radial displacement between tubing and casing is ignored. With these assumptions, the analytical solution to single string buckling problem can be easily applied to concentric pipe system. The stability and post buckling elastic behavior of concentric pipes can be described by using the summed forces and sum of moments of inertia. The space configuration of Christman's model is shown as Figure 8 and Figure 9.

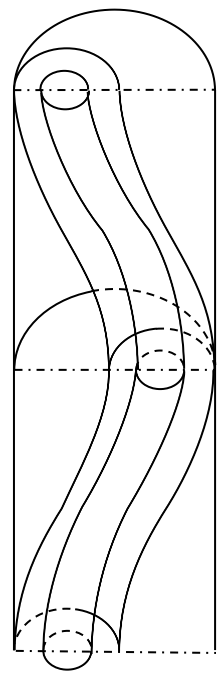

Figure 8 Christman's Concentric Pipes Model, Christman (1976)

However, inner and outer pipes of a set of concentric pipes system can be subject to separate axial loads in real practice, so both pipes could buckle separately until they are in contact. This contact interaction between pipes certainly has a large impact on the final buckling configuration of dual string system. Besides, the simple arithmetic sum of property or loads of individual pipes can't be used to properly evaluate the effect of loads on an overall system. The system capacity could be overestimated by using the dual string system to take the load that is initially applied to individual pipe. Christman's model obviously can't adequately solve these problems. For an extreme situation where the forces in tubing and casing have same values but opposite signs, the Christman's model will predict no buckling because the net force of cross section is zero. However, the new analysis will predict a buckling, which will be discussed in later chapter.

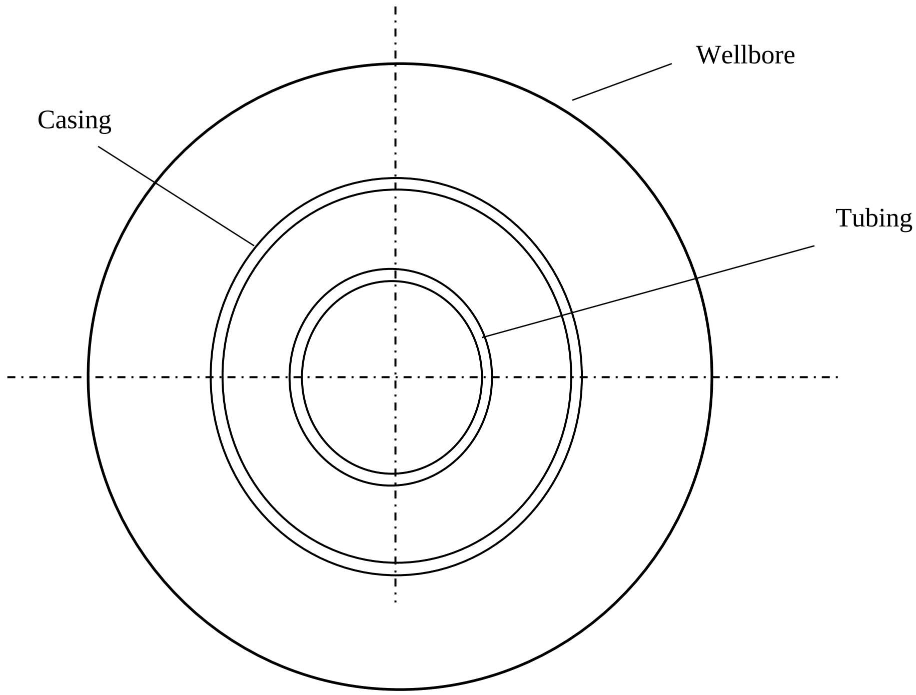

Figure 9 Christman's Concentric Pipes Model Cross Section, Christman (1976)

Mitchell (2012) made modifications on Christman's model and presented a mathematical model for dual string buckling. He divided concentric pipes buckling into two contact categories by explicitly calculating the contact forces between the pipes and with the external wellbore. Both of this two buckling configurations are assumed to buckle helically. The two cases are as follows:

1. Tubing and casing buckles together with tubing in contact with the casing and casing in contact with wellbore.
2. Tubing is assumed to buckle into contact with the casing, but there is no contact between the casing and wellbore.

All results are analytic and easy to be used in practical application. The model developed in case 1 scenario made a great modification on Christman's model by taking the radial displacement between casing and tubing into consideration. Also, buckling force can be separately applied on casing and tubing instead of evenly shared by the sum of cross section.

In this study, Mitchell used contact force criteria to determine to distinguish between case 1 and Case 2. This criterion stated that if dual string system takes a helical buckling form in case 1, the contact force between dual strings and between casing and wellbore should be positive. Otherwise the tubing and casing will fit together and buckle into helical shape without contact between casing and wellbore. The comparison of assumptions for this two models is shown in Table 4.

The problem with above statement is that the assumed configuration doesn’t conform to real situation. Take loading induced buckling in vertical well for example, as buckling force increases the drill string typically goes from a sinusoidal buckling configuration to a helical buckling configuration. During this process, the contact between drill string and well bore will start from a point contact, which is sinusoidal buckling stage. Then as buckling force keeps increasing above certain critical value, drill string will form helical buckling configuration because the further radial displacement is constrained by wellbore. The assumed situation, where dual string system buckles into helical shape without contact with wellbore is impossible in real case. More comments will be made on Mitchell’s model in latter section. Besides, dual string buckling phenomenon doesn’t catch a lot of attention in design or field practice. The influence of dual string buckling has not been well considered in tubular designing yet. Furthermore, Case studies are still needed on how this interaction between casing and tubing impact the final configuration of dual string system to better understand the dual string buckling mechanism.

Table 4 Comparison between Christman's Model and Mitchell's Model

	Assumption Comparison
Christman's Model (1976)	1. Radial clearance between dual strings should be small enough, so radial displacement between dual strings is negligible. 2. Stability load is the arithmetic sum of loads on individual string. 3. The total system stiffness is the arithmetic sum of individual moment of inertia. 4. Dual string system buckles into helical configuration with casing continuously in contact with wellbore.
Mitchell's Model (2012)	1. Radial displacement within dual string system is considered. 2. Stability load is applied on individual string separately. 3. The stability load of long pipe in vertical wells is zero, so the inner string buckles initially and be in continuous contact with casing. 4. The dual string system buckles into helical configuration. The buckling configuration is further divided into two scenarios: (i) outer string is in contact with wellbore; (ii) there is no contact between outer string and wellbore.

CHAPTER 3
ANALYSIS OF THE PROBLEM

3.1 Introduction

The rapid development of drilling technology makes many reservoirs accessible and brings up new challenges as well. The buckling behavior of tubulars plays an important role in drilling operations control and must be taken serious consideration in drilling design. Although a comprehensive numerical simulator is very popular nowadays, an analytical model will help to provide more insight to understand the mechanism behind. Furthermore, analytic results can serve as a reference to verify numerical result or provide a simple result when numerical analysis is not available.

Oil wells typically have multiple concentric casing strings. Most of the previous research has shown methods to determine buckling behavior of single string under complex loadings. An accurate buckling analysis is important for many reasons. Buckling of tubulars can cause reversal bending stress along cross section, which is a major concern in design to avoid fatigue failure. Besides, buckling induced length change will apply a considerable axial load on a fixed packer or cause excessive axial displacement for a free packer, so it is very necessary to develop a reliable buckling model.

This section aims to bring up an analytical mathematical model, based on minimum energy theory, to describe the post buckling behavior of dual string systems. It is quite different from buckling analysis for single string that multiple string could be in contact with each other and fit together to fit a final buckling configuration. So effect of this contact interaction should be well considered in this model and evaluated in further analysis. Although this model is derived based on two pre-assumed space configuration of dual string system, it is a good attempt to give insight into mechanism of dual string buckling. Also, the newly derived model should be verified with previous literature before it is applied to case study. Some of the parameters that is caused by buckling are evaluated and compared with previous research.

3.2 Problem Description

For a set of concentric casing and tubing inside wellbore, Lubinski's model only consider the buckling of inner tubing while assume the outer casing to be rigid. This is commonly true especially when the outer casing is very well supported laterally, like well cementing. However, none of strings are ideally rigid, and there are still some scenarios where casing can have free lateral displacement. These conditions allow the casing to displace with tubing together. It is very necessary to derive a model for dual string buckling.

Lubinski (1950) first studied the buckling problem of a long pipe in a vertical wellbore. His conclusion is that the stability force, as Eq.(1), for a long pipe is usually so small that it is normally ignore in calculation. So we assume the tubing will initially buckle in vertical well. Another important stability criteria is first developed by Paslay and Dawson (1984), as is shown by Eq. (5), which considers the stabilizing effect of wellbore inclination to buckling. We only use this criteria for inclined well or horizontal well situation.

If an inner tubing is subject to an axial force, it will typically buckle into a sinusoidal or helix shape and be in contact with external casing. It is possible that the external casing will buckle due to the contact force from inner tubing. Another situation is that both casing and tubing are subject to compressive forces, they will buckle individually and fit together to form a final space configuration as a system. Besides, the buckling of this dual string system should be constrained in the wellbore. It is noticed that in either of above situation, the contact force between dual strings or between casing and external wellbore should be positive to have physical meaning. In following section, we will use proper symbols to describe this situation.

The following Figure 10 illustrates dual string system cross section configuration. The smaller pipe represents tubing inside and larger pipe represents casing. The external wellbore is assumed to be rigid in this study. The radial clearance of tubing with respect to casing is described as r_{tc}, while radial clearance of casing with respect to wellbore is described as r_{cc}. Expressions for r_{tc} and r_{cc} are given by

$$r_{tc} = r_{ci} - r_{te} \quad \text{and} \tag{9}$$

$$r_{cc} = r_w - r_{ce}, \tag{10}$$

where r_{ci} is inner radius of casing, r_{te} is external radius of tubing, r_w is inner radius of wellbore, r_{ce} is external radius of casing.

Christman (1976) first attempted to address this buckling problem of dual string system by simplifying it into a composite single pipe in context of Lubinski's single string buckling analysis. Mitchell (2012) proposed that when both strings buckle together under compressive axial loads, the buckled configuration must fit together so that contact forces between the two strings or between casing and wellbore are positive and wouldn't occupy the same space. Mitchell (1986) derived the contact force expression between a helically buckled string and wellbore. Before referring to Mitchell's contact force expression, we will first introduce the cylindrical coordinate in which the geometry helix is described, as shown in Figure 11 .

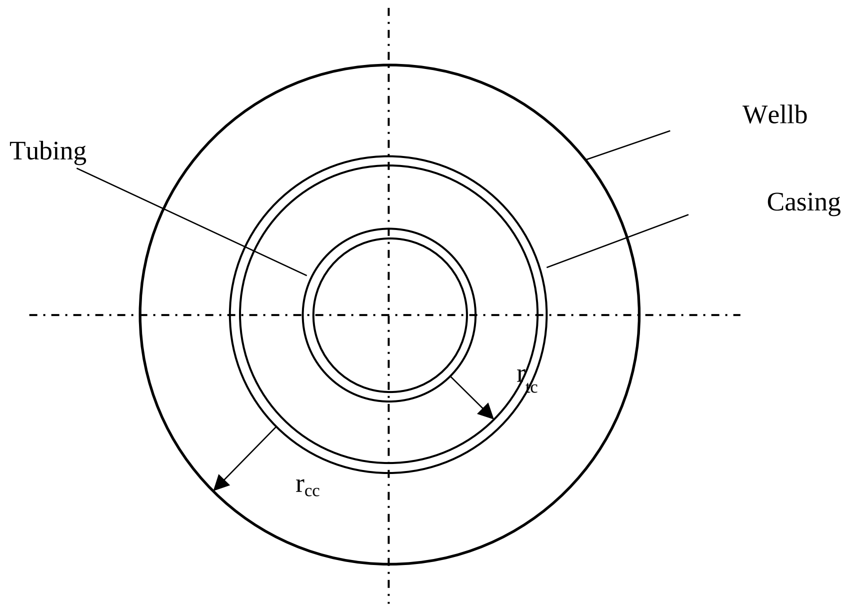

Figure 10 Dual String System Configuration

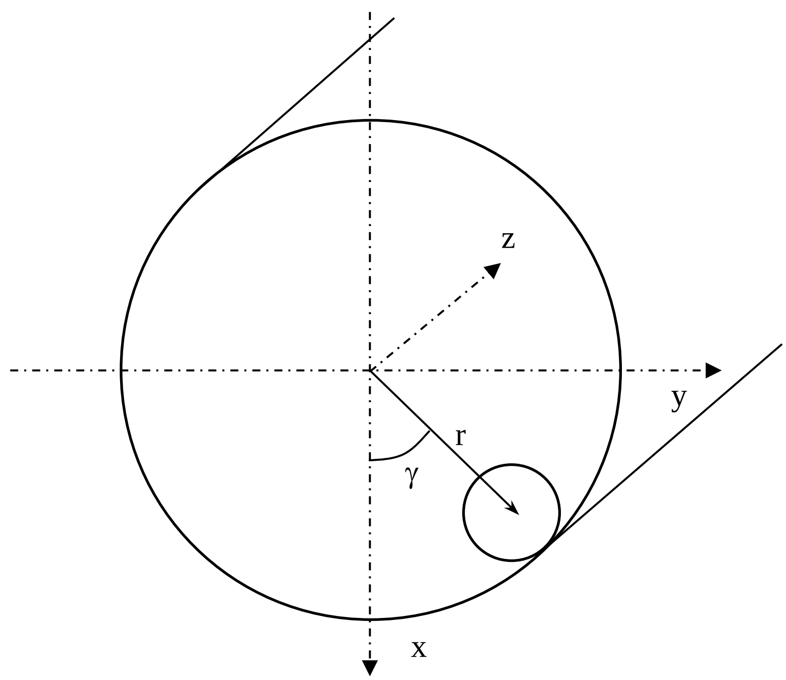

Figure 11 Helical Buckling Geometry and Coordinates

The geometry of the helix is described by the following equations as

$$x = r \cdot cos\gamma \quad \text{and} \tag{11}$$

$$y = r \cdot sin\gamma, \tag{12}$$

where γ is the angular coordinate, r is the string radial clearance.

The angular coordinate g is important, because it can be related with helical pitch using

$$y' = 2\pi/p, \tag{13}$$

where the ‘ denotes d/dz, p is the pitch of helical buckling.

In this cylindrical coordinate, Mitchell (1986) gave the expression for contact force between helically buckled string and wellbore as

$$W_n = r(F - EI\gamma'^2)\gamma'^2, \tag{14}$$

where W_n is the contact force, F is buckling force, r is the radial clearance between string and wellbore, E is young’s modulus, I is moment of inertia of cross section.

We will the above contact force this as criteria in this study to divide dual string buckling into two different categories in vertical scenario. This will be commented in latter section. Summary for the above two model is shown in Table 5.

As previously mentioned in chapter two, Lubinski (1962) conducted force equilibrium analysis on a tubular portion and very well studied the effect of inner and outer fluid pressure on buckling force distribution along tubing. The final expression for the effect of fluid pressure on a tubing without ends is expressed by

$$\mathrm{F} = \mathrm{F_a} + \mathrm{P_i A_i} - \mathrm{P_o A_o}, \tag{15}$$

where F is buckling force, F_a is axial actual compressive loads, P_i is inner fluid pressure of tubular, P_o is outer fluid pressure of tubular, A_i is area corresponding to inner radius of tubular, A_o is area corresponding to outer radius of tubular.

Table 5 Model Summary for Dual String Buckling System

<table>
<tr><td></td><td>Assumption Comparison</td></tr>
<tr><td rowspan="4">Christman's Model (1976)</td><td>1. Radial clearance between dual strings should be small enough, so radial displacement between dual strings is negligible.
2. Stability load is the arithmetic sum of loads on individual string.
3. The total system stiffness is the arithmetic sum of individual moment of inertia.
4. Dual string system buckles into helical configuration with casing continuously in contact with wellbore.</td></tr>
<tr><td>Potential Problem</td></tr>
<tr><td>1. Radial clearance between dual strings usually can be very large in common practice, in which scenario this model largely underestimate deformation of inner string due to buckling.
2. The third assumption only holds true for small radial clearance.
3. Only one buckling configuration is considered which is not sufficient for all scenarios.</td></tr>
<tr><td></td></tr>
<tr><td rowspan="4">Mitchell's Model (2012)</td><td>Assumption Comparison</td></tr>
<tr><td>1. Radial displacement within dual string system is considered.
2. Stability load is applied on individual string separately.
3. The stability load of long pipe in vertical wells is zero, so the inner string buckles initially and be in continuous contact with casing.
4. The dual string system buckles into helical configuration. The buckling configuration is further divided into two scenarios: (i) outer string is in contact with wellbore; (ii) there is no contact between outer string and wellbore.</td></tr>
<tr><td>Potential Problem</td></tr>
<tr><td>The major problem is that the second scenario in assumption 4 is not possible to exist in reality. It can't consider the influence of radial clearance with respect to wellbore, which will result in discontinuity in solution.</td></tr>
</table>

3.3 Dual String Buckling Model Derivation

In this section we consider the situation of small strain, so material of dual string system keeps elastic constitutive relation. Then the beam theory is applied on dual string system to find bending strain energy expression by curvature. The potential energy expression for buckled dual string system is the sum of potential energy of individual pipe. The equilibrium is achieved by minimizing the total potential energy of the system.

3.3.1 Derivation Assumptions

Major assumptions in buckling analysis are as follows,

i. Dual string system assumes either a sinusoidal or helical buckling configuration.
ii. Boundary condition is ignored.
iii. Slender elastic beam theory is applied to relate bending strain energy to curvature.
iv. Wellbore is assumed to be rigid and constant cross-sectional area. Besides, the undulation of wellbore is not considered.
v. Only static fluid effect is considered in this study.
vi. Dynamic effect and friction between casing and pipe and with wellbore are ignored for simplification.
vii. Dual strings are assumed to have constant sectional area, so the effect of connectors is not considered.

Clearly the contact interaction between tubing and casing directly impact the final configuration of dual string system. Let's make an analogy to single string buckling process and consider a loading process where the axial compressive force on tubing and casing increases from zero. As is mentioned in Lubinski's (1950) study, the critical buckling force for single string in vertical well is so small that the sinusoidal buckling of tubing and casing will initiate at the very beginning. As the axial compressive force increases, the initially individually buckled tubing and casing may be in contact. During this time the configurations of tubing and casing have to fit together. This contact interaction makes tubing and casing behave like a dual string system. During a long period of time, this dual string system will take the form of sinusoidal buckling configuration. As the axial compressive force increases further, this dual string system goes through an unstable stage where the configuration can be either sinusoidal buckling or helical buckling. The dual string system can made the transition from sinusoidal buckling to helical buckling above certain critical compressive force. After that the dual strings ride up the wellbore and buckle helically together.

The above analysis is an analogy to buckling process of single string. It should be noticed that the real buckling process of dual string should be much more complicated than this. The above analysis simplifies the real situation and serves as theoretical basis for model derivation. According to the buckling process, the tubing string and casing string may interact in two distinct ways: by point contact, which is sinusoidal buckling and by continuous contact, which is helical buckling. So in this study we will build up the analytical model for these two scenarios respectively.

3.3.2 Helical Buckling of Dual String System

When the compressive buckling force is large enough for dual string system, the dual string system is assumed to have the helical buckling configuration. The helically buckling dual string system is assumed to have continuous contact with wellbore, while inner tubing is continuously in contact with outer casing. Another assumption is made that within the dual string system casing and tubing have the same pitch along wellbore direction. The condition where buckling force is constant along wellbore is considered.

The cross section of fully buckled dual string system configuration is shown as Figure 12, Space configuration of helical buckling of dual string system is shown as Figure 13.

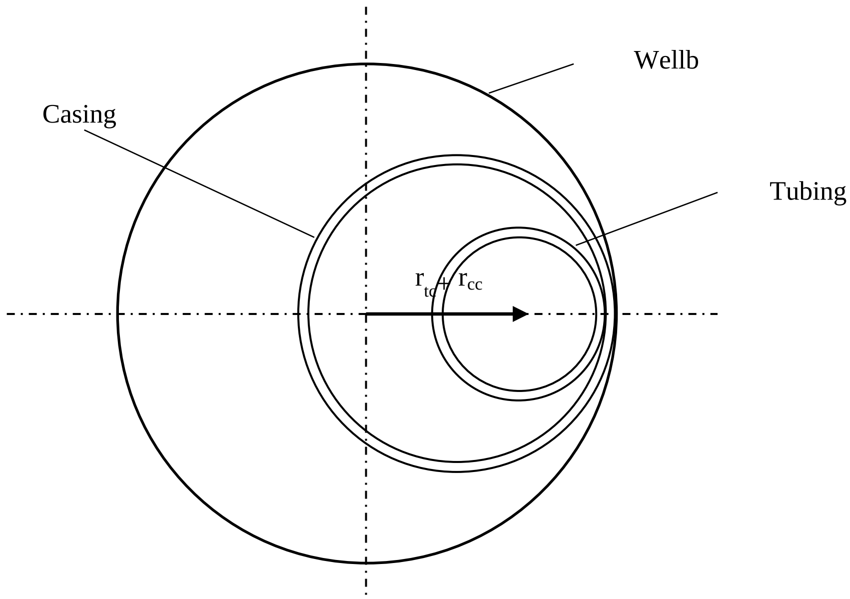

Figure 12 Casing in Contact with Wellbore

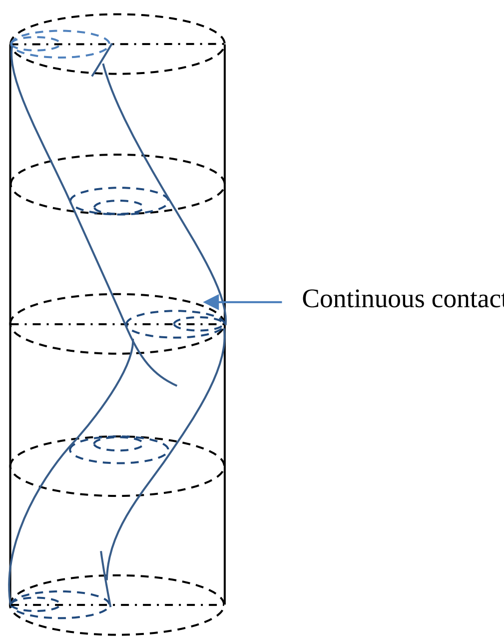

Figure 13 Helical Buckling Configuration of Dual String System

In the following study, we will add a subscript 1 and 2 to previously defined parameters to denote tubing and casing in a dual string system respectively for simplification. It is noticed that in this helical buckling situation the radial displacement of tubing becomes the sum of tubing radial clearance and casing radial clearance. So the radial displacement of tubing and casing are expressed by

$$r_1 = r_{tc} + r_{cc} \quad \text{and} \tag{16}$$

$$r_2 = r_{cc}. \tag{17}$$

We apply the minimum energy theory to the total potential energy of dual string system (derivation details in APPENDIX A) and find the force-pitch relationship. This model shows that pitch is a variable along drill string that corresponds to a buckling force at certain depth. The expression of this model is given by

$$p = \pi\sqrt{\frac{8E(I_1{r_1}^2+I_2{r_2}^2)}{F_1{r_1}^2+F_2{r_2}^2}}, \tag{18}$$

where p is the pitch of helix at certain depth with unit in inch, parameters E, I and F are the same as previously defined, subscripts 1 or 2 are added to these parameters to assign them to tubing or casing, r_1 and r_2 are defined in above text. It is also noticed that this dual string buckling model can be easily simplified into Lubinski's (1962) single string buckling model as Eq. (3).

Mitchell (2012) studied the helical buckling configuration by applying the virtual work principle. The final expression derived is given as

$$\beta^2 = \frac{F_1{r_1}^2+F_2{r_2}^2}{2E(I_1{r_1}^2+I_2{r_2}^2)}, \tag{19}$$

where β is parameter related with helix geometry .Notice that this parameter b is related with helix pitch, p, by

$$p = \frac{2\pi}{\beta}. \tag{20}$$

By substituting Eq. (20) into Eq. (19), we get the exact same expression as Eq.(18). In this way the newly derived model verified Mitchell’s (2012) previous research.

In the above model derivation process, we assume buckling force, F, to be positive when it is compressive force and negative if it is tensile force. So Eq. (18) is valid only for

$$F_1 {r_1}^2 + F_2 {r_2}^2 > 0. \tag{21}$$

It is still noticed that even F_1 and F_2 has equal value with opposite signs, which means the sum of buckling forces at cross section of dual string system could be zero, there is still a possibility of buckling of this dual string system according to Eq. (18).

As previously mentioned, this helically buckling configuration of dual string system only form as buckling force increase to a very large value. Under this condition the contact forces between dual strings and casing string with wellbore should both be positive. Mitchell (1986) has solved for the contact force between helically buckled string and wellbore using Eq. (14). Combine Mitchell’s result Eq.(13) with Eq. (14) and substitute parameters in this situation, the contact forces equilibrium equations are given by

$$r_1 \left[F_1 (\tfrac{2\pi}{p})^2 - EI_1 (\tfrac{2\pi}{p})^4 \right] = W_{tc} \quad \text{and} \tag{22}$$

$$r_2 \left[EI_2 (\tfrac{2\pi}{p})^4 + F_2 (\tfrac{2\pi}{p})^2 \right] = -W_{wc} + W_{tc}, \tag{23}$$

where Wwc is contact force between wellbore and casing, Wtc is contact force between casing and tubing, the parameters r_1, r_2, E, I_1, I_2, p are same as previous definition. Rearrange above equations and contact force Wwc is given by

$$W_{wc} = r_1\left[F_1(\frac{2\pi}{p})^2 - EI_1(\frac{2\pi}{p})^4\right] + r_2\left[EI_2(\frac{2\pi}{p})^4 + F_2(\frac{2\pi}{p})^2\right]. \quad (24)$$

So the prerequisite criteria for helically buckling of dual string to occur is given by

$$W_{tc} > 0 \quad \text{and} \quad W_{wc} > 0. \quad (25)$$

If there is a value for pitch that can satisfy all the prerequisite conditions for helical buckling, including Eq.(21) and Eq.(25), the bending moment and bending stress can be given by (Crandall 1959)

$$M_1 = EI_1 r_1(\frac{2\pi}{p})^2, \quad (26)$$

$$M_2 = EI_2 r_2(\frac{2\pi}{p})^2, \quad (27)$$

$$\sigma_{m1} = \frac{M_1 r_{te}}{I_1}, \text{ and} \quad (28)$$

$$\sigma_{m2} = \frac{M_2 r_{ce}}{I_2}. \quad (29)$$

where M is the bending moment, σ_m is the maximum stress at cross section, I, r, r_{te}, r_{ce} and p are the same as previously defined, subscript 1,2 represent tubing and casing respectively.

Lubinski (1962) also gave the expression for drill tubular weight per unit length in presence of fluid by

$$w = w_s + w_i - w_o, \quad (30)$$

where w is weight per length with buoyancy effect, w_s is weight per length in air, w_o is weight of outside liquid displaced per unit length, w_i is weight of liquid in the tubing per unit length.

Then Lubinski (1962) further gave the expression for length change due to helically buckling by

$$\Delta L_{b_1} = -\frac{{r_1}^2{F_1}^2}{8EIw} \text{ and} \quad (31)$$

$$\Delta L_{b_2} = -\frac{{r_2}^2{F_2}^2}{8EIw}, \quad (32)$$

where ΔL_b is the length change due to buckling, F_1, F_2, E, I_1 ,I_2 and w are the same as previously defined.

3.3.3 Sinusoidal Buckling of Dual String System

In last section we established the mathematical model for buckling force-pitch relationship and stated the prerequisite criteria for dual string system to form helically buckling configuration. Then the next question would be: what is the space configuration if the prerequisite criteria given by Eq.(25) is not satisfied at certain depth?

As the buckling of dual string system develops with increasing buckling force, the configuration of dual string system goes through a sinusoidal buckling stage, unstable transition stage and finally helically buckling stage. Although the duals string shape at transition stage is kind of arbitrary, the length of drill string at this unstable stage is usually short and using a sinusoidal shape for approximate can be acceptable. So if the prerequisite criterion for helical buckling is not satisfied, we will assume a sinusoidal buckling configuration for this dual string system.

This section introduces how a mathematical model of force-pitch relationship is established for sinusoidal buckling. The assumption that dual strings have the same pitch still applies in this study. Sinusoidal buckling space configuration of dual string system is shown as Figure 14. The contact interaction between tubing and casing or between casing and wellbore is by point contact.

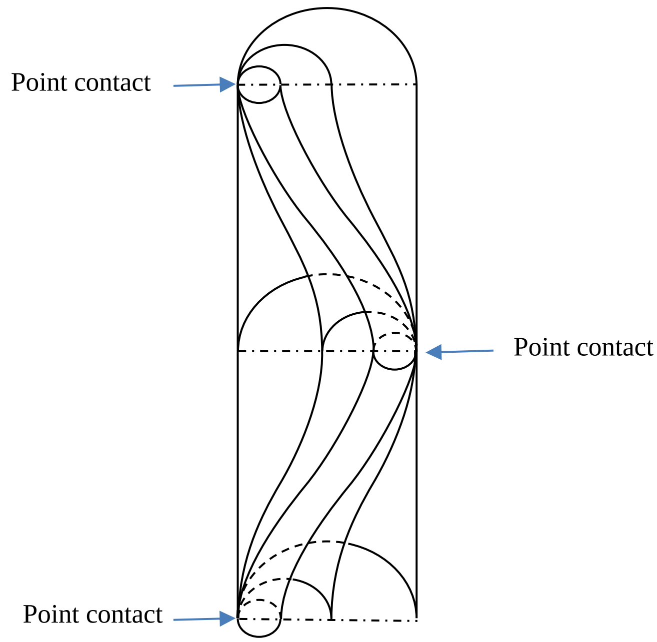

Figure 14 Sinusoidal Buckling Configuration of Dual String System

Similar to previous method, the minimum energy theory is applied to the total potential energy of dual string system (derivation details in APPENDIX B). This model also shows that pitch is a variable, which corresponds to a buckling force at certain depth. The expression of this model is given by

$$p = 2\pi\sqrt{\frac{\pi E(I_1 r_1 + I_2 r_2)}{F_1 {r_1}^2 + F_2 {r_2}^2}}, \tag{33}$$

where p is the pitch of sinusoidal curve at certain depth with unit in inch, parameters r, E, I and F are the same as previously defined, subscripts 1 or 2 are added to these parameters to assign them to tubing or casing. Notice that the prerequisite condition Eq. (21) should be satisfied before apply this model.

If it is determined that a dual string system conforms to a sinusoidal buckling, the bending moment can be given by (derivation details can be found in APPENDIX B)

$$M_1 = -\frac{4\pi^2 r_1 E I_1}{p^2} \sin(\frac{2\pi x}{p}) \text{ and} \tag{34}$$

$$M_2 = -\frac{4\pi^2 r_2 E I_2}{p^2} \sin(\frac{2\pi x}{p}), \tag{35}$$

where M is the bending moment, σ_m is the maximum stress at cross section, I, r and p are the same as previously defined, subscript 1,2 represent tubing and casing respectively. The Eq. (28) and Eq. (29) can still be used to calculate maximum stress at cross section.

The length change due to sinusoidal buckling can be expressed by (derivation details can be found in APPENDIX B)

$$\Delta L_{b1} = \frac{\pi {r_1}^2}{4p}\left[\sin\left(\frac{4\pi l}{p} + 2\varphi_i\right) - \sin(2\varphi_i)\right] + \frac{\pi^2 {r_1}^2 l}{p^2} \text{ and} \tag{36}$$

$$\Delta L_{b2} = \frac{\pi {r_2}^2}{4p}\left[\sin\left(\frac{4\pi l}{p} + 2\varphi_i\right) - \sin(2\varphi_i)\right] + \frac{\pi^2 {r_2}^2 l}{p^2}, \tag{37}$$

where φ_i term is the phase when x_1 is equal to zero.

CHAPTER 4
MODEL VERIFICATION

4.1 Introduction

In later chapter analytical model has been proposed to describe the buckling behavior of dual string system. Newly derived models should be well verified before application. There are many techniques that can be utilized to verify a model. Including, but not limited to, conducting lab experiments, acquiring field data from real practice and comparing modeling result with widely acknowledged literature.

Some previous studies were conducted through analysis of experiment results, e.g. Cheatham and Chen (1988), McCann and Suryanarayana (1995). However, seldom experiment was conducted to research buckling behavior of dual string system. Besides, the phenomenon of dual string buckling didn't get enough attention in design or field practice. There are no public available field observation data to compare with. In this section the proposed analytical model for dual string buckling will be verified by comparing the example case result in widely acknowledged previous literature.

This section will start with calculation procedure to illustrate how to use this new model in application. Previously the solution in helical scenarios can be verified by Mitchell's (2012) solution. Then Lubinski's (1950) exact solution for sinusoidal buckling of string will be used to verify the newly derived model.

4.2 Calculation Procedure

As previously mentioned, the tubular buckling can cause bending moment and thus probably a large stress at the cross section. Besides, length change due to buckling accounts for an important portion of length change in drill string, which is an important consideration during packer design. For helical buckling scenario, the largest bending moment usually occurs at the bottom, thus the maximum bending stress occurs at cross section at bottom assuming a uniform tubular. However, the bending moment is reversely varying in sinusoidal buckling scenario, so it is necessary to calculate the bending moment along drill string to get the maximum bending moment. Besides, if the cross section is not uniform, it is necessary to calculate the bending moment distribution along drill string as design reference.

In the later chapter the buckling model for dual string system is derived in the context of constant buckling force. Although the buckling force usually varies along the drill string in real practice, the buckling force can be assumed to be constant at certain depth and its nearby region. So if the drill string is discretized into numerous segments and the length of segments is small enough, a constant buckling force can be assumed within one segment while buckling force can vary between different segments. After discretization the newly derived model can be used to get pitch, bending moment, bending stress and length change due to buckling within each segment. Finally all segments can be assembled together and all the variables can be determined along drill string. In order to apply this model in practical scenario, the calculation procedure is illustrated as follows:

i. Discretize the dual string system into numerous segments along pipe direction. Number the segments from bottom up, e.g. from segment interval $[x_1, x_2]$ to segment interval $[x_i, x_{(i+1)}]$ as shown in Figure 15.

ii. If the dimensions of dual string system are known, a proper method or model should be used to determine the buckling force at the calculation starting point, which is x_1 in this scenario. This buckling force can be determined from real field data or from literature model, e.g. Lubinski's model (1962) for buckling force at packer.

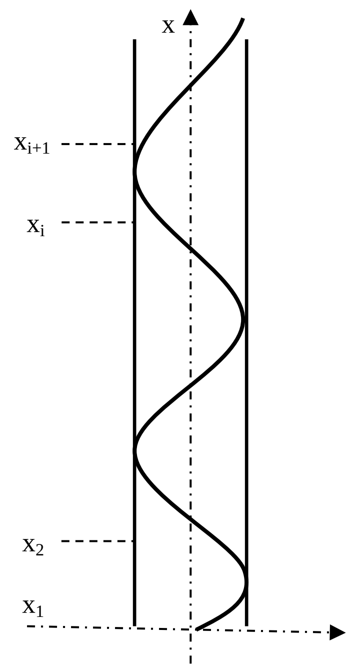

Figure 15 Discretization of String

iii. Assume buckling force within each segment keeps constant. This assumption is valid as long as the segment length is not too large. It is also noticed that the buckling force within each segment can be determined from previous segment. The relationships is expressed as

$$F_{x_{(i+1)}} = F_{x_{(i)}} - w * l_{i-(i+1)}, \tag{38}$$

where w is weight per length with buoyancy effect, which is given by Eq. (30), $F_{x_{(i+1)}}$ is buckling force at depth with coordinate of $x_{(i+1)}$, $l_{i-(i+1)}$ is the length of segment. Besides, the segment length $l_{i-(i+1)}$ can either be constant or variable. Usually we select segment length larger than 0.2 times pitch for high accuracy.

The reason is explained in APPENDIX C and will be further discussed in case studies of later chapters.

iv. For each segment, calculation starts from node i to get the pitch for segment interval [x_i, $x_{(i+1)}$], then tubing shape for this interval is determined using this constant pitch with either a helical shape or sinusoidal shape. For each segment, we will first assume the dual string system take the helical buckling configuration and calculate the pitch for this segment. Then this pitch will be substituted into prerequisite condition for helical buckling, specifically Eq.(21) and Eq.(25). If this prerequisite condition is satisfied, then the helical buckling assumption is verified. Otherwise, the sinusoidal buckling configuration will be used to determine buckling configuration.

v. After calculation on interval [x_i, $x_{(i+1)}$], i+1 becomes a new starting point, and step iii and step iv is continuously repeated until neutral point is reached in vertical well situation.

4.3 Model Verification

As previously mentioned, the dual string buckling solution for helical buckling configuration can be simplified to the exact expression of Lubinski's (1962) helical buckling model of single string. Besides, Mitchell's (2012) model for helical buckling with wellbore contact is the same as this new model in nature. Thus we conclude that the helical buckling model for dual string system can be readily used in practical case study. In this chapter, we will focus on verify the sinusoidal buckling solution for dual string buckling using Lubinski's (1950) widely acknowledged research on sinusoidal buckling of single string.

Lubinski (1950) conducted detailed study on sinusoidal buckling behavior of single string in vertical well scenario. By establishing the differential equation for force equilibrium and solving with power series approximation, he obtained very accurate solution for sinusoidal buckling with low order. When buckling order become very large, his solution is off the real situation. Results of first order and second order sinusoidal buckling are calculated with Lubinski's model, which we will assume it is the real case. We will calculate and compare the string space configuration, bending moment, bending stress and length change due to buckling with result from new model in this section. The detailed geometrical information of tubular in this case study can be found in APPENDIX D. We will start from introduce some concepts used in Lubinski's (1950) research and then conclude with a result comparison.

The length in feet of one dimensionless unit, which is abbreviated as DU, is given by the following expression as

$$m = \sqrt[3]{\frac{EI}{w}}, \tag{39}$$

where m is length in feet of one dimensionless unit, E, I and w are the same as previously defined. According to Lubinski's (1950) study, this length doesn't vary appreciably from one type of drill string to another and is usually between 40 and 65 ft.

When weight on bit reaches critical value, the drill string deforms from straight to sinusoidal buckling. The buckling shape at the critical value of the first order and second order sinusoidal buckling were plotted in Figure 16 Shape of Buckled Curves ComparisonFigure 16 (a) and (b) respectively. It is obviously observed that the new model can describe a very close shape configuration with Lubinski's result, which shows that there is very high accuracy in calculation using new model.

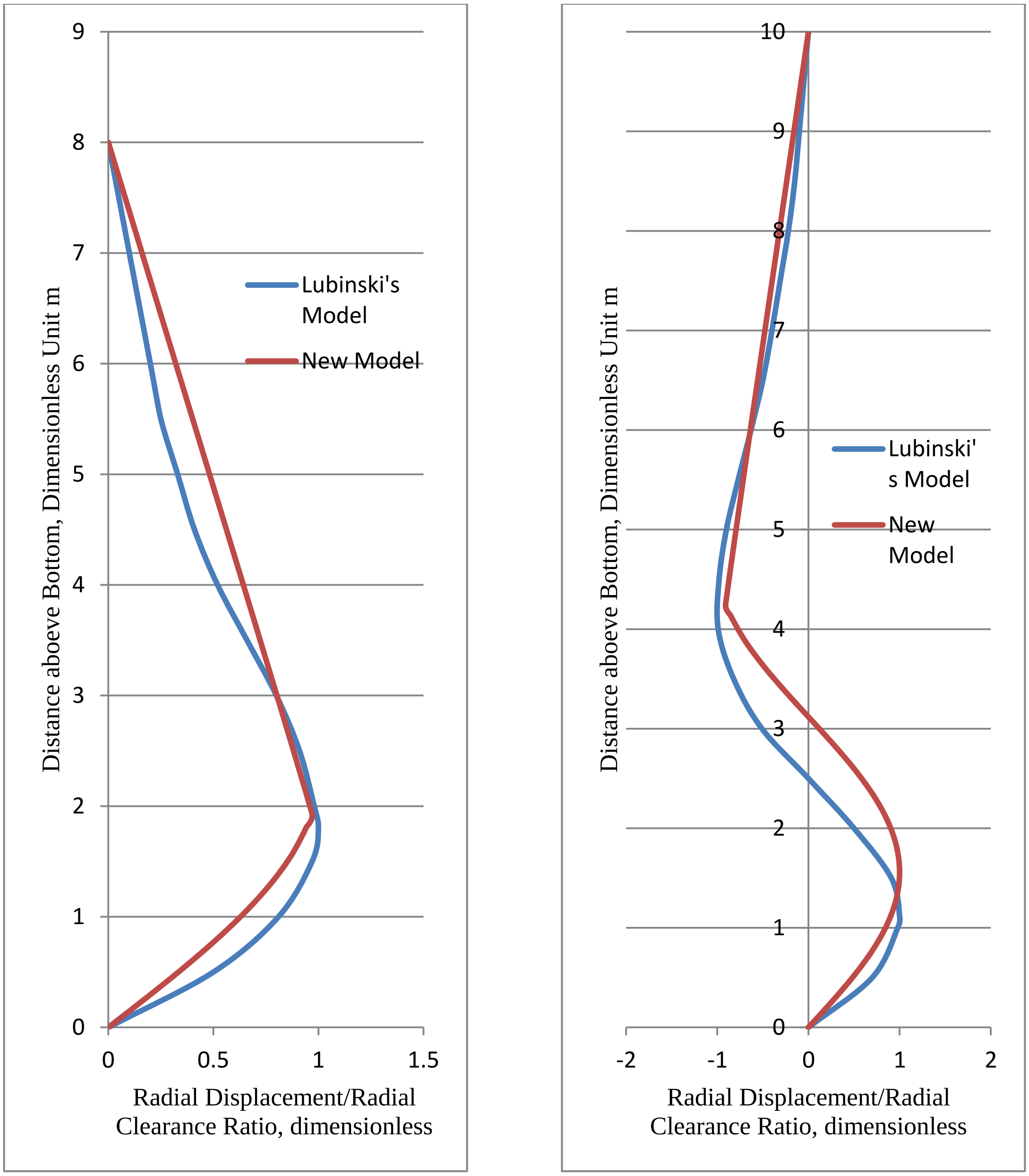

(a) (b)

Figure 16 Shape of Buckled Curves Comparison

Also we can notice that there is a discontinuity at 1.94 DU from bottom on first order sinusoidal buckling configuration and a discontinuity at 4.22 DU from bottom on second order sinusoidal buckling configuration. Actually this discontinuity position corresponds to position of the neutral point of tubular. This buckling model can only describe the buckling configuration in compressive section while not applicable to the tensile section of tubular, so we use a straight line to connect tensile section. The result will be acceptable because the major deformation, bending moment and length change due to buckling exist in the compressive section. Also there is a small position different for point where drill string is in contact with wellbore. That is because in real case Lubinski observed a fast downward displacement of tangential point as this second order buckle happens.

Lubinski also define the bending moment coefficient i by the following expression as

$$i = \frac{d^2y}{dx^2}\frac{m^2}{r} \text{ and} \tag{40}$$

$$M = iwmr. \tag{41}$$

where all parameters are previously defined. For any given size of drill pipe or drill collars, the weight per unit length, w, and the length of one dimensionless unit are all constant. So the bending moment M will increase in proportional to the radial clearance and bending moment coefficient i. This coefficient i is unique to a certain buckling configuration. We compare the coefficient result with Lubinski's model in second order sinusoidal buckling condition, as shown in Figure 17.

As we can see from Figure 17, this coefficient i is varying along the drill string, which indicates that bending moment in sinusoidal buckled tubular varies along the string. Lubinski's model predicts the maximum bending moment occurs around 0.84 DU from the bottom, while this model predicts the maximum bending moment around 1.5 DU from the bottom. As is previously discussed, Lubinski observed a fast downward displacement of tangential point as this second order buckle happens, while the pitch in this model can only gradually changes.

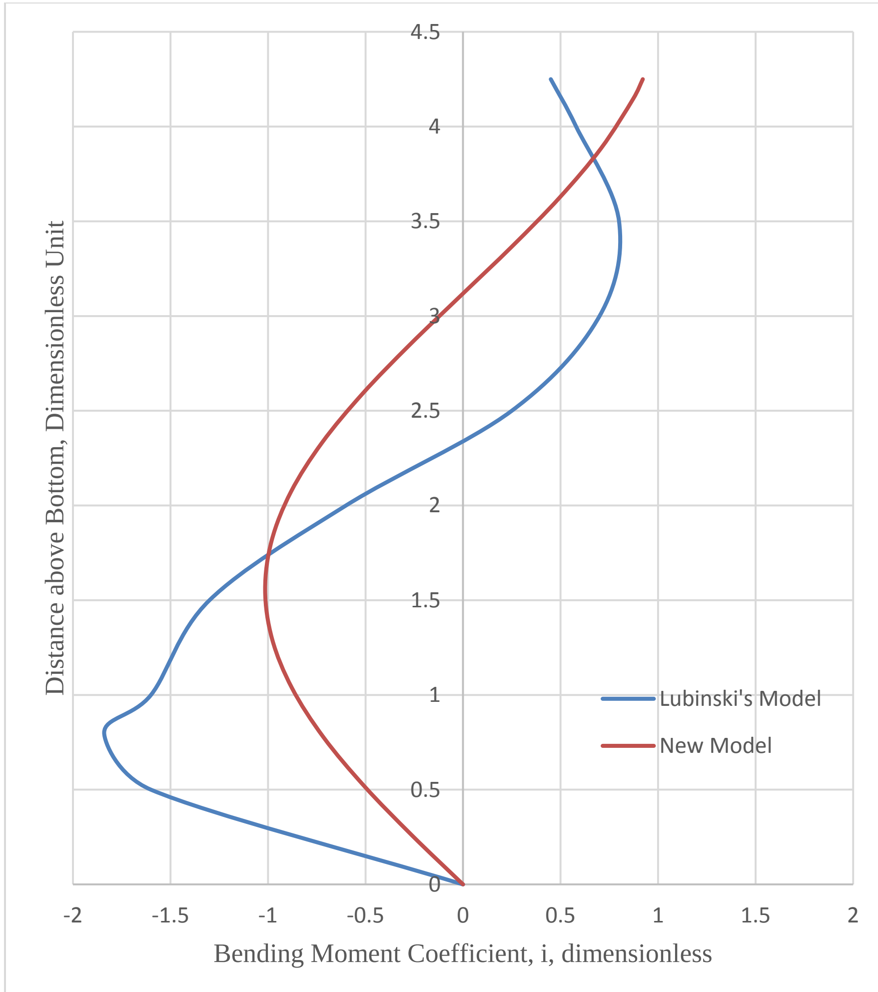

Figure 17 Bending Moment Coefficient Comparison

Besides, there is a linear approximation in derivation of this model (derivation details are explained in APPENDIX C). The influence of this process is like make an average distribution of bending energy over the pitch. The bending energy seems to smoothly distribute along the string instead of increasing or dropping suddenly like Lubinski's model. So this explains why the maximum bending moment coefficient from Lubinski's model is 1.84, while coefficient from this model is 1.02. However, the predicted result with new model still follow a very close trend with results from Lubinski's model.

Then we will calculate the magnitude of maximum stresses generated by the bending moment due to buckling. The following study considers the condition at which the second order buckling contact the wellbore. The maximum coefficient value i is directly determined by previous study as 1.84 in Lubinski's study and 1.02 from newly derived model. The maximum stresses have been calculated with 6 ¼ inch. Drill collar in a12 lb/gal mud, the detailed geometrical information can be found in Table 12 in APPENDIX D.

As is shown in Figure 18, the maximum bending stress from Lubinski's model is about 40% higher than that from the newly derived model. As previously discussed, this new model tend to average the energy over the pitch, so the maximum moment predicted is less than Lubinsk's result accordingly. So it should always bear in mind in practical application that this new model could possibly underestimate the maximum bending stress. Besides, field data in real case is also needed to determine which model better fits the real situation.

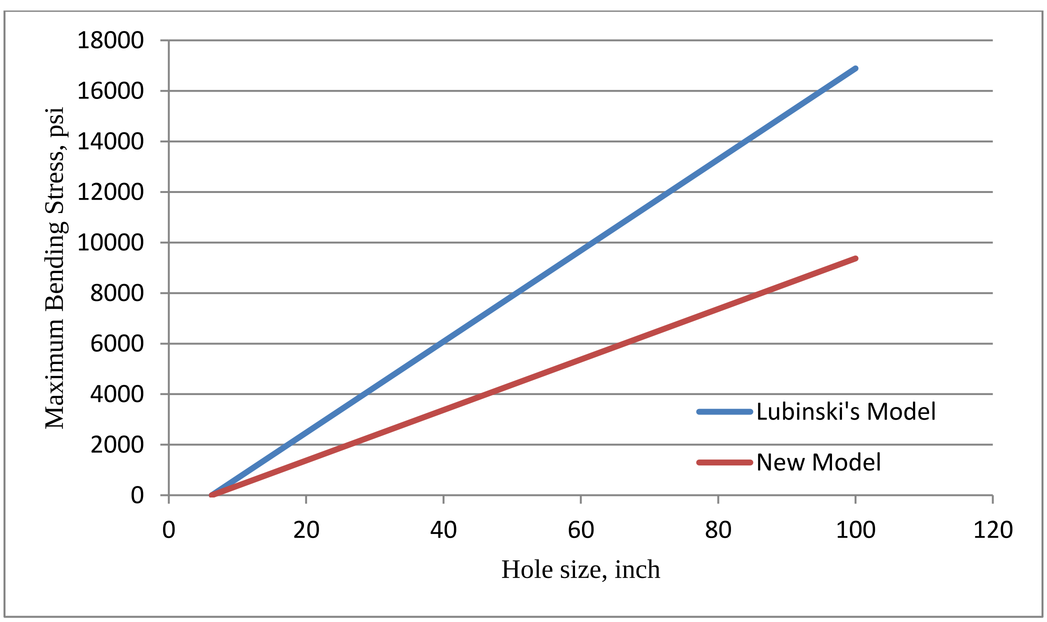

Figure 18 Maximum Bending Stress Comparison

It is also noticed in above figure that once buckling configuration is determined, the bending moment will be in proportional to wellbore diameter. In real cases, if the drill string is rotating and continuously in contact with formation, it could potentially generate a large cavity in certain formations. Large cavities will directly increase the hole diameter, and if the maximum bending moment happens to be close to this region, this can cause very large bending stress at cross section, which also needs to be considered in practice.

Lubinski (1950) introduced another kelly displacement coefficient, q, to describe the displacement due to buckling by the expression as

$$\Delta L_b = q\frac{r^2}{m}, \tag{42}$$

where ΔL_b, r and m are previously defined. The coefficient q depends on the distance between the bit and the neutral point, which is proportional to the weight on bit. For a given size of drill collar or drill pipe in a wellbore and a given density, the unit length, m, and radial clearance is constant, this length change due to buckling only depends on q.

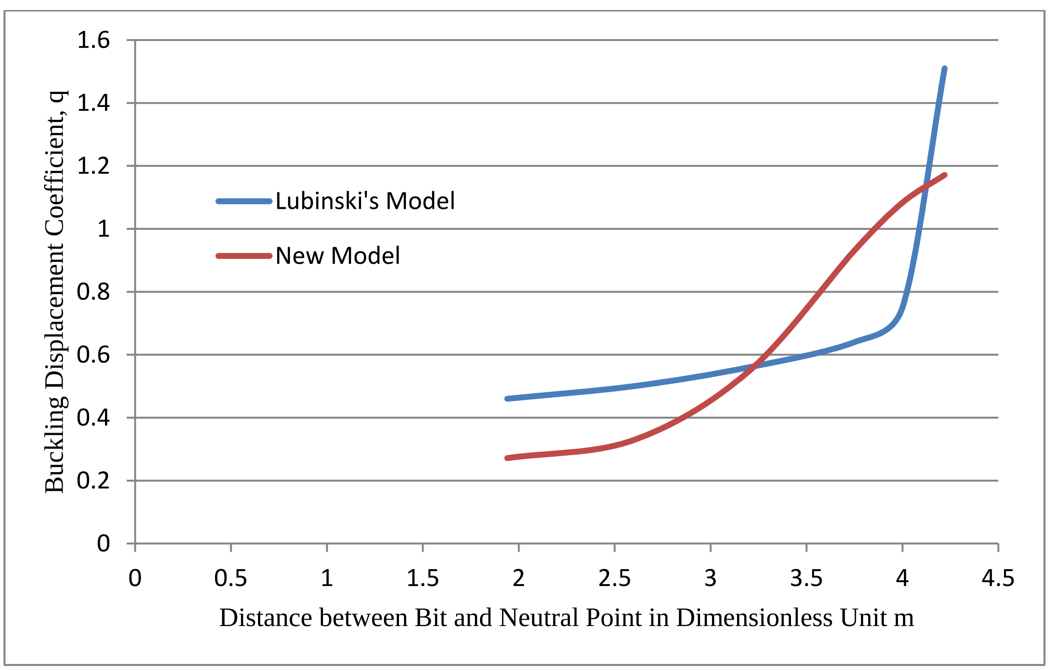

Figure 19 Comparison of Displacement Coefficient

As is shown in Figure 19, the buckling induced displacement coefficient from new model is very close to the result from Lubinski's model. The abscissa of curve start point is around 1.94 DU, which corresponds to the critical buckling force of first order buckling. The abscissa of curve end point is around 4.22 DU, which corresponds to the critical buckling force of second order buckling that contacts the wellbore. So this plot corresponds to the length change due to buckling from first order sinusoidal buckling to second order sinusoidal buckling.

In summary, this chapter first illustrates the calculation procedure of applying the newly derived model in real case study. After that the proposed analytical model for predicting buckling behavior of dual string system has been verified by a case study using widely acknowledged Lubinski's model. The study shows that the newly derived model can accurately describe the real situation. Attention should be paid to maximum moment and stress prediction, because the new model potentially may underestimate the maximum bending moment.

CHAPTER 5
EXAMPLE CALCULATION AND DISCUSSION

5.1 Introduction

In previous chapter we developed analytical model for helical and sinusoidal buckling of dual string system. Furthermore, the widely acknowledged Lubinski's model (1950) and Mitchell's model (2012) have been used and successfully verified the prediction accuracy of the newly derived model.

Currently the post buckling behavior of single string has been under extensive research and numerous case studies have been conducted on this subject. The assumption of these studies that the casing should be rigid can be invalid at certain conditions. There are only a few studies on this subject. Christman (1976) brought up a composite pipe model with arithmetic summed property of dual string system, which was based on unreasonable assumptions at certain condition. Mitchell (2012) made improvement on Christman's model but didn't conduct enough case studies and explore the mechanism for dual string buckling behavior.

This section aims to contribute to better understanding the buckling mechanism of dual string system by conducting several case studies on different parameters. We will start with Lubinski's (1962) example, which will be the base example. Then different parameters are varied to evaluate its effect on buckling behavior of dual string system. Finally Christman's model and Mitchell's model are applied in case study and comparison between these three models is conducted. The mechanism of dual string buckling system will be explored.

5.2 Model Application for Case Study

For comparison convenience, an example has been chosen from Lubinski's (1962) research on helical buckling. This example is for a high pressure squeeze-cementing operation. The geometrical information for casing and tubing is included in Table 13 and Table 14 in APPENDIX D. In the Lubinski's example, the wellbore for 7 in. casing was not specified, so we are assuming a typical bore diameter of 8 ½ in. There is a packer (A_p=8.30 sq in.) at the depth of 10,000 ft.

Both the tubing and annulus are full of 30 degree API crude oil at the same time the tubing is initially sealed in the packer. Thereafter, the crude oil in tubing is displaced by 15 ppg cement slurry, as in a squeeze cementing operation. Assume the fluid between wellbore and casing is brine with 10ppg weight. Finally the pressure p_i =5,000 psi and p_o =1,000 psi are applied at surface to the tubing and annulus respectively.

Bottomhole pressure is calculated without considering the effect of flow. This corresponds to the most severe condition during a cementing operation that there is little or no flow. It is already proven in Lubinski's research that in the presence of both the inside pressure, P_i , and outside pressure, P_o, the tubing behaves as if it is subjected to a buckling force as

$$F = A_p(P_i - P_o), \qquad (43)$$

where A_p is the area of packer bore, P_i is the inner pressure of tubing at certain depth and P_o is the outer pressure of tubing at certain depth. This formula is chosen to determine the buckling force at bottom of tubing. Eq. (30) and Eq. (38) will be used in this study to determine the buckling force at any depth along the tubing and casing. By substituting the above numerical values, we can get that buckling force at bottom of tubing is 66,400 lbf.

There are five scenarios which are specifically designed to study the buckling behavior of a dual string system, as is shown in Table 6, where F_1 is the buckling force on tubing at packer depth, F_2 is the buckling force on casing at packer depth, .and r_w is the wellbore radius.

Table 6 Buckling Force Conditions for Case Study

Case No.	F_1 (lbf)	F_2 (lbf)	r_w (inch)
1	66,400	0	4.25
2	66,400	66,400	4.25
3	132,800	0	4.25
4	66,400(single string)	0	4.25
5	66,400	0	5

There are usually two general field practice scenarios where buckling of dual string system occurs. The first situation is that the inner string buckles into contact with the outer casing and the casing buckles subsequently due to the contact load generated by the inner pipe, which is designed as case 1. The second situation is that both strings have compressive axial buckling forces and buckles together. The final resultant configuration should make the buckling behavior of dual string fit together, which is designed as case 2. Case 3 and case 5 are designed to explore the how the buckling force and radial clearance impact the post buckling behavior of dual string system. Case 4 is designed to compare the difference of buckling behavior between single string and dual string system. Post buckling parameters, including pitch variation, bending moment, bending stress and length change due to buckling, are studied in this section.

5.2.1 Field Case 1-Results and Analysis

The case 1 is specifically designed to study the buckling behavior of dual string system that is induced by the initial buckling of inner string. The influence of casing weight is not considered for Case 1. In this scenario the dual string system is predicted to form a sinusoidal buckling configuration.

The buckling pitch along tubing is plotted in Figure 20. The expanded figure is shown in Figure 21. The pitch of sinusoidal shape is 54 ft. at bottom hole and increases very slowly from bottom up until it reaches around 7,500 ~ 8,000 ft. The neutral point of tubing is at 8,637 ft. It is observed that the buckling pitch increases very rapidly at the near neutral point region. This is because buckling force at the near neutral point region is very close to the critical stability of sinusoidal buckling, which is a very small value. In other word, this region is actually a transition region between sinusoidal shape and straight shape. As the distance from bottom keeps increasing above the neutral point, the tubing is in tensile zone and behaves more like a straight shape.

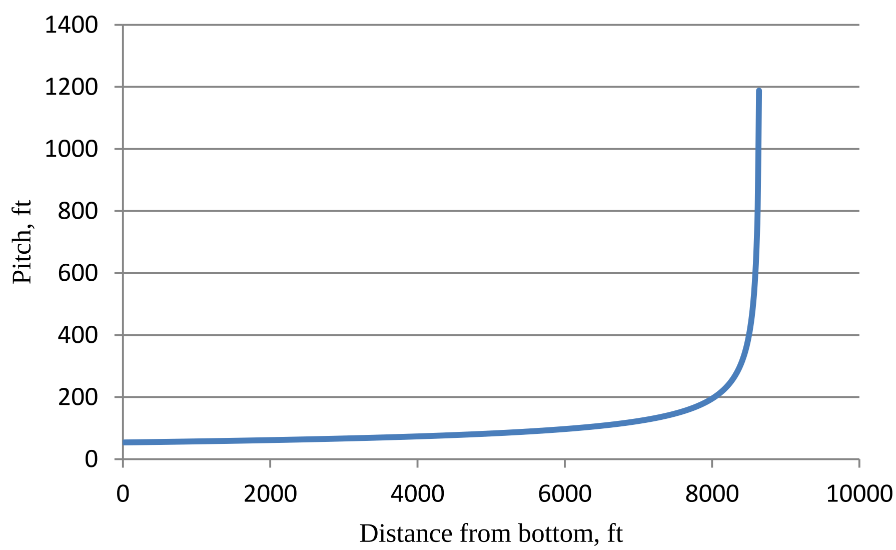

Figure 20 Pitch along Tubing in Case 1

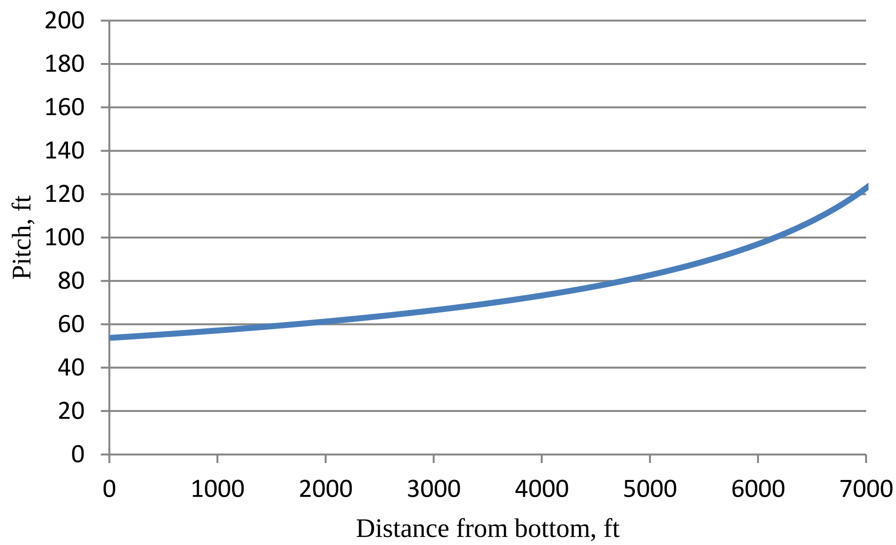

Figure 21 Pitch along Tubing in Case 1(Expanded Plot)

It is also noticed that the buckling pitch varies slowly from 54 ft to 120 ft in a large portion of buckling section (around 7,000 ft. of tubing). As is stated during model derivation (details in APPENDIX B and APPENDIX C), the length segment during calculation is preferred to be larger than 0.2 times pitch for an accurate approximation. The segment length selected in this study is 20 ft, which ensures that the prediction from this model gives a very accurate prediction. Furthermore, the maximum bending moment, maximum bending stress and length change due to buckling mainly occurs at the bottom portion of tubing, where the newly derived model can ensure a very high accuracy.

The bending moment in tubing along tubing is shown in Figure 22. For simplicity and clearness in demonstration, we only plot the bending moment from bottom to 2,000 ft. up along the tubing. This reversal sign of bending moment indicates that the dual string system conforms to the sinusoidal buckling configuration. It should also be noticed that the amplitude of bending moment is supposed to be symmetrical about the x axis while the plot is not. The reason is because calculation within every segment is based on the starting and ending point of the interval, when the segment length is very close to buckling pitch, calculation probably skips the maximum point which is within this segment. To verify this explanation, we reduce the segment length to 10 ft. and generate the bending moment in tubing plot as Figure 23. It is obvious that as the segment length decreases, the bending moment becomes symmetrical about the x axis.

However, we only care about the outer contour of this bending moment plot to determine the maximum bending moment, as shown by dash line in Figure 22 and Figure 23. Calculation with different length segment both predict a descending trend of bending moment from bottom up and a maximum bending moment around 865 lbf-ft near the bottom of tubing. Although using the segment length 20 ft. may potentially make the plot miss some peak value point, it is very unlikely that all the maximum point is skipped. In this case study we keep using the 20 ft length segment, which can also predict an accurate maximum bending moment.

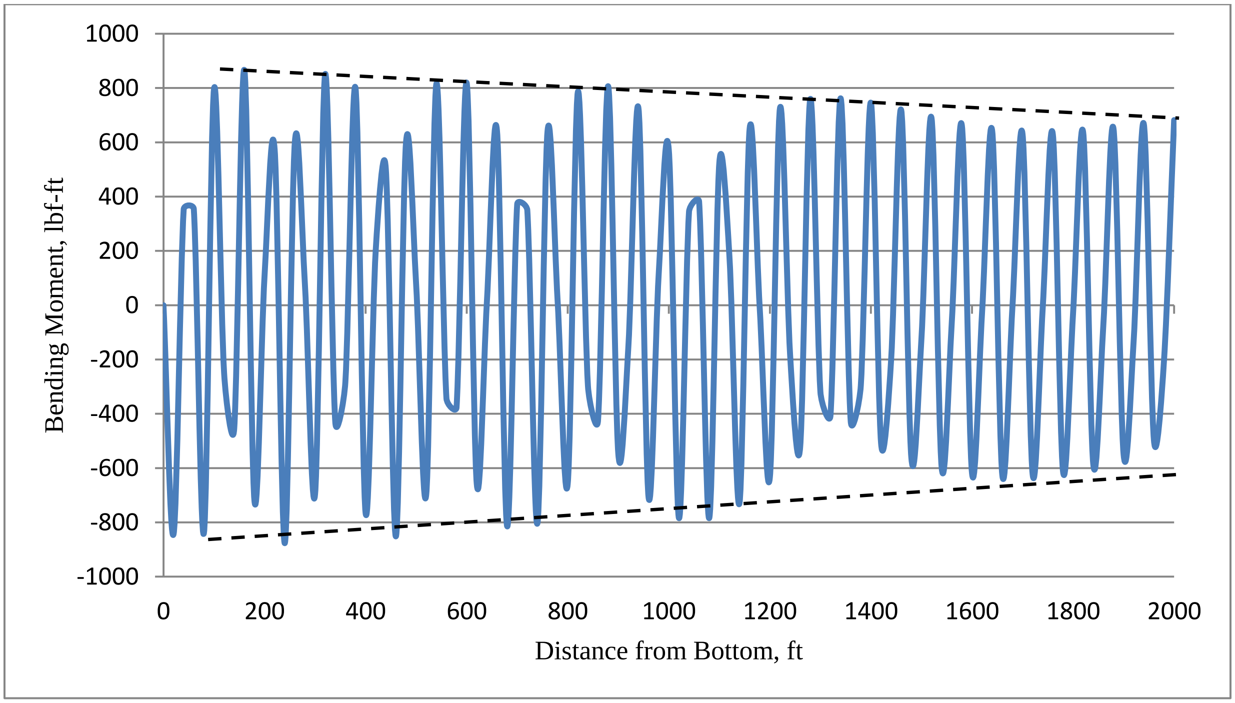

Figure 22 Bending Moment in Tubing with Segment Length = 20 ft.

The bending moment in casing can be calculated in similar way and results are plotted in Figure 24. The maximum bending moment in casing is 8,680 lbf-ft at the same depth of maximum bending moment point in tubing near the bottom. The dashed line represents the maximum bending moment contour. So the bending stress in tubing and casing can be plotted accordingly in Figure 25. The dashed line represents the maximum bending stress contour. The descending dash line shows that the bending moment amplitude are decreasing from bottom up and will become very small near neutral point.

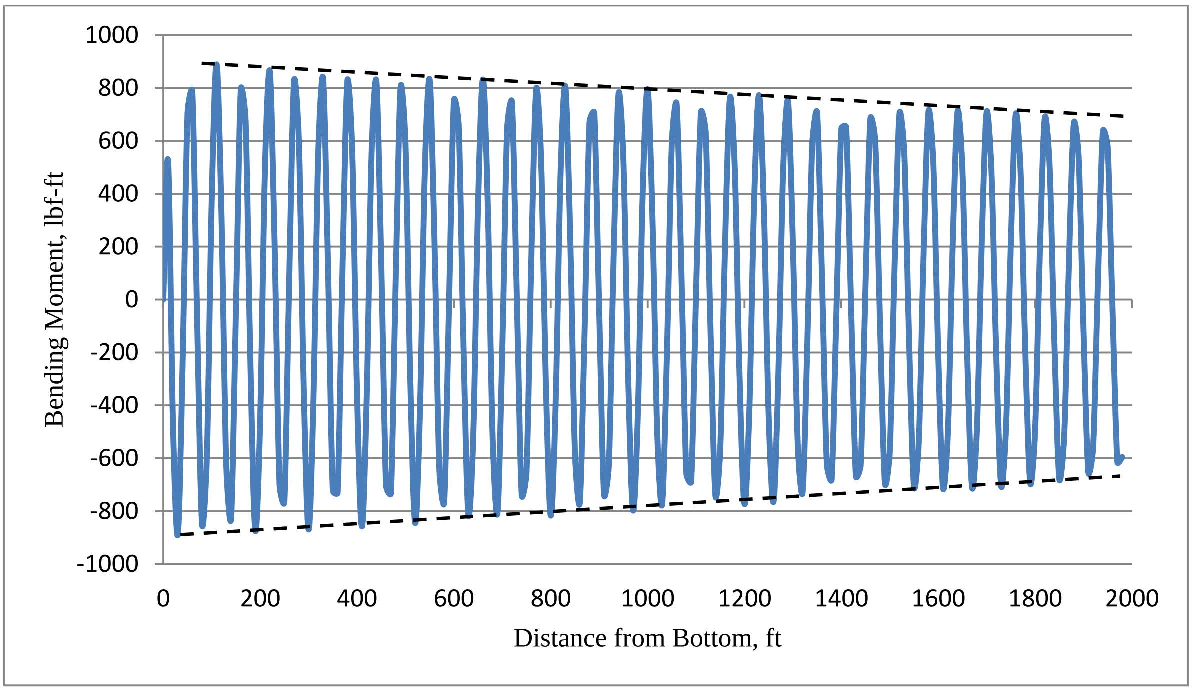

Figure 23 Bending Moment in Tubing with Segment Length = 10 ft.

Notice that if the buckling of dual string system occurs, the casing helps to take a large portion of bending moment due to its high bending stiffness capacity in dual string system. The bending moment in tubing only accounts for a small portion. It can also be read from Figure 25 that the maximum bending stress in tubing is 783 psi and maximum bending stress in casing is 606 psi. So the final resultant maximum stress at cross section of tubing is close to the maximum stress at cross section of casing.

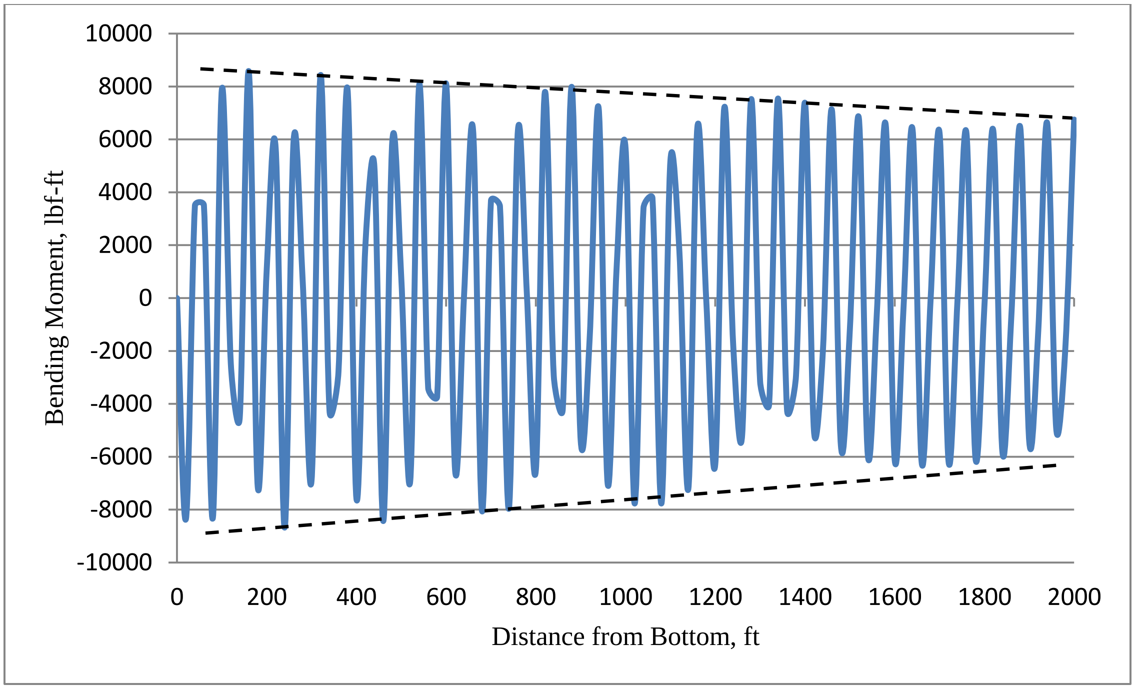

Figure 24 Bending Moment in Casing in Case 1

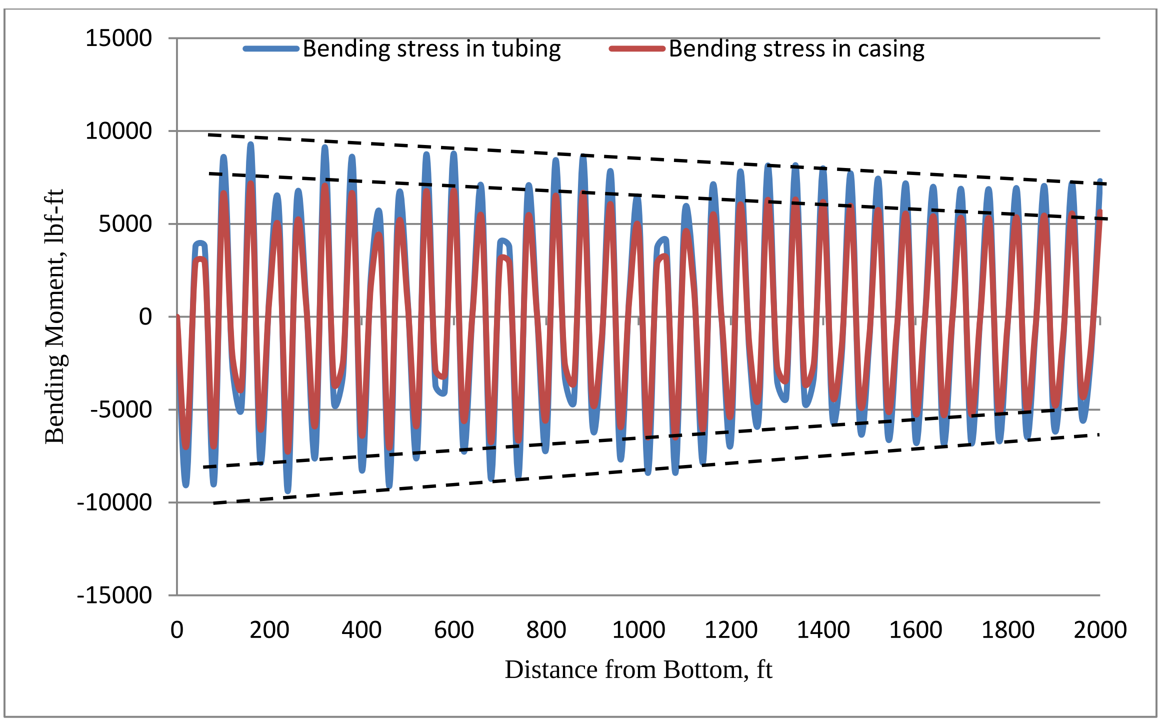

Figure 25 Bending Stress in Casing and Tubing in Case 1

5.2.2 Field Case 2-Results and Analysis

The case 2 is specifically designed to study the buckling behavior of dual string system that the inner tubing and outer casing buckles simultaneously and fit together to the final configuration. In this scenario the dual string system is predicted to form a sinusoidal buckling configuration. In this case the buckling force at bottom of tubing and casing are both designed to be 66,400 lbf. Another difference from case 1 is that the influence of casing weight on buckling force in casing is considered. Although the buckling forces at the bottom of casing and tubing are designed to be same, the buckling forces along casing and along tubing are decreasing at different rate from bottom up. The neutral points of casing and tubing are calculated to be different depth, with casing at 4,080 ft. and tubing at 8,637 ft. from bottom up.

The pitch and distance from bottom relationship of buckling configuration in case 2 are plotted in Figure 26 and the expanded plot of the same figure is shown in Figure 27. It is noticed that the calculation is conducted from bottom hole to 7,500 ft. from bottom, above which position the prerequisite condition, Eq. (21), for this model is not satisfied any more. It is also noticed that the buckling pitch of the region near 7,500 ft is increasing very rapidly. It is very likely that the dual string system undergoes a transition from sinusoidal buckling shape to straight shape. The buckling pitch of dual string system at bottom is 51.3 ft, which is less than buckling pitch at bottom in case 1 due to buckling force on casing.

It deserves attention that although the axial force in casing transit from compressive to tensile force above 4,080 ft. in casing, this model can still predict a sinusoidal buckling configuration for dual string system. The outer casing buckles under the large contact force between buckled tubing and casing. However, this section of casing in tensile force can largely constrain the buckling of dual string system. As is shown in Figure 26, the buckling pitch of dual string system increase rapidly above 7,000 ft. from bottom, where the buckling force in casing is considered to be zero. It can also be inferred that when the prerequisite condition, Eq. (21), is not satisfied any more, the duals string system transit into straight shape.

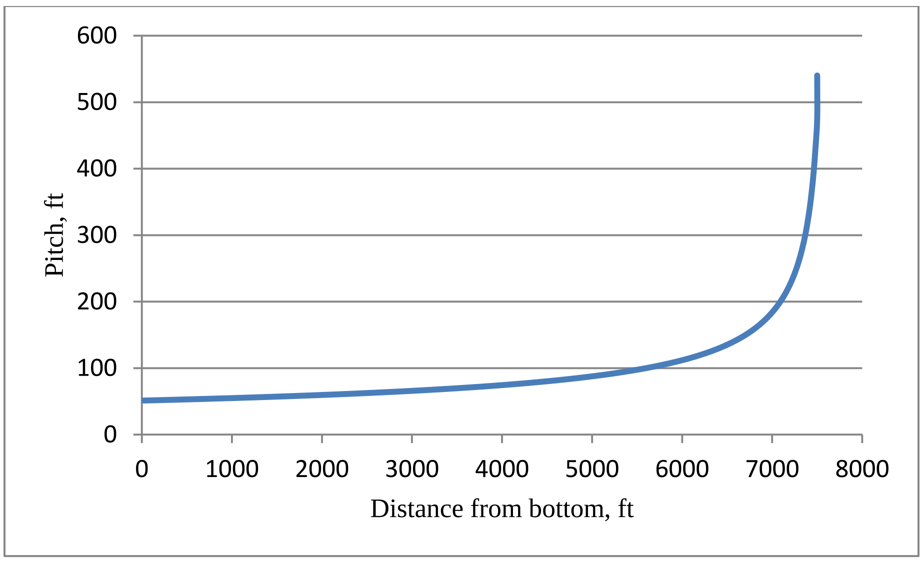

Figure 26 Buckling Pitch along Tubing in Case 2

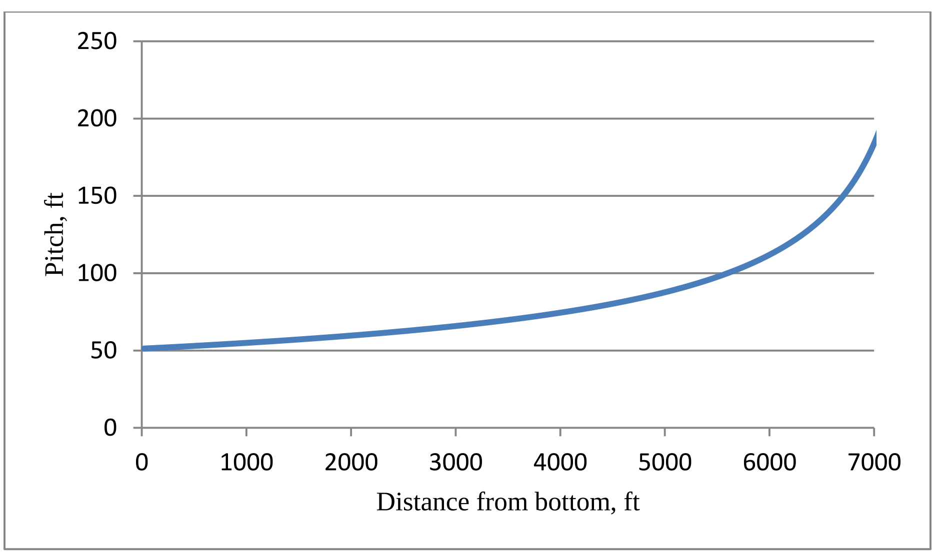

Figure 27 Buckling Pitch along Tubing in Case 2 (Expanded Plot)

The bending moment in tubing and casing along wellbore are plotted in Figure 28 and Figure 29, respectively. For simplicity and clearness in demonstration, we only plot the bending moment from bottom to 2,000 ft. above bottom. The outer contour of bending moment is represented by dash line in Figure 28 and Figure 29, which predict a descending trend as it goes from bottom up. This conforms to our understanding that large bending moment occurs at region where buckling force is the highest. The bending moment becomes very small value at near the neutral point region, as the dual string system behaves more like a straight shape. By reading from Figure 28 and Figure 29, we can find that the maximum bending moment in tubing is 980 lbf-ft and the maximum bending moment in casing is 9,706 lbf-ft. The maximum bending stress at cross section in casing and tubing can be plotted accordingly in Figure 30. It can also be read from Figure 30 that the maximum bending stress in tubing is 876 psi and maximum bending stress in casing is 678 psi.

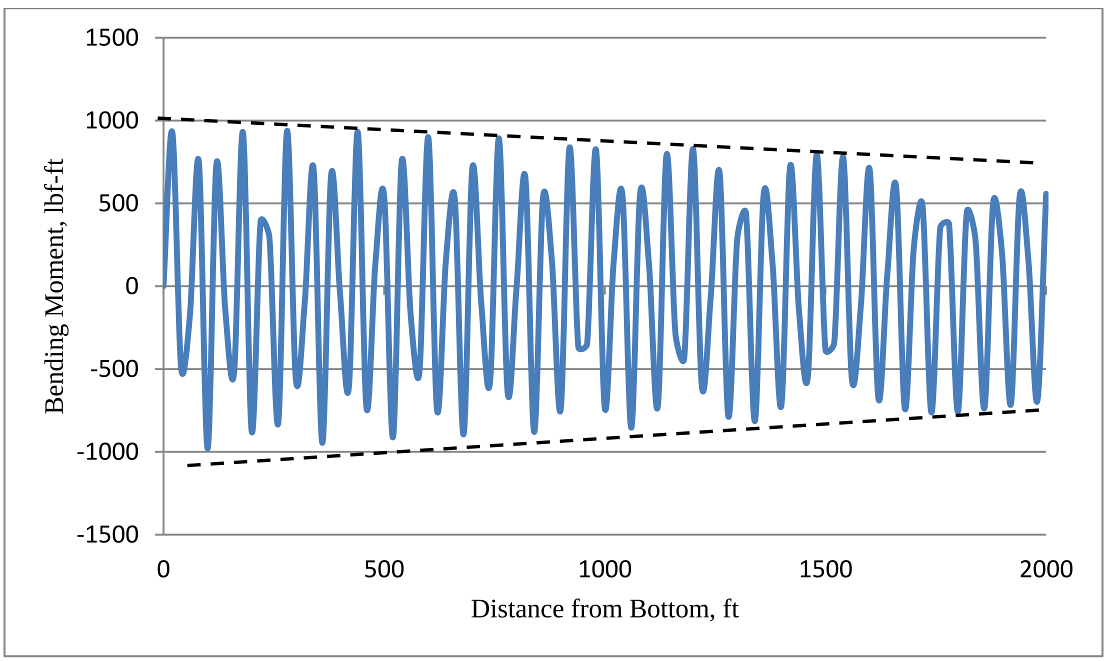

Figure 28 Bending Moment in Tubing in Case 2

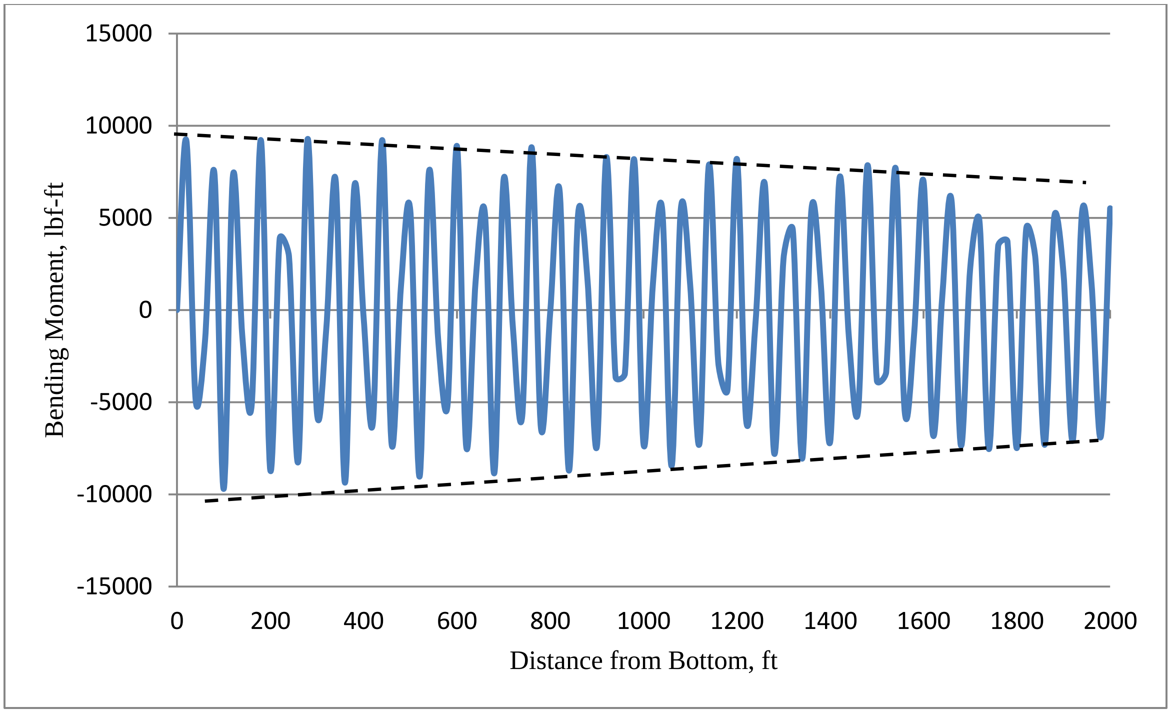

Figure 29 Bending Moment in Casing in Case 2

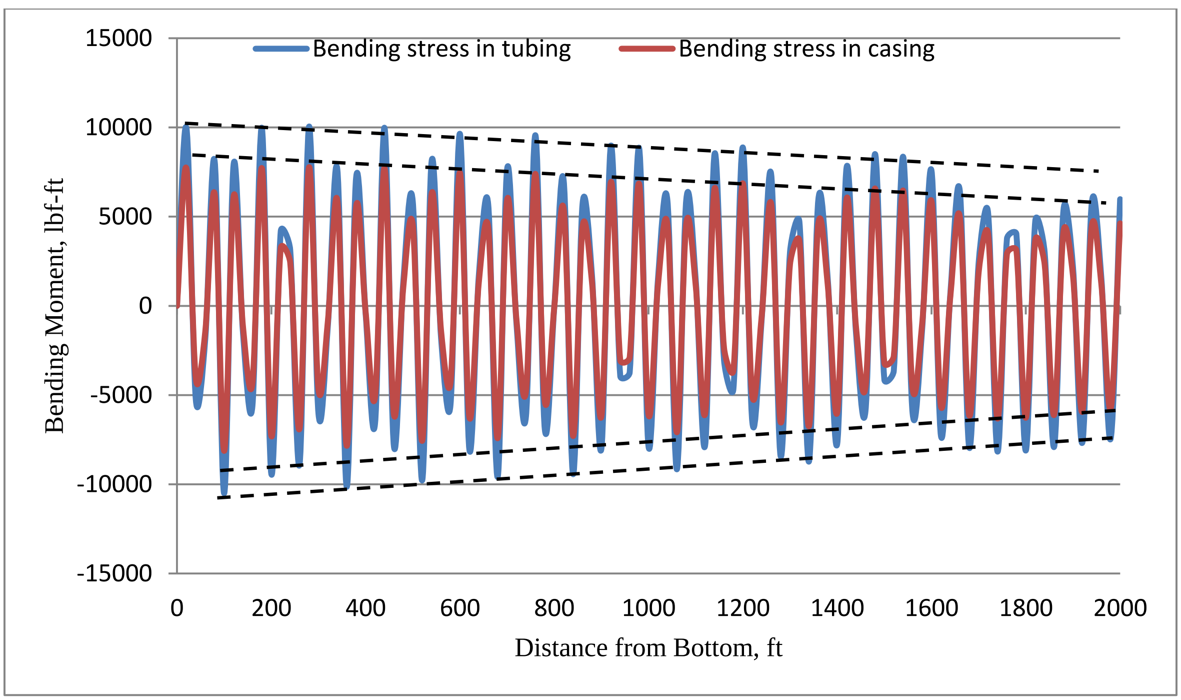

Figure 30 Bending Stress in Casing and Tubing in Case 2

5.2.3 Field Case 3-Results and Analysis

The case 3 is specifically designed to study the influence of buckling force on buckling behavior of dual string system. The influence of casing weight is not considered for Case 3. In this scenario the dual string system is predicted to form a sinusoidal buckling configuration.

In Case 3 the buckling force at bottom of tubing is increased to 132,800 lbf. Actually there are many operations that could potentially increase the buckling force by a large scale, e.g. applying very high surface pressure inside of tubing or conducting operation on mud or cement with heavy weight. However, in this case it should be stated that the Case 3 is specifically designed only for research purpose, so it probably seldom happen in real practice.

The relationship between buckling pitch and distance from bottom is plotted in Figure 31. As is shown in Figure 31, the buckling pitch of dual string system is 38 ft.at bottom of tubing and gradually increases to 58 ft. at surface. In this case the buckling force at bottom of dual string system is so high that it buckles all the way to the surface. The neutral point is actually above the tubing surface point. Compared with Case 1, the buckling pitch of dual string decreased significantly as two times of initial buckling force is applied.

The bending moment in tubing and casing along wellbore are plotted in Figure 32 and Figure 33, respectively. For simplicity and clearness in demonstration, we still only plot the bending moment from bottom to 2,000 ft. above. Reading from Figure 32 and Figure 33, we can find that the maximum bending moment in tubing is 1,764 lbf-ft and the maximum bending moment in casing is 17,466 lbf-ft. Maximum bending moment in Case

3 increases almost twice as the buckling force doubles. Based above bending moment calculation, the maximum bending stress in casing and tubing can be plotted accordingly in Figure 34. Reading from Figure 34, we can find that the maximum bending stress in tubing is 1,576 psi and maximum bending stress in casing is 1,218 psi.

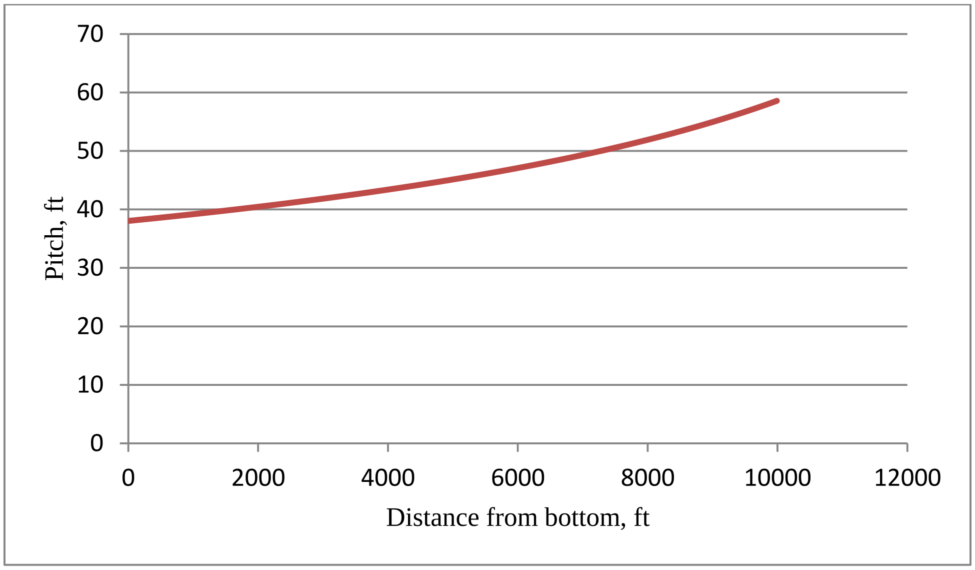

Figure 31 Buckling Pitch along Tubing in Case 3

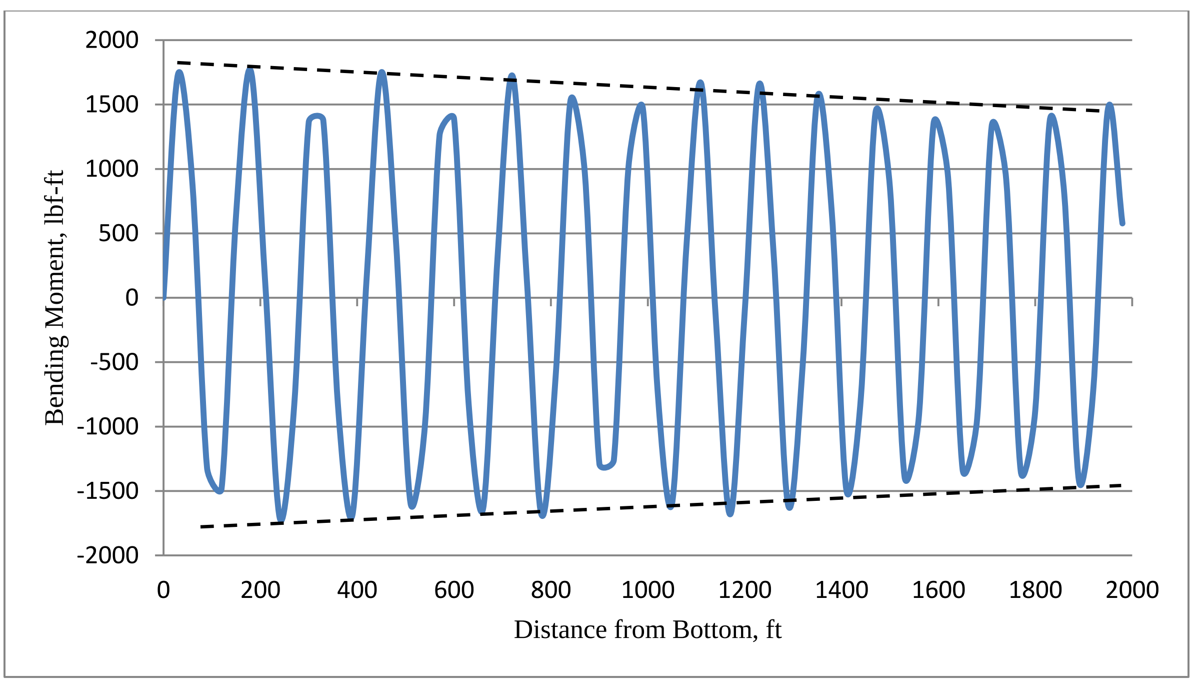

Figure 32 Bending Moment in Tubing in Case 3

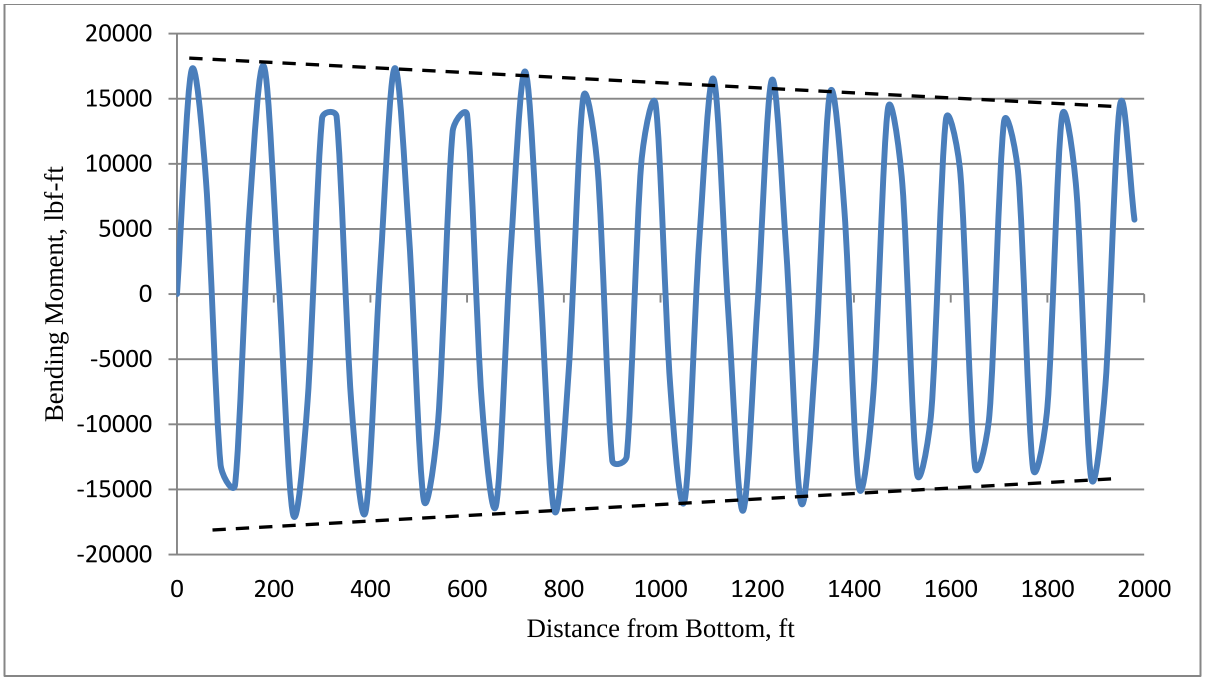

Figure 33 Bending Moment in Casing in Case 3

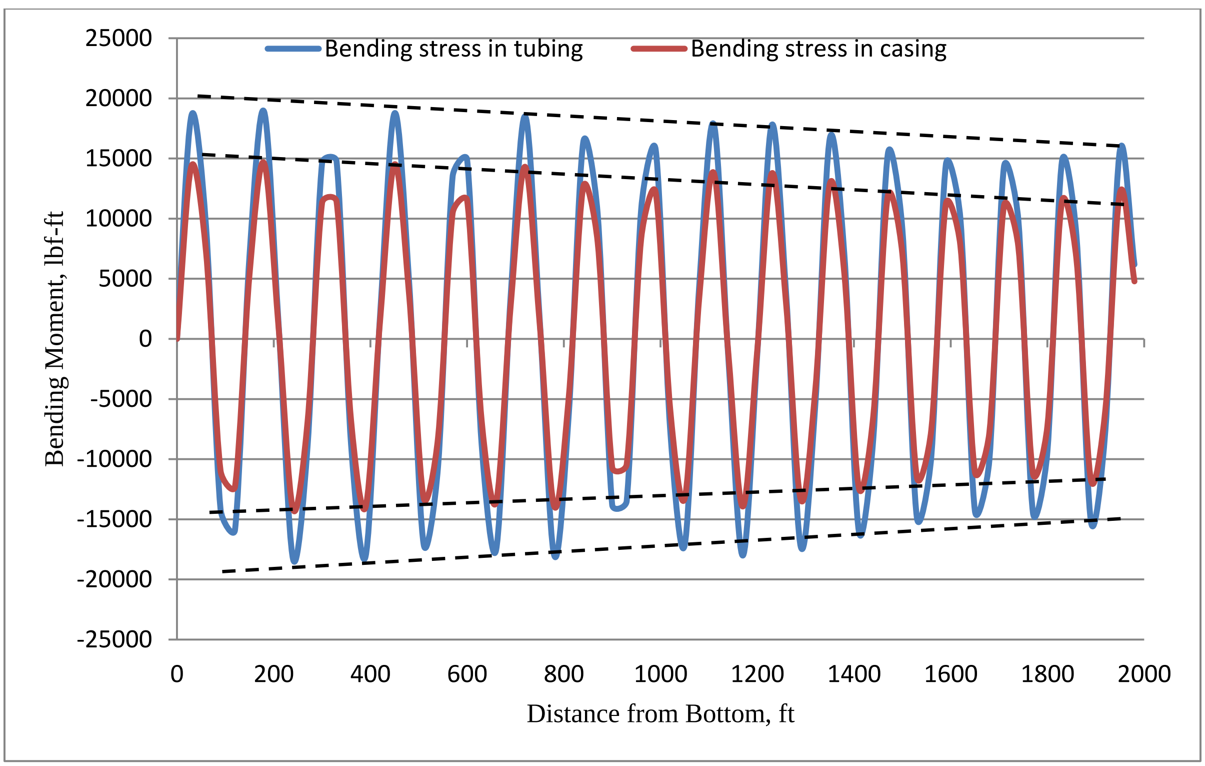

Figure 34 Bending Stress in Casing and Tubing in Case 3

One interesting finding is that there is less number of waves in Figure 32, Figure 33 and Figure 34 compared with previous case study. This is also determined by the ratio of buckling pitch and the length of selected segment. As the length of segment is at the similar magnitude of buckling curve, it is possible that the end point of a segment can skip the nearby region of point with maximum bending moment, but it is very unlikely that all end point fall out of that nearby region. The outer contour of bending moment has to be plotted to indicate maximum value. Since buckling pitch varies along tubing, the ratio of pitch and length of segment is changing, so this is why the curve is symmetrical in certain length section and changes in other section. Fixing this problem needs skills in properly selecting segment length and the outer contour line should always be used to help to predict an accurate value.

5.2.4 Field Case 4-Results and Analysis

The case 4 is specifically designed to study the difference between buckling behavior of a single string and dual string system under the same buckling force. In this scenario the single string is predicted to form a helical buckling configuration. Calculation for a single string buckling can be conducted by using Lubinski's (1962) model.

The buckling force applied at bottom of tubing is 66,400 lbf , which is the same as Case 1. The relationship between buckling pitch and distance from bottom is plotted in Figure 35 and an expanded plot of the same figure is shown in Figure 36. The neutral point is at 8,640 ft from bottom up. The buckling pitch starts from 20 ft at bottom and increases very slowly until around 7,300 ft. Then the buckling pitch increases very rapidly in the near neutral point region.

The bending moment and bending stress of cross section at different depth is plotted against distance from bottom in Figure 37 and Figure 38. It should be noticed that the bending moment in tubing of helical buckling has the same positive sign, which is different from the reversal bending moment in sinusoidal buckling. It is easily observed that the bending moment has a linear relationship with distance from bottom. The maximum bending moment and bending stress always occur at the bottom of tubing, where the buckling force is the largest and pitch is the smallest. Reading from Figure 37 and Figure 38, we can find the maximum bending moment in tubing is 4,454 lbf-ft and the maximum bending stress in tubing is 47,742 psi.

5.2.5 Field Case 5-Results and Analysis

The case 5 is specifically designed to study the influence of radial clearance on the final buckling behavior of dual string system. The loading condition and geometrical dimension are the same as Case 1 except for the wellbore dimension. In this scenario the dual string system is predicted to form a helical buckling configuration.

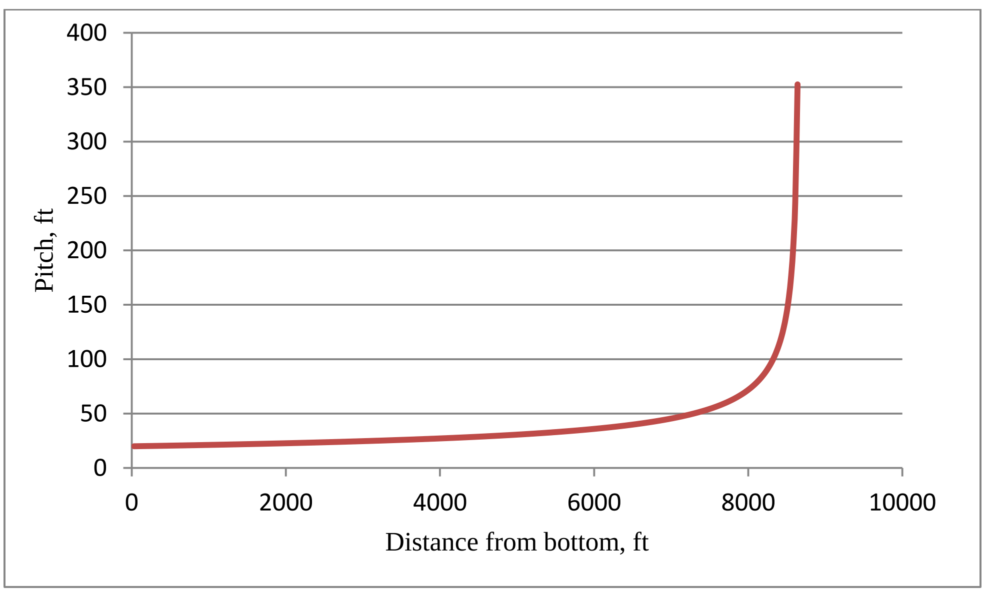

Figure 35 Pitch along Tubing in Case 4

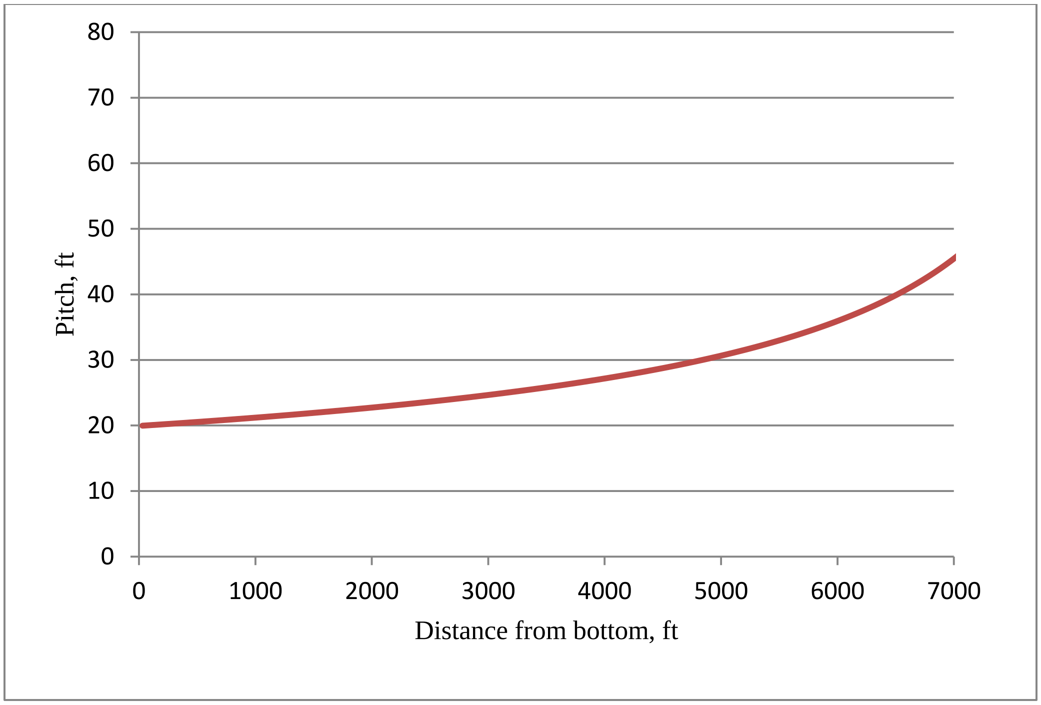

Figure 36 Pitch along Tubing in Case 4 (Expanded Plot)

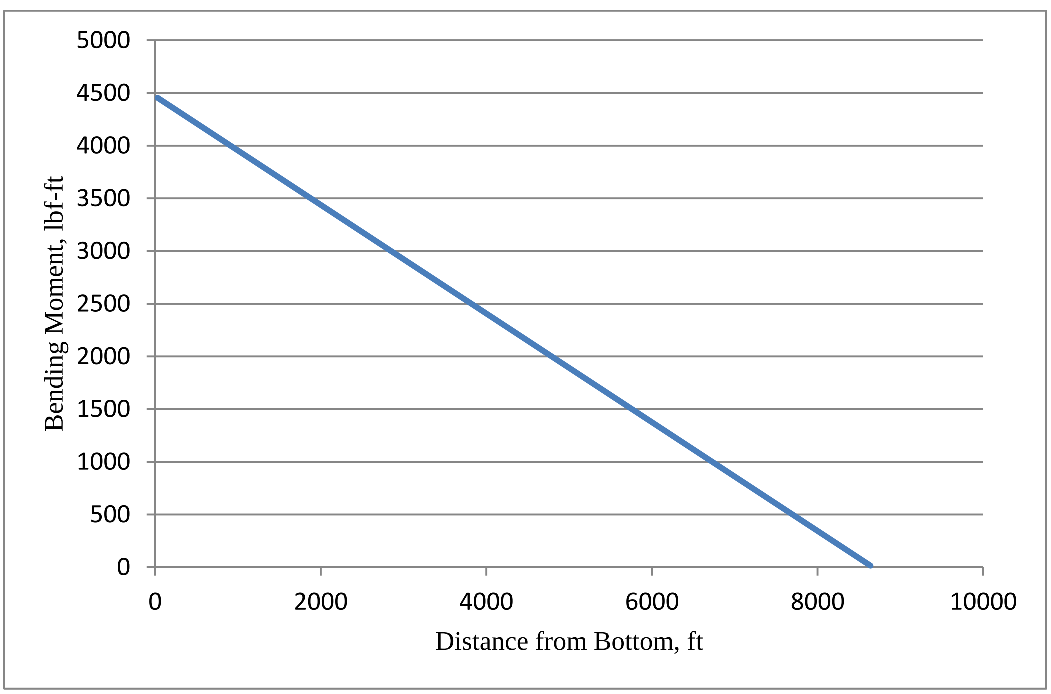

Figure 37 Bending Moment in Tubing in Case 4

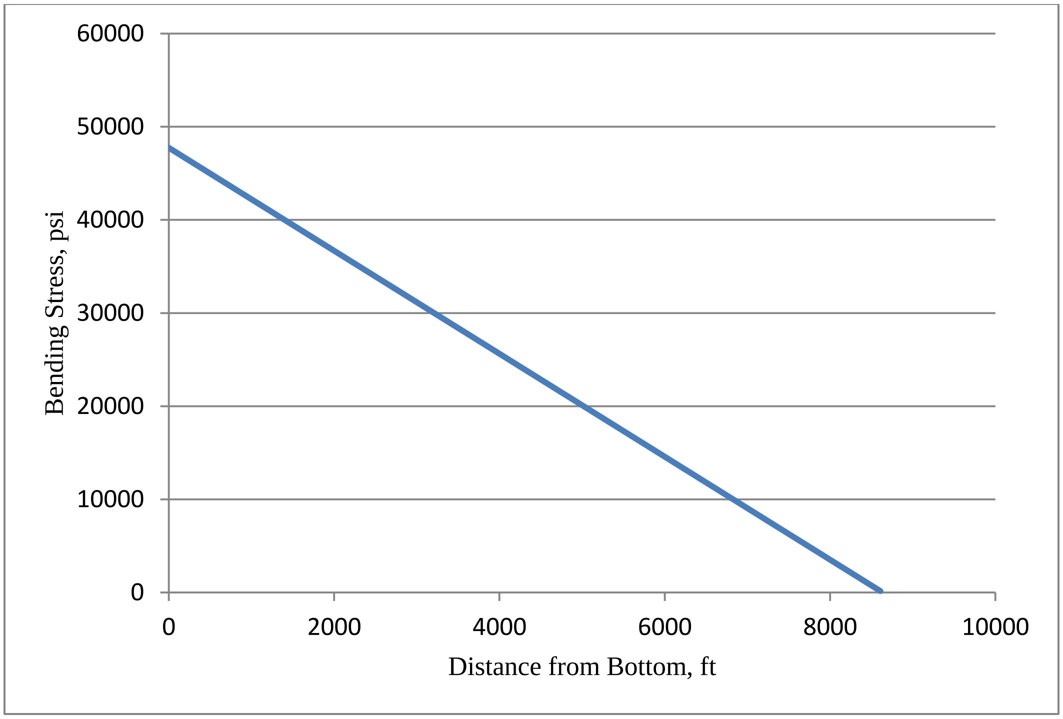

Figure 38 Bending Stress in Tubing in Case 4

The relationship between buckling pitch and distance from bottom is plotted in Figure 39 and an expanded plot of the same figure is shown in Figure 40. The buckling pitch of dual string system at bottom is 57.4 ft. The buckling pitch increases very gradually as it goes up until around 6,500ft. As is mentioned in previous case study, the rapid increase in buckling pitch corresponds to a transition stage to straight shape.

The bending moment of tubing and casing cross section at different depth is plotted against distance from bottom in Figure 41 and Figure 42. It is easily observed that the bending moment has a linear relationship with distance from bottom in case 5. The maximum bending moment and bending stress always occur at the bottom of tubing, where the buckling force is the largest and pitch is the smallest. Reading Figure 41 and Figure 42, we can find the maximum bending moment in tubing is 1,043 lbf-ft and the maximum bending moment in casing is 15,677 lbf-ft.

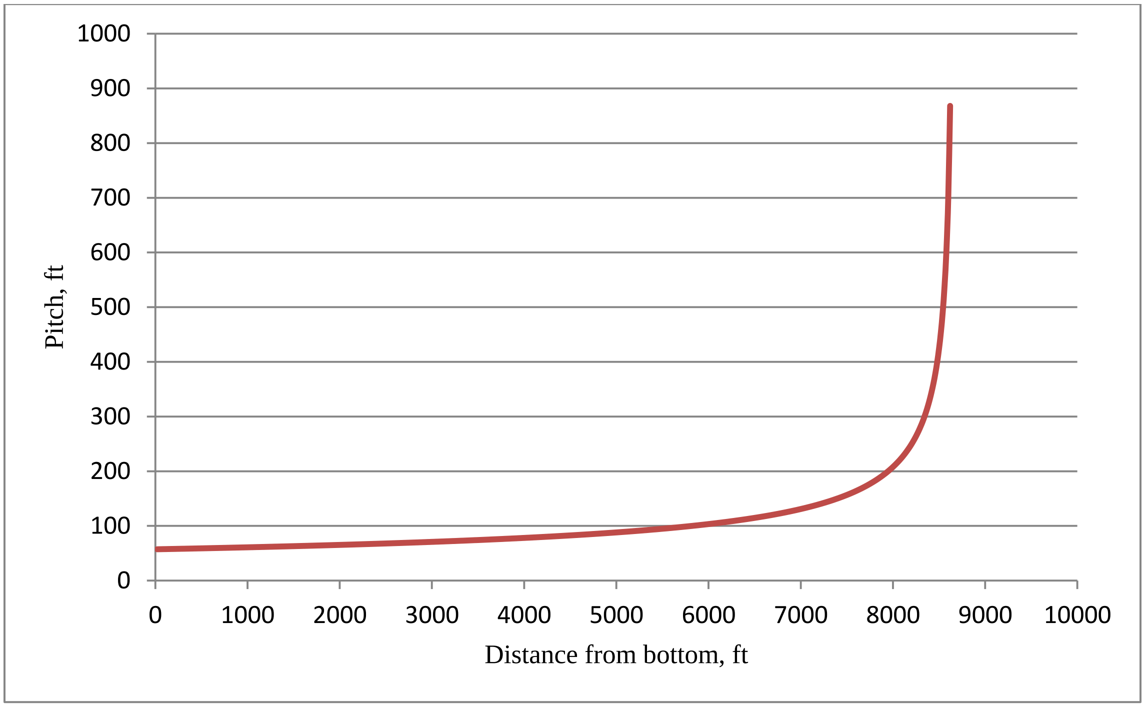

Figure 39 Pitch along Tubing in Case 5

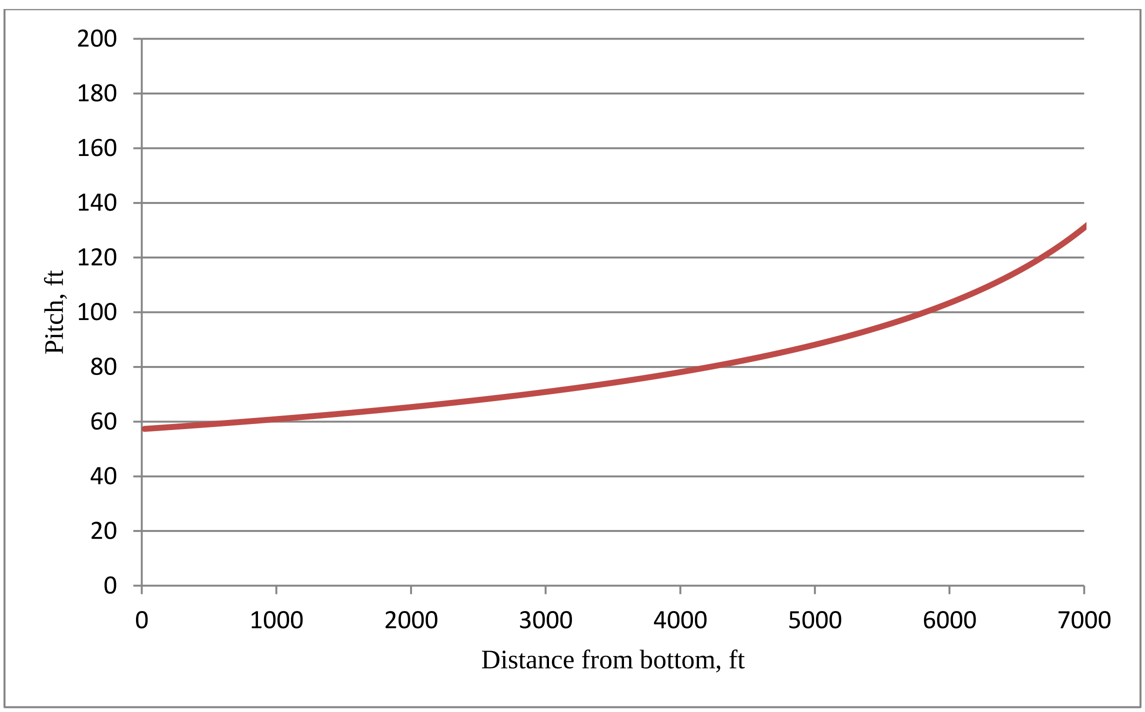

Figure 40 Pitch along Tubing in Case 5 (Expanded Plot)

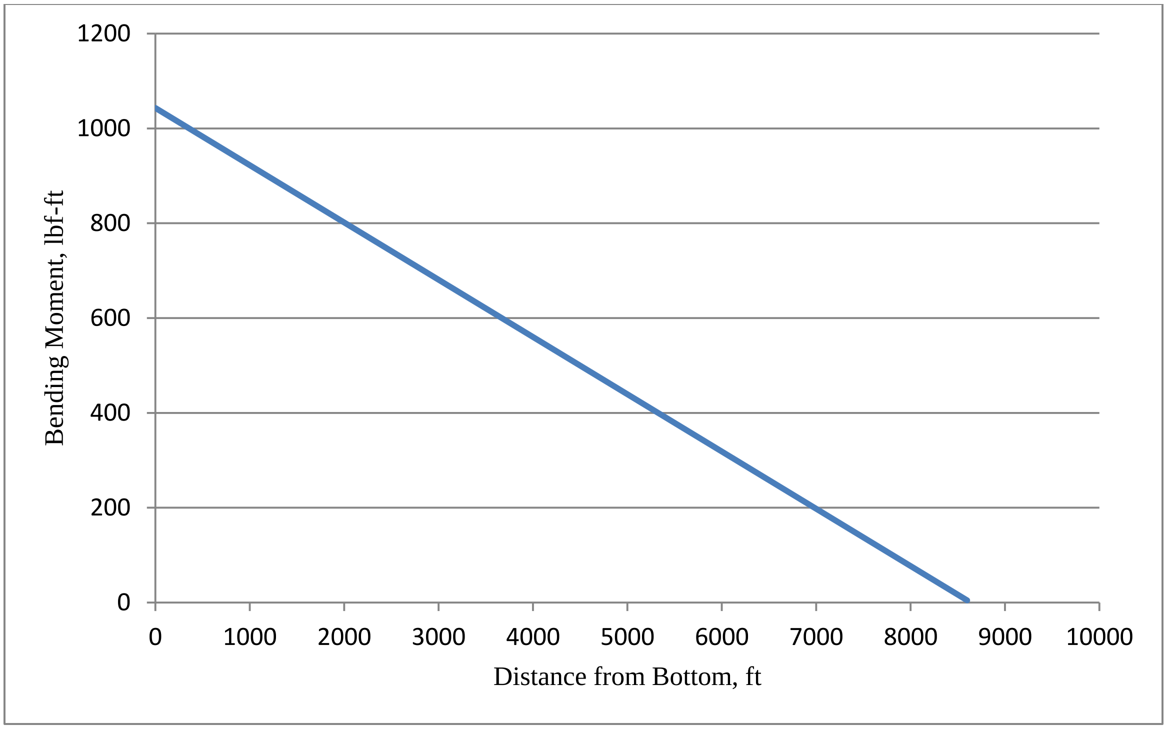

Figure 41 Bending Moment in Tubing in Case 5

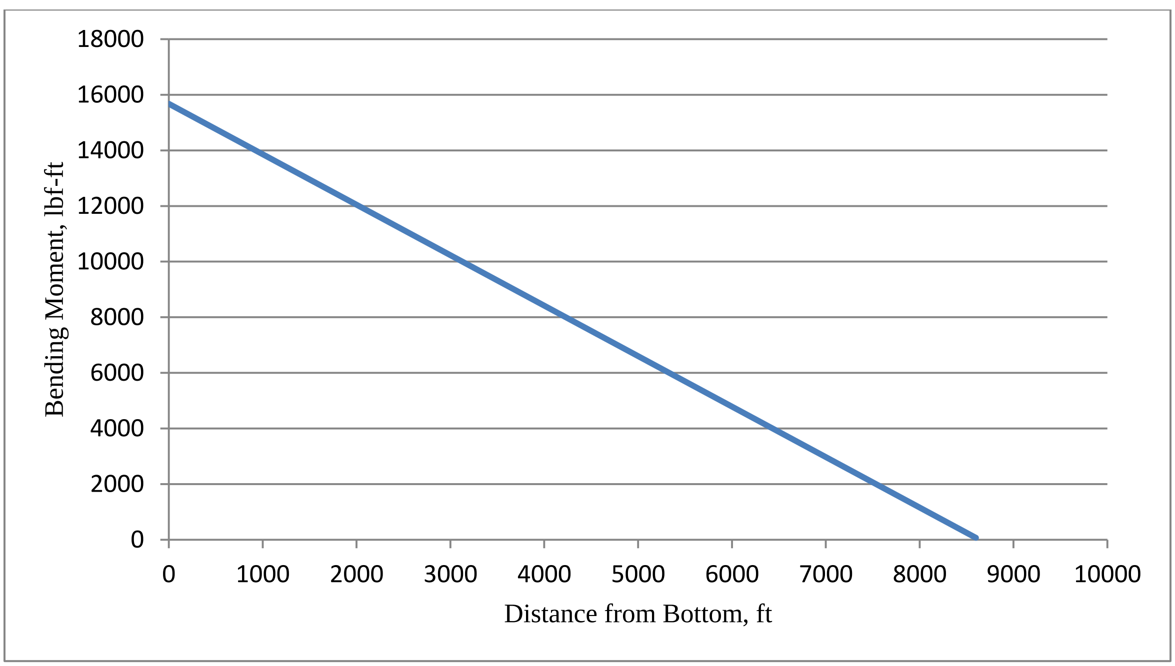

Figure 42 Bending Moment in Casing in Case 5

Based on the bending moment result, the bending stress in casing and tubing can also be accordingly determined, as is shown in Figure 43. The maximum bending stress in casing is 13,127 psi and the maximum bending stress in tubing is 11,182 psi at bottom.

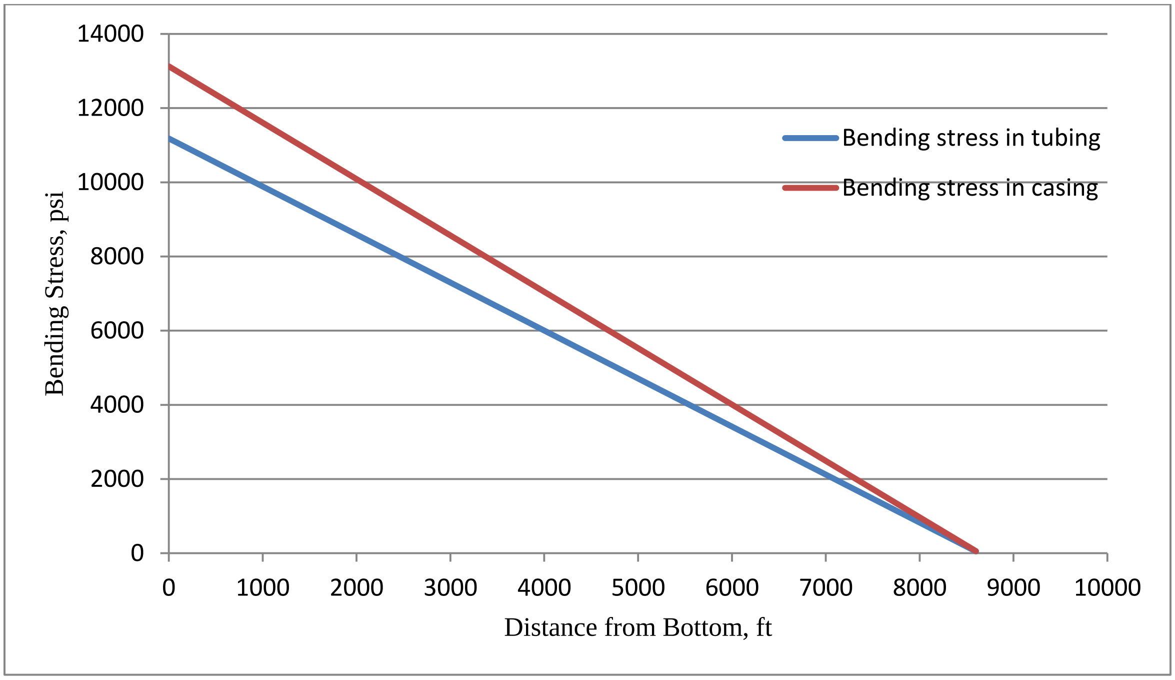

Figure 43 Bending Stress in Casing and Tubing in Case 5

5.3 Case Study Summary

This chapter specifically designed five scenarios based on real practice to explore the mechanism of dual string buckling and investigate on the influence of parameters like buckling force and radial clearance on buckling behavior of dual string system. In the end, we aim to propose useful engineering suggestions based on our case study for reference in practical design or operations.

All the calculation results are summarized in the following Table 7. Since buckling pitch is varying along the tubing, the pitch value at bottom of tubing is selected in the following table. Among all the parameters in Table 7, M_t is the maximum bending moment in tubing, M_c is the maximum bending moment in casing, σ_t is the maximum bending stress in tubing, σ_c is the maximum bending stress in casing and ΔL_b is the length change due to buckling. The length change due to buckling is an important parameter in design, which will be commented in this section

Table 7 Case Study Result Summary

Case No.	Pitch (ft.)	M_t (lbf-ft.)	M_c (lbf-ft.)	σ_t (psi)	σ_c (psi)	ΔL_b (in.)
1	53.4	877	8,680	7,268	9,396	6.86
2	51.3	980	9,706	10,507	8,127	6.62
3	38.1	1,764	17,466	18,907	14,625	22.60
4	20.0	4,454	NA	47,742	NA	46.09
5	57.4	1,043	15,677	11,182	13,126	21.94

Case 1 is designed as the base scenario for comparison, where the buckling force is only applied on inner tubing. Case 2 keeps all the conditions the same except that apply buckling force on casing and take the effect of weight into consideration. The final dual string buckling configuration in Case 2 show that there is only a small decrease in buckling pitch. Besides, there is a slight increase in maximum bending moment and maximum bending stress in Case 2. So the increase of buckling force in casing doesn't significantly impact the buckling configuration of dual string system.

It deserves attention that the change of length due to buckling in Case 2 is less than case 1. The reason is because the influence of casing weight is considered in Case 2. With the distance from bottom increasing, the neutral point in casing is first reached at 4,080 ft. In the region from 4,080 ft to 7,500 ft, the axial force in casing is in tension, which tends to suppress the buckling of inner tubing. It is obviously noticed in Figure 44 that the buckling pitch in Case 2 increases rapidly above 4,080 ft. As the dual string system behaves more like a straight line shape, the change of length decreases. Besides, the length of compressive section in Case 2 is less than that of case 1. This can also reduce the change of length due to buckling.

It is also noticed that the Eq. (21) can be used to predict the transition region of dual string system from sinusoidal buckling to straight shape. Thus the neutral point of a dual string system can be defined as the point in dual string where the expression is satisfied as

$$F_1 {r_1}^2 + F_2 {r_2}^2 = 0, \tag{44}$$

where F_1 is the buckling force in tubing, F_2 is the buckling force in casing, r_1 is the radial clearance of tubing and r_2 is the radial clearance of casing. This can be further verified by Figure 44.

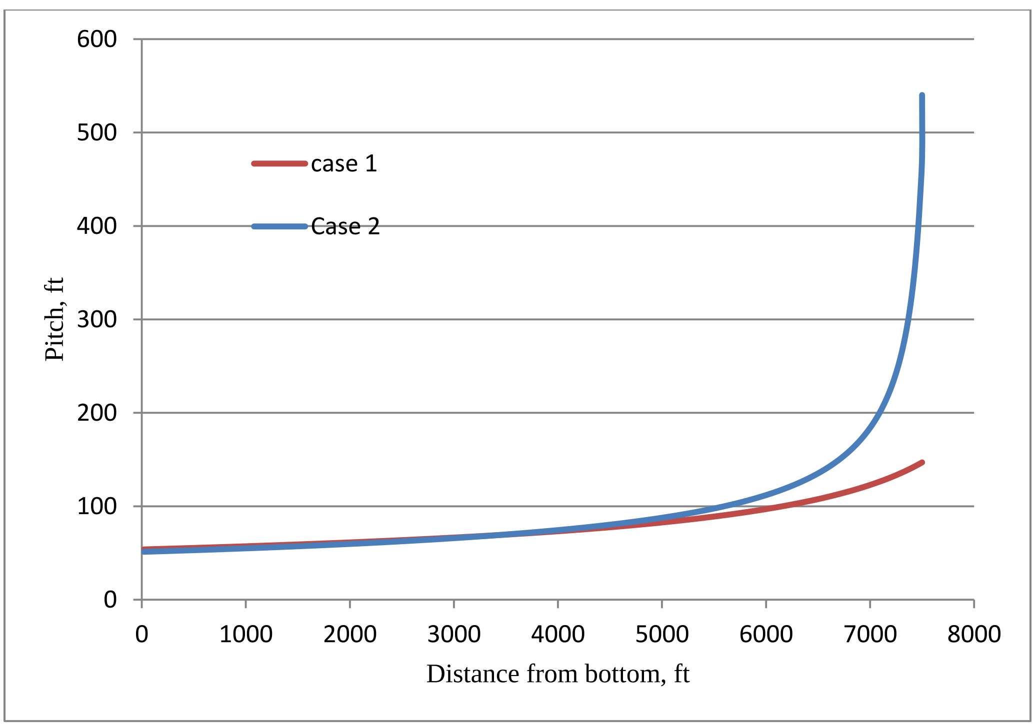

Figure 44 Buckling Pitch along Tubing in Case 1 and Case 2

When Case 3 is compared with Case 1, Case 3 keeps all the conditions the same except that the buckling force at bottom of tubing is increased twice. It is observed that the increase of buckling force on tubing significantly reduces the buckling pitch at bottom and increases the maximum bending moment and stress in tubing and casing. Since the buckling pitch is much smaller and deformation due to buckling is more severe, the change of length due to buckling is significantly increased. So the change of buckling force in tubing has more influence final buckling behavior than change of buckling force in casing. The mechanism is that the casing has a much higher stiffness capacity than tubing.

When Case 4 is compared with Case 1, Case 4 describes a scenario where a single string buckles inside a casing at the same condition as Case 1 except that the casing is assumed to be rigid in Case 1. The buckling shape of a long pipe in vertical wells can typically be assumed to be a helically buckling configuration. It is observed that the buckling deformation of a single string is much more severe than that of a dual string system. The much more bending moment, bending stress and change of length due to buckling can develop for single string buckling under the same buckling load. This is because the buckling loads on dual string system turn out to be shared by casing and inner string. Casing usually accounts for a large portion of buckling loads due to much higher stiffness capacity. So the prerequisite condition should be carefully checked before application of dual string model in design. Application of this dual string model in tubular design may properly save cost but could potentially cause tubular failure by overestimating the contribution of outer casing in buckling.

Besides, it should be noticed that the change of length due to buckling in Case 4 is much larger than previous cases. Another reason is that the buckling of a single long pipe in Case 4 is assumed to be a helical configuration, which is a spatial shape, while the buckling of dual string in previous three cases is in sinusoidal configuration, which is a plane shape, the change of length due to buckling is larger for spatial configuration even at the same pitch. So if the sinusoidal buckling of dual string system is verified to be the real case, the change of length due to buckling could be much smaller.

When Case 5 is compared with Case 1, Case 5 keeps all the conditions the same except that the dual string system is buckled in a larger wellbore, where the radial clearance for tubing and casing is even larger. As the radial clearance increases, the dual string system buckles into a helical shape in space. So in real practice, a large radial clearance could possibly change the buckling configuration from sinusoidal buckling to helical buckling. For example, if there is a large cavity on the wellbore at certain soft formation, the buckling shape of tubular changes from sinusoidal buckling to helical buckling, which will further increase the contact force, this increased contact could possibly further increase the cavity on the wellbore.

Although the buckling pitch at bottom in case 5 is a little larger than the pitch in Case 1. The maximum bending moment, maximum bending stress and change of length due to buckling of dual string system in Case 5 is the larger than that in Case 1 under the same buckling load. So the radial clearance of dual string system has a very significant influence on final buckling configuration.

5.4 Model Comparison with Previous Solutions

In this section we aim to exam the calculation accuracy of different prediction model for dual string buckling by applying .Christman's (1976) model and Mitchell's (2012) model on the same Lubinski's example.

Christman's model takes dual string system as a composite pipe with summed properties of individual pipe. He also assumes that the buckling load on cross section of composite pipe is the sum of buckling load on individual pipes. In this way the buckling problem of dual string system is simplified into a single string buckling problem. Then the previous model of force pitch relationship for single string can be applied on this situation. Christman's model can be expressed as

$$p = \pi\sqrt{\frac{8E\bar{I}}{\bar{F}}}, \tag{45}$$

where $\bar{I}$ is the sum of individual moment inertia, and $\bar{F}$ is the sum of individual buckling force.

Mitchell (2012) studied the helical buckling configuration by applying the virtual work principle. The final expression derived is given as Eq. (19). This expression is only for the situation where tubing buckles into casing while casing is in contact with wellbore.

The prerequisite condition for above helically buckling of dual string to occur is given by Eq. (25). Otherwise, the dual string system buckles into the second scenario. Tubing is assumed to buckle into contact with the casing, but there is no contact between the casing and wellbore. The space configuration is as shown in Figure 50. The buckling pitch can be given by

$$\beta^2 = \frac{F_1(v+r_1)^2+F_2v^2}{2E(I_1(v+r_1)^2+I_2{r_2}^2)}, \tag{46}$$

where v is the radial displacement of casing and v can be solved by the following equations as

$$v^3 + av^2 + bv + c = 0, \tag{47}$$

where

$$a = 3\varepsilon r, \tag{48}$$

$$b = [4\varepsilon - 1 + \varphi(2\varepsilon - 1)r^2], \tag{49}$$

$$c = \varepsilon(1 + \varphi)r^3, \tag{50}$$

$$\varepsilon = \frac{I_t}{I_t + I_c}, \text{ and} \tag{51}$$

$$\varphi = \frac{F_1}{F_1 + F_2}. \tag{52}$$

5.4.1 Comparison between Christman's Model and New Model

As previously stated in chapter 2, the major assumption for Christman's model is that radial clearance between dual strings is small enough so radial displacement with dual strings can be neglected. This section we will evaluate the influence of radial displacement with dual strings on the final buckling behavior of dual string system. Three cases are specifically designed for this purpose. The following Table 8 shows the comparison between these three cases. All the other conditions including loads and casing parameters are same with Case 1except that larger inner tubing is used for Case 7and Case 8. Furthermore, different solution models are used to compare the prediction difference. The geometrical information for 4-1/2" casing is listed in Table 15 in APPENDIX D.

Table 8 Case Study for Influence of Radial Displacement

Case No.	Inner Tubing Diameter (in.)	Model Used for Solution
1	2-7/8”	New Model
6	2-7/8”	Christman’s Model
7	4-1/2”	New Model
8	4-1/2”	Christman’s Model

Christman’s model derived expressions for pitch, bending stress and length change due to buckling, which will be used for comparison in this research. The pitch along tubing relationship is plotted in Figure 45 and expanded plot is Figure 46. For the same scenario, Christman’s model predicts a helical buckling configuration with a much higher pitch. The maximum bending stress in tubing and casing is shown in Figure 47. The maximum stress occurs at bottom with 691 psi in tubing and 1,684 psi in casing.

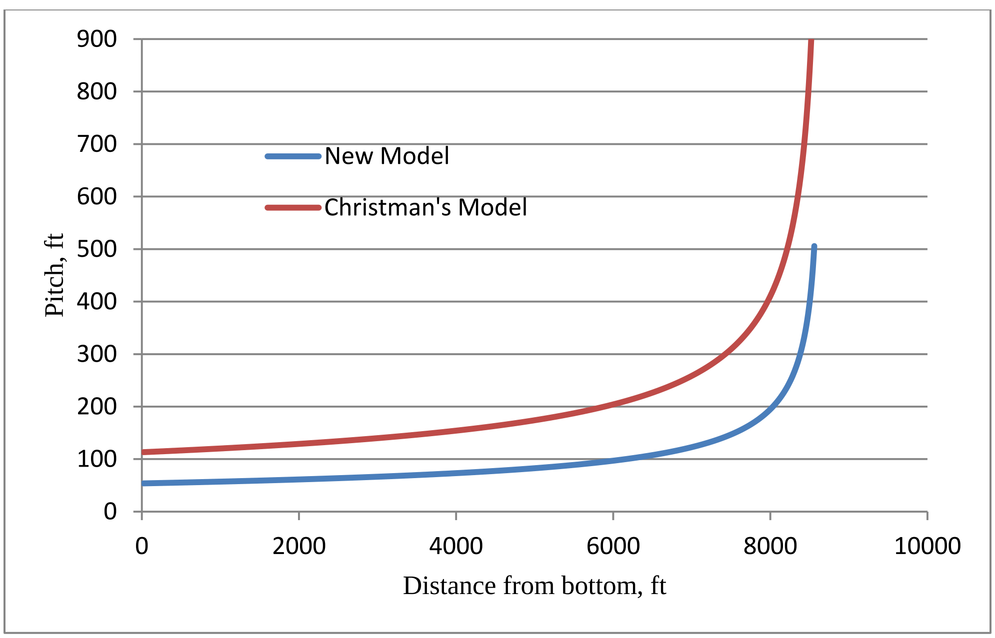

Figure 45 Comparison of Pitch between Case 1 and Case 6

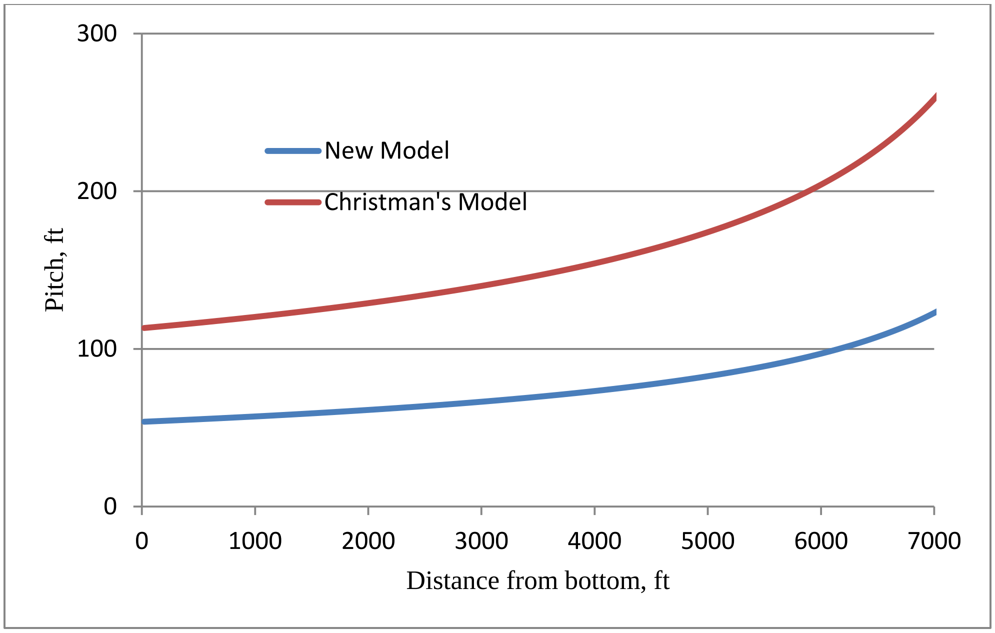

Figure 46 Pitch Comparison between Case 1 and Case 6 (Expanded Plot)

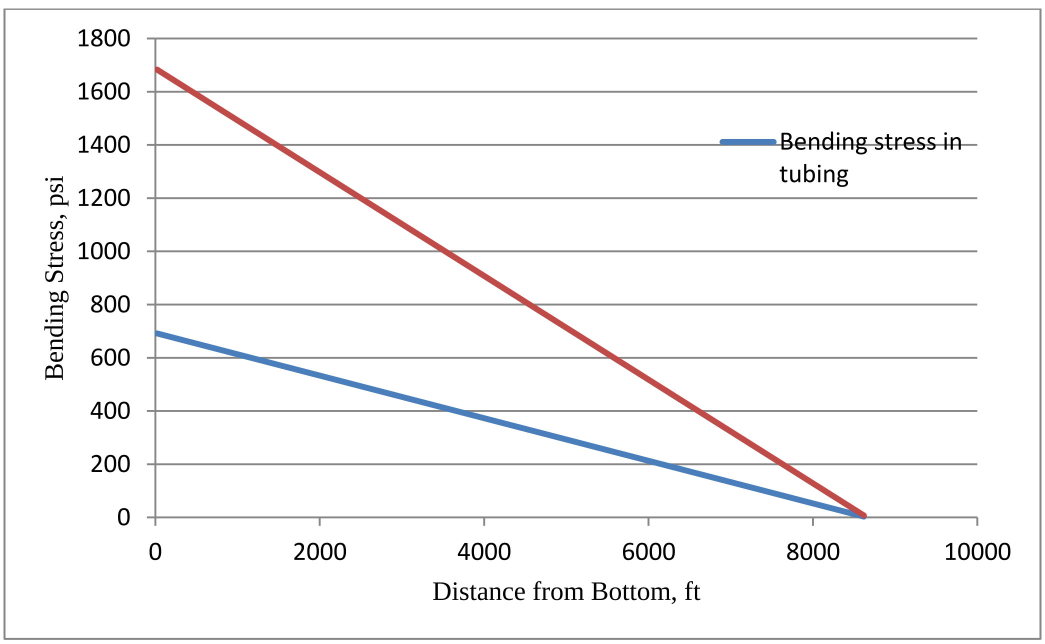

Figure 47 Bending Stress in Tubing and Casing in Case 6

If all the conditions keep the same except that the 2-7/8” tubing is replace by a 4-1/2” tubing, application of new model and Christman’s model to this new scenario corresponds to the result of Case 7 and Case 8. Comparison of pitch along string in Case

7 and Case 8 is shown in Figure 48 and the expanded plot is show in Figure 49. The final results in these four cases are summarized and compared in Table 9, where the pitch refers to the pitch at bottom.

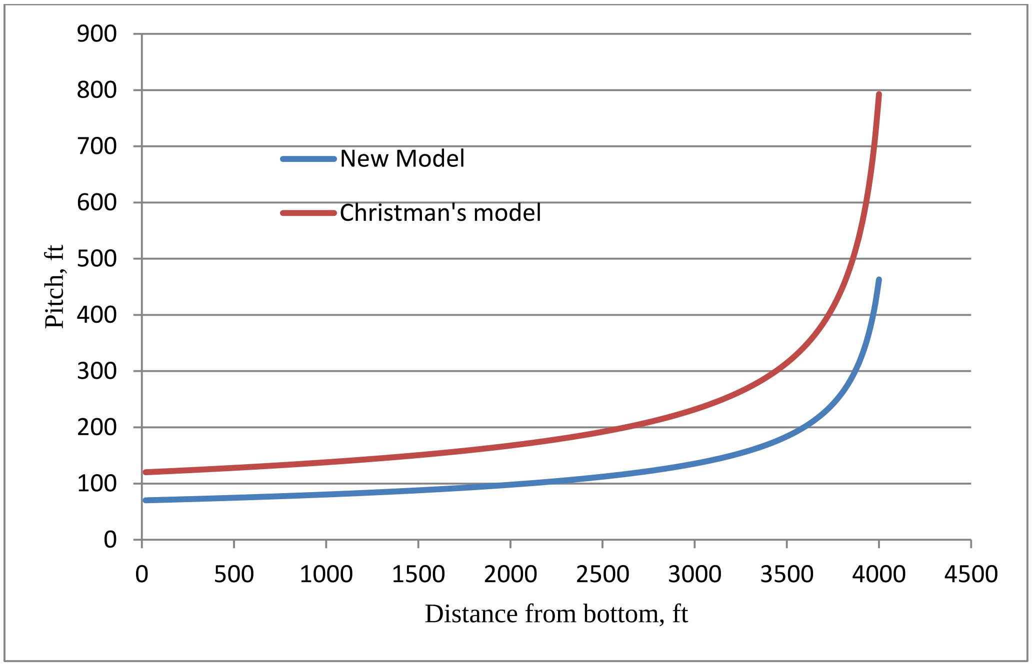

Figure 48 Comparison of Pitch in Case 7 and Case 8

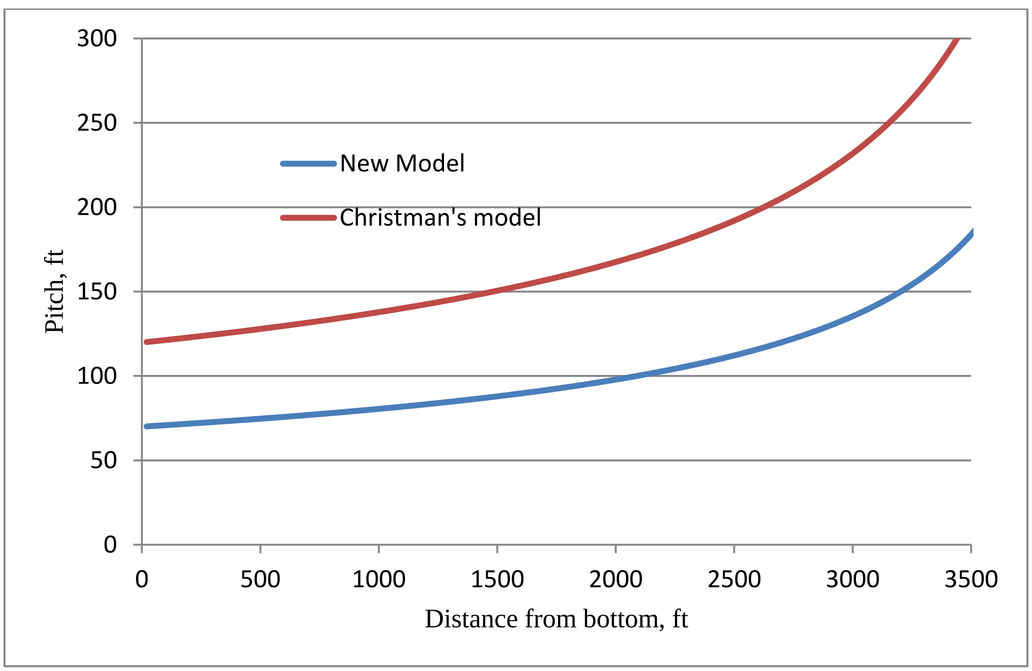

Figure 49 Pitch Comparison in Case 7 and Case 8 (Expanded Plot)

Table 9 Summary of Case Study Result

Case No.	Pitch (ft.)	σ_t (psi)	σ_c (psi)	ΔL_b (in.)	Buckling Configuration
1	53.4	7,268	9,396	6.86	Sinusoidal buckling
6	113.3	692	1,683	0.31	Helical buckling
7	70.2	5,815	4,386	1.64	Helical buckling
8	120.1	962	1,496	0.13	Helical buckling

In Case 1 and Case 6, the radial clearance between casing and tubing is very large. The Christman's model gives quite different prediction of buckling configuration with new model, because the prerequisite of small radial clearance for Christman's model is not satisfied in this situation. The assumed radial displacement of inner tubing is much less than real case, thus largely underestimates the deformation of tubing due to buckling. So the bending stress and length change due to buckling in Case 6 are much less than the result from Case 1. Then the inner 2-7/8" tubing is replaced by a 4-1/2" tubing, so the radial clearance is largely reduced in Case 7 and Case 8. For these two cases, both Christman's model and new model predict a helical buckling configuration with pitch of 120.1ft and 70.2 ft, respectively. As the radial clearance between dual strings decrease, the prediction result from Christman's model is more close to result from new model. However, the Christman's model still underestimates the bending stress and length change due to buckling by a large scale.

5.4.2 Comparison between Mitchell's Model

The major problem with Mitchell's model is that it assumes an unrealistic configuration for buckling of dual string system, which is shown in Figure 50. As is previously mentioned, the Eq. (46) (47) gives the solution for buckling of dual string system without wellbore contact. It is observed that that solution is independent of wellbore radius. This section will specifically design Case 9 to illustrate the influence of radial clearance with respect to wellbore. For Case 9, all the conditions are kept the same except that the wellbore radius is increased from 8 ½" to 9 ½". The calculation result is shown in Table 10. The subscript (a) indicates that it is the result from Mitchell's model, while subscript (b) indicates that it is result from newly derived model. Clearly the result shows that as wellbore radius increases from 8-1/2" to 10", Mitchell's model predicts a solution with discontinuity. However, the result from newly derived model shows that the bending stress and length change due to buckling increase gradually as wellbore radius increases, which is more close to real situation.

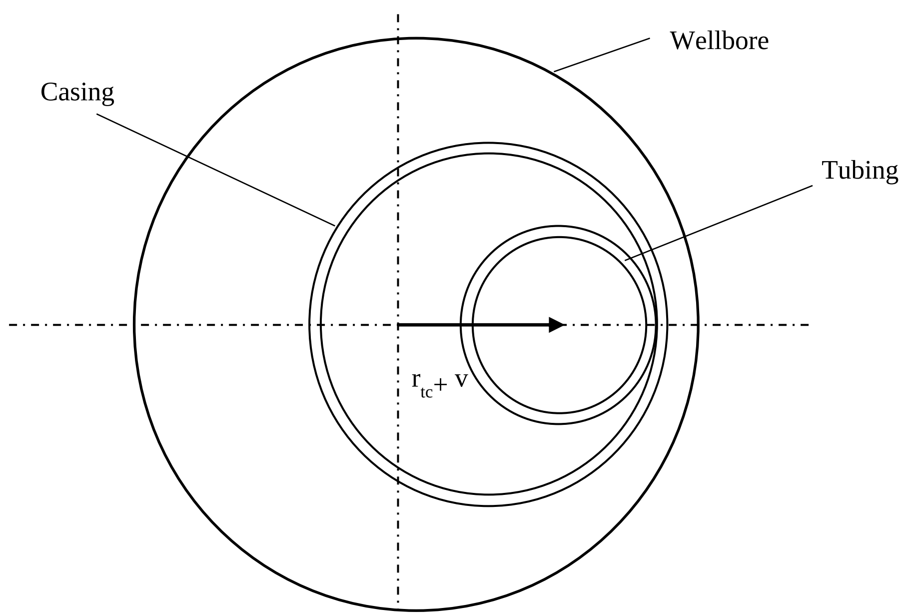

Figure 50 Helical Buckling without Wellbore Contact, Mitchell 2012

Table 10 Case Study with Mitchell's Model and New Model

Case No.	Wellbore Radius (in.)	Pitch (ft.)	σ_t (psi)	σ_c (psi)	ΔL_b (in.)
1(a)	8-1/2	20.4	47,620	3997	NA
9(a)	9-1/2	20.4	47,620	3997	NA
1(b)	8-1/2	53.4	7,268	9,396	6.86
9(b)	9-1/2	56.6	10,451	11,117	9.09
5	10	57.4	11,182	13,126	21.94

In a brief summary, clearly Christman's model is an unrealistic one because it assumes the axial load is shared by two separate pipes. So it overestimates the stiffness capacity of dual string systems and may give an unsafe reference for design. That is the reason why the buckling pitch predicted tends to be larger than other models. In reality the concentric pipes interact with each other by contact force. Mitchell's model correctly analyzes this interaction mechanism and gives correct prediction for fully helical buckling configuration with wellbore contact, which can be verified by this new model. However, the scenario where helical buckling forms without wellbore contact is far from reality, because helical buckling usually evolves from sinusoidal buckling with wellbore constrain. It is very difficult to for dual string system to form helical buckling without wellbore contact. The pitch predicted from new model gives a more reasonable pitch than Mitchell's model in this case.

CHAPTER 6
CONCLUSION

6.1 Summary

- An analytical mathematical model has been brought up to describe the post buckling behavior of dual string systems based on minimum energy theory. Effect of contact interaction has been considered in this model and evaluated in analysis.
- Calculation procedure has been designed to apply this new model in application. Lubinski's (1950) exact solution for sinusoidal buckling of string has been used to verify the newly derived model.
- Case study has been conducted to further explore and better understand the buckling mechanism of dual string system. The influence of different parameters on final buckling configuration has been investigated.
- Case study has been designed for comparison between previous models with newly derived model. Results show that new model gives a more reliable prediction in many scenarios.

6.2 Conclusion and Engineering Suggestions

- Although this model is derived based on two pre-assumed space configuration of dual string system, it is a good attempt to give insight into mechanism of dual string buckling.
- Compared with the change of buckling force in outer casing, the change of buckling force in inner tubing has much larger impact on final buckling configuration of dual string.

- Tension in outer casing tends to suppress the buckling deformation of inner tubing.
- The neutral point position and near neutral point region of dual string system can be determined using Eq. (44).
- In dual string system, outer string tends to stand more moments due to higher stiffness compared with inner string.
- Application of this dual string model in tubular design may properly save cost but could potentially cause tubular failure by overestimating the contribution of outer casing in buckling. the prerequisite condition should be carefully checked before application of dual string model in design.
- An increase in the radial clearance of dual string system can significantly change the final buckling configuration
- By model comparison, it is found that Christman's model tends to overestimate the stiffness of dual string system because of neglecting the radial clearance between dual strings.
- Mitchell's model assumes an unrealistic scenario where dual string system is self-balanced and independent of wellbore. The solution in this scenario can't properly explain the influence of clearance with respect to wellbore on dual string buckling system.
- This newly derived model properly solves the problems in Christman and Mitchell's model and is able to give a more reliable prediction for practical use.

REFERENCES

Azar, J. J., & Samuel, G. R. (2007). Drilling Engineering. PennWell Books.

Cheatham Jr, J. B. (1984). "Helical Postbuckling Configuration of a Weightless Column under the Action of an Axial Load." *Society of Petroleum Engineers Journal*, 24(04), 467-472.

Cheatham, J. B., & Chen, Y. C. (1988, January). "New Design Considerations for Tubing and Casing Buckling in Inclined Wells." In *Offshore Technology Conference*. Offshore Technology Conference.

Chen, Y. C., Lin, Y. H., & Cheatham, J. B. (1990). "Tubing and Casing Buckling in Horizontal Wells" (includes associated papers 21257 and 21308). *Journal of Petroleum Technology*, *42*(02), 140-191.

Chen, Y. C., & Cheatham, J. B. (1990). "Wall Contact Forces on Helically Buckled Tubulars in Inclined Wells." *Journal of Energy Resources Technology*, *112*(2), 142-144.

Christman, S. A. (1976, January). "Casing Stresses Caused by Buckling of Concentric Pipes." In SPE Annual Fall Technical Conference and Exhibition. Society of Petroleum Engineers.

Crandall, S.H. (1959). An Introduction to the Mechanics of Solids, 414-415. New York: McGraw-Hill Book Company.

Cunha, J. C. (2003, January). "Buckling of Tubulars inside Wellbores: a Review on Recent Theoretical and Experimental Works." In SPE Production and Operations Symposium. Society of Petroleum Engineers.

Dawson, R. (1984). “Drill Pipe Buckling in Inclined Holes.” *Journal of Petroleum Technology*, 36(10), 1-734.

Hammerlindl, D. J. (1977). “Movement, Forces, and Stresses Associated with Combination Tubing Strings Sealed in Packers.” *Journal of Petroleum Technology*, *29*(02), 195-208.

He, X., & Kyllingstad, A. (1995). “Helical Buckling and Lock-up Conditions for Coiled Tubing in Curved Wells.” *SPE Drilling & Completion*, *10*(01), 10-15.

Kuru, E., Martinez, A., Miska, S., & Qiu, W. (2000). “The Buckling Behavior of Pipes and Its Influence on the Axial Force Transfer in Directional Wells.*” Journal of energy resources technology*, 122(3), 129-135.

Kwon, Y. W. (1988). “Analysis of Helical Buckling.” *SPE drilling engineering*, *3*(02), 211-216.

Lubinski, A. (1950, January). “A Study of the Buckling of Rotary Drilling Strings.” In Drilling and Production Practice. American Petroleum Institute.

Lubinski, A., & Althouse, W. S. (1962). “Helical Buckling of Tubing Sealed in Packers.” *Journal of Petroleum Technology*, 14(06), 655-670.

McCann, R. C., & Suryanarayana, P. V. R. (1994, January). “Experimental Study of Curvature and Frictional Effects on Buckling.” In Offshore technology conference. Offshore Technology Conference.

Mitchell, R. F. (1982). “Buckling Behavior of Well Tubing: The Packer Effect.” *Society of Petroleum Engineers Journal*, 22(05), 616-624.

Mitchell, R. F. (1986). “Simple Frictional Analysis of Helical Buckling of Tubing.” SPE Drilling Engineering, 1(06), 457-465.

Mitchell, R. F. (1988). “New Concepts for Helical Buckling." SPE Drilling Engineering, 3(03), 303-310.

Mitchell, R. F. (1996). “Comprehensive Analysis of Buckling with Friction.” *SPE Drilling & Completion*, *11*(03), 178-184.

Mitchell, R. F. (1997). “Effects of Well Deviation on Helical Buckling.” *SPE Drilling & Completion*, 12(01), 63-70.

Mitchell, R. F. (1999). “Buckling Analysis in Deviated Wells: A Practical Method.” *SPE drilling & completion*, 14(01), 11-20.

Mitchell, R. F. (2002, January). “New Buckling Solutions for Extended Reach Wells.” In IADC/SPE Drilling Conference. Society of Petroleum Engineers.

Mitchell, R. (2012). “Buckling of Tubing Inside Casing.” *SPE Drilling & Completion*, 27(04), 486-492.

Miska, S., & Cunha, J. C. (1995, January). “Analysis of Helical Buckling of Tubulars Subjected to Axial and Torsional Loading in Inclined Wellbores.” In *SPE Production Operations Symposium*. Society of Petroleum Engineers.

Miska, S., Qiu, W., Volk, L., & Cunha, J. C. (1996, January). “Analysis of Axial Force Along Coiled Tubing in Inclined/Horizontal Wellbores.” InInternational conference on horizontal well technology. Society of Petroleum Engineers.

O'Brien, T. B. (1984). “Why Some Casing Failures Happen.” *World Oil;(United States)*, *199*(1).

Paslay, P. R., & Bogy, D. B. (1964). “The Stability of a Circular Rod Laterally Constrained to Be in Contact with an Inclined Circular Cylinder.” *Journal of Applied Mechanics*, 31(4), 605-610.

Paslay, P. R. (1994, January). "Stress Analysis of Drillstrings." In *University of Tulsa Centennial Petroleum Engineering Symposium*. Society of Petroleum Engineers.

Samuel, R. and Gao, D. 2014. Horizontal Drilling Engineering – Theory and Applications. Houston: SigmaQuadrant Publishers.

Samuel, R. and Gao, D. 2015. 501 Solved Problems and Calculations for Drilling Operations. Houston: SigmaQuadrant Publishers.

Wang, C. Y. (1986). "A Critical Review of the Heavy Elastica." *International Journal of Mechanical Sciences*, 28(8), 549-559.

Wu, J., & Juvkam-Wold, H. C. (1993, January). "Study of Helical Buckling of Pipes in Horizontal Wells." In *SPE Production Operations Symposium*. Society of Petroleum Engineers.

Wu, J., & Juvkam-Wold, H. C. (1995). "Buckling and lockup of tubulars in inclined wellbores*." Journal of energy resources technology*, 117(3), 208-213.

APPENDIX A

The force pitch relationship for helically buckling of dual string system will be derived in this section, based on a long, weightless string of pipe or rods subject to compression. Based on the geometry of helically buckled pipe, as is shown in Figure 51, the following equation is derived as

$$\sin\theta = \frac{p}{\sqrt{p^2+4\pi^2 r^2}} \qquad \text{and} \tag{A- 1}$$

$$F_P = F_a/\sin\vartheta, \tag{A- 2}$$

where F_P is force load along the pipe axis, F_a is force load along axis of helix.

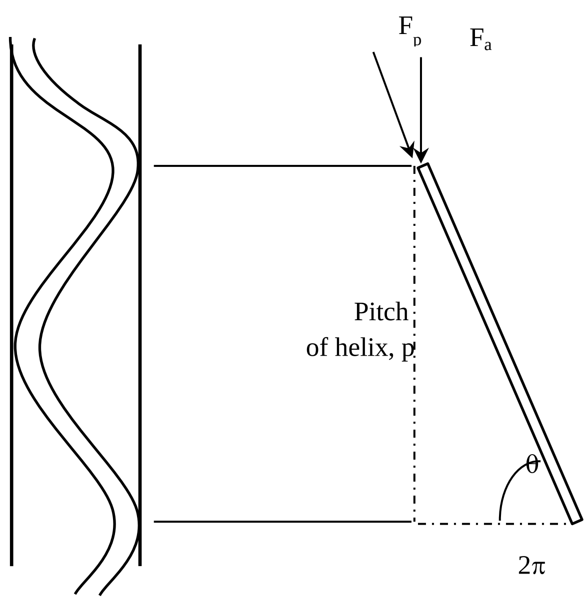

Figure 51 Geometry of Helically buckled pipe

In this study, we used the definition rule for simplification that subscript 1 represents for tubing, while subscript 2 represents for casing. The total potential energy includes contributions from:

i. Compressive strain energy of dual string is expressed by

$$U_c = \frac{F_{P1}{}^2 L_1}{2A_1 E} + \frac{F_{P2}{}^2 L_2}{2A_2 E} \quad \text{and} \tag{A- 3}$$

$$\mathrm{U_c} = \frac{\mathrm{F_{a1}}^2 \mathrm{L_1}}{2\mathrm{A_1 E}}\left(\frac{\mathrm{p^2+4\pi r_1{}^2}}{\mathrm{p^2}}\right) + \frac{\mathrm{F_{a2}}^2 \mathrm{L_2}}{2\mathrm{A_2 E}}\left(\frac{\mathrm{p^2+4\pi r_1{}^2}}{\mathrm{p^2}}\right), \tag{A- 4}$$

where A is cross section area, so A_1 is cross section area of tubing, A_2 is cross section area of casing; L is length of pipe subject to compression, E is Young's modulus, p is pitch of helix; r is radial clearance, so r_1 is radial displacement of tubing, r_2 is radial displacement of casing, r_1 and r_2 can be expressed as

$$r_1 = r_{tc} + r_{cc} \quad \text{and} \tag{A- 5}$$

$$r_2 = r_{cc}. \tag{A- 6}$$

ii. Bending strain energy of a helix can be expressed by

$$U_b = \frac{L_1 E I_1 C_1{}^2}{2} + \frac{L_2 E I_2 C_2{}^2}{2} \quad \text{and} \tag{A- 7}$$

$$C = \frac{4\pi^2 r}{p^2+4\pi^2 r^2}. \tag{A- 8}$$

where C is curvature of helix. The curvature expression is discussed in Lubinski's (1962) paper.

Substitute (A- 8) into (A- 7) to get

$$\mathrm{U_b} = \frac{8\pi^4 \mathrm{r_1}^2 \mathrm{EI_1 L_1}}{(\mathrm{p^2+4\pi^2 r_1{}^2})^2} + \frac{8\pi^4 \mathrm{r_2}^2 \mathrm{EI_2 L_2}}{(\mathrm{p^2+4\pi^2 r_2{}^2})^2}. \tag{A- 9}$$

iii. Potential energy due to external forces is given by

$$\mathrm{U_f = L_{h1}(F_{a1} + P_{i1}A_{i1} - P_{o1}A_{o1}) + L_{h2}(F_{a2} + P_{i2}A_{i2} - P_{o2}A_{o2}).} \quad \text{(A- 10)}$$

The above expression is thoroughly discussed in Lubinski's (1962) paper. We directly take the result expression.

Length of buckled pipe system along the helix axis is expressed by

$$L_h = \frac{p}{\sqrt{p^2+4\pi^2r^2}} L(1 - \frac{F_a}{EAsin\theta}). \quad \text{(A- 11)}$$

The total potential energy of single string can be expressed by

$$U = \mathrm{U_c + U_b + U_f}. \quad \text{(A- 12)}$$

The minimum energy method requires that the first variation with respect to p is zero when the buckling configuration reaches equilibrium. Above equations can be combined and substituted into the following expression

$$\frac{\partial \mathrm{U}}{\partial \mathrm{p}} = 0. \quad \text{(A- 13)}$$

In real practice, p is usually several magnitudes above radial clearance, r. Consider $p \gg 2\pi r$, the following expression exists as

$$p^2 + 4\pi^2 r^2 \approx p^2. \quad \text{(A- 14)}$$

By rearrangement, the formula for p is expressed as

$$\mathrm{p} = \sqrt{\frac{8\pi^2 \mathrm{E}(\mathrm{I_1 r_1{}^2 L_1 + I_2 r_2{}^2 L_2})}{\mathrm{r_1{}^2 L_1}\left(\mathrm{F_1} - \frac{\mathrm{F_{a1}}^2}{\mathrm{EA_1}}\right) + \mathrm{r_2{}^2 L_2}(\mathrm{F_2} - \frac{\mathrm{F_{a2}}^2}{\mathrm{EA_2}})}}. \quad \text{(A- 15)}$$

For stress less than 100,000 psi, $\frac{F_a}{AE} < 0.0034$; at the same time, casing length is equal to tubing length approximately, $L_1 \approx L_2$. So the final pitch force relationship is expressed as

$$p = \pi \sqrt{\frac{8E(I_1 {r_1}^2 + I_2 {r_2}^2)}{F_1 {r_1}^2 + F_2 {r_2}^2}}. \qquad \text{(A- 16)}$$

For a weightless string without fluid pressure effect, the corresponding pitch, p, will be constant along wellbore. On the other hand, if the string is not weightless, that means the buckling force,F_1 and F_2, and thus the pitch, p, will vary along the string. It is noticed that this model can also predicts variable pitch along wellbore. This was also discussed in Lunbinski's (1962) paper.

APPENDIX B

The force pitch relationship for sinusoidal buckling of dual string system will be derived in this section, based on a long, weightless string of pipe or rods subject to compression.

The buckling shape of casing or tubing can be described by a centerline that connects the center of every cross section of casing or tubing. Since the sinusoidal buckling configuration lies within a two dimensional plane, we build a Cartesian coordinate on the plane where sinusoidal buckling forms, Set the origin at the center of down hole and x,y axis direction as is shown in Figure 52. So the largest lateral displacement of tubulars should be radial clearance with respect wellbore. The lateral displacement expression is the same as Eq.(16) and Eq.(17).

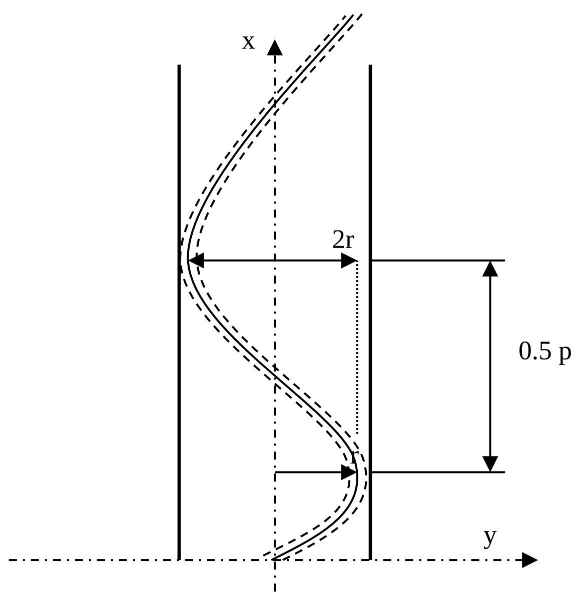

Figure 52 Sinusoidal Buckling Configuration of tubular center line

The shape of tubing and casing centerline can be expressed as

$$y_1 = r_1 \sin(2\pi \frac{x}{p} + \varphi_i) \quad \text{and} \tag{B- 1}$$

$$y_2 = r_2 \sin(2\pi \frac{x}{p} + \varphi_i). \tag{B- 2}$$

where parameters r_1, r_2, p are the same as previously defined, φ_ι represents initial phase and it is zero in this situation if string end is at the down hole center.

In derivation of analytical solution below, we make an approximation that the axial and bending strain energy is evenly distributed along a sinusoidal wave, which will be commented in APPENDIX C. We still follow the definition rule for simplification that subscript 1 represents for tubing, while subscript 2 represents for casing. We will start from deriving potential energy expression for a single string. This expression will be the same for tubing and casing except that the specific value to substitute is different, e.g. different value of r_1 and r_2 are substituted into parameter of radial displacement, r. The total potential energy includes contributions from:

i. Compressive strain energy of one string is expressed by

$$U_c = \frac{{F_a}^2}{2A_s E} \int_0^L \left[1 + \left(\frac{dy}{dx}\right)^2\right] dx. \tag{B- 3}$$

The derivative of y can be expressed as

$$y' = \frac{2\pi r}{p} \cos(\frac{2\pi x}{p}). \tag{B- 4}$$

Substitute (B- 4) into (B- 3) and we get

$$U_c = \frac{{F_a}^2}{2A_s E} \int_0^L \left[1 + \frac{4\pi^2 r^2}{p^2} cos^2(\frac{2\pi x}{p})\right] dx = \frac{4{F_a}^2 L}{AE} [\frac{1}{8} + (\frac{1}{4}\pi^2 + \frac{1}{2}\pi)\frac{r^2}{p^2}], \tag{B- 5}$$

where A is the cross section area, Fa is the actual axial compressive load, L is the length of unstressed pipe, all the other parameters are previously defined. Notice that there is a linear approximation for integral in above equation to make it analytically solvable. This approximation accuracy will be commented in APPENDIX C.

ii. Bending strain energy of one string is expressed by

$$U_b = \frac{LEIC^2}{2} = \frac{EI}{2}\int_0^L [\left(\frac{y''}{1+y'^2}\right)^{\frac{3}{2}}]^2\, dx. \tag{B- 6}$$

The second derivative of y can be expressed as

$$y'' = -\frac{4\pi^2 r}{p^2}\sin(\frac{2\pi x}{p}). \tag{B- 7}$$

Substitute (B- 7) into (B- 6) and we get

$$U_b = \frac{EI}{2}\left(\frac{4\pi^2 r}{p^2}\right)^3 \int_0^L \frac{-\frac{p}{2\pi}sin^2\left(\frac{2\pi x}{p}\right)}{\left[1+\frac{4\pi^2 r^2}{p^2}cos^2\left(\frac{2\pi x}{p}\right)\right]^3} dcos(\frac{2\pi x}{p}). \tag{B- 8}$$

For a common practice, usually we have p>10ft, radial clearance r is at magnitude of 1 inch, so the term $\frac{2\pi^2 r^2}{p^2} \approx 0$. By rearranging above equations, the final form of bending energy is solved and expressed by

$$U_b = \frac{16\pi^3 EIrL}{p^4}, \tag{B- 9}$$

where all the parameters are previously defined. Notice that there is another linear approximation for integral in above equation to make it analytically solvable. This approximation accuracy will also be commented in APPENDIX C.

iii. From Figure 52, Potential energy for external force of one string is expressed by

$$U_f = \frac{FL*\frac{1}{2}p}{\sqrt{\frac{1}{4}p^2+4r^2}} = \frac{FLp}{\sqrt{p^2+16r^2}}. \tag{B- 10}$$

The total potential energy for dual string system is the sum of individual potential energy and can be expressed by

$$\mathrm{U} = \mathrm{U_{c1}} + \mathrm{U_{b1}} + \mathrm{U_{f1}} + \mathrm{U_{c2}} + \mathrm{U_{b2}} + \mathrm{U_{c2}}. \tag{B- 11}$$

The minimum energy method requires that the first variation with respect to p is zero when the buckling configuration reaches equilibrium. Above equations can be combined and substituted into the following expression

$$\frac{\partial \mathrm{U}}{\partial \mathrm{p}} = 0. \qquad \text{(B- 12)}$$

In real practice, p is usually several magnitudes above radial clearance, r. so we have $p \gg 2\pi r$. For stress less than 100,000 psi, $\frac{F_a}{AE} < 0.0034$ holds true. Besides, casing length is equal to tubing length approximately, $L_1 \approx L_2$. By rearrangement, the final pitch force relationship is expressed as

$$p = 2\pi\sqrt{\frac{\pi E(I_1 r_1 + I_2 r_2)}{F_1 {r_1}^2 + F_2 {r_2}^2}}. \qquad \text{(B- 13)}$$

It is noticed that if the dual string system is determined, the only variable in above equation will be buckling force. For a weightless string without fluid pressure effect, the corresponding pitch, p, will be constant along wellbore. On the other hand, this model can also predicts variable pitch along wellbore, if the buckling force F_1 and F_2 are varying from bottom to top, thus the pitch, p, will vary along the string correspondingly.

Let us define the bending moment by the following equation as

$$M = EI\frac{d^2y}{dx^2}. \qquad \text{(B- 14)}$$

where M is the bending moment. By substituting Eq. (B- 7) into Eq.(B- 14), we can get the bending moment expression for each string as

$$M_1 = -\frac{4\pi^2 r_1 E I_1}{p^2}\sin\left(\frac{2\pi x}{p}\right) \text{ and} \qquad \text{(B- 15)}$$

$$M_2 = -\frac{4\pi^2 r_2 E I_2}{p^2}\sin\left(\frac{2\pi x}{p}\right). \qquad \text{(B- 16)}$$

The length L of a curve between two points of abscissas equal to x_1 and x_2 can be expressed by

$$L = \int_{x_1}^{x_2} \sqrt{1 + (\frac{dy}{dx})^2} dx. \qquad \text{(B- 17)}$$

In the drilling operations, y, which corresponds to the radial clearance, is very small compared with drill string length x. Therefore, after expanding the square root term into series, all the terms except for the first two can be neglected. Thus we obtain the expression as

$$L = (x_2 - x_1) + \frac{1}{2}\int_{x_1}^{x_2} (\frac{dy}{dx})^2 dx. \qquad \text{(B- 18)}$$

Since the (x_2-x_1) term is the projection length of the drill string on the axis of the hole, the length change due to buckling is equal to

$$\Delta L_b = \frac{1}{2}\int_{x_1}^{x_2} (\frac{dy}{dx})^2 dx. \qquad \text{(B- 19)}$$

where ΔL_b is the length change due to buckling. By substituting Eq. (B- 4) into Eq. (B-19) and setting the [x_1, x_2] interval to [0, l], the final expression is as

$$\Delta L_{b1} = \frac{\pi {r_1}^2}{4p}\left[\sin\left(\frac{4\pi l}{p} + 2\varphi_i\right) - \sin(2\varphi_i)\right] + \frac{\pi^2 {r_1}^2 l}{p^2} \text{ and} \qquad \text{(B- 20)}$$

$$\Delta L_{b2} = \frac{\pi {r_2}^2}{4p}\left[\sin\left(\frac{4\pi l}{p} + 2\varphi_i\right) - \sin(2\varphi_i)\right] + \frac{\pi^2 {r_2}^2 l}{p^2}, \qquad \text{(B- 21)}$$

where φ_i term is the phase when x_1 is equal to zero. During the pitch derivation process ignoring the initial phase φ_i doesn't have much influence on the final expression, because it is removed when linear approximation is applied. However, for length change due to buckling, its influence has to be considered.

APPENDIX C

This section is designed to illustrate the linear approximation we use in model derivation of APPENDIX A and APPENDIX B. After that we will evaluate how much influence it has on the final result.

The Figure 53 shows a simple sine wave in a Cartesian coordinate. The expression of this sine wave function is given by

$$y = \sin(\frac{4\pi x}{p}), \tag{C- 1}$$

where 0.5p is the pitch of sine wave.

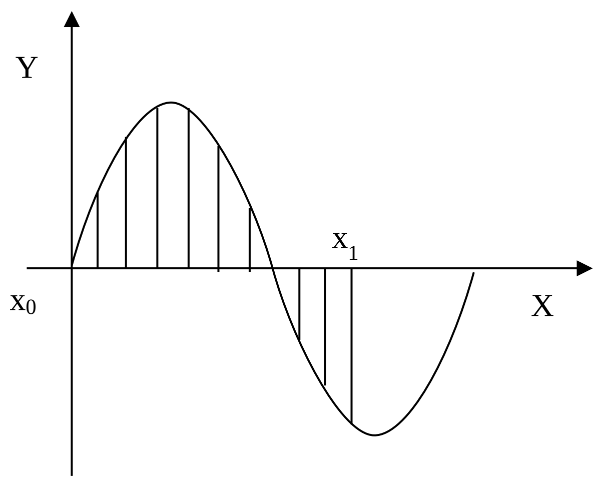

Figure 53 Integration of Sine wave

If we would like to obtain the shadowed area, we can directly integrate the sine wave function over interval [x_0, x_1], the expression is given by

$$Accurate\ integration = \int_{x_0}^{x_1} |\sin(\frac{4\pi x}{p})|dx. \tag{C- 2}$$

However, we would like to derive a simple analytical solution without the trigonometric functions in order to be applied easily in practice. So a linear approximation is used to replace this integral, as is shown in Figure 54. This approximate line is determined in the way that the covered area under this line is the same as the area covered by sine wave on a quarter pitch. The approximation can be expressed by

$$Approximatin = \frac{x_1 - x_0}{\frac{1}{8}p} \int_0^{\frac{p}{8}} \sin(\frac{4\pi x}{p}) dx. \quad \text{(C- 3)}$$

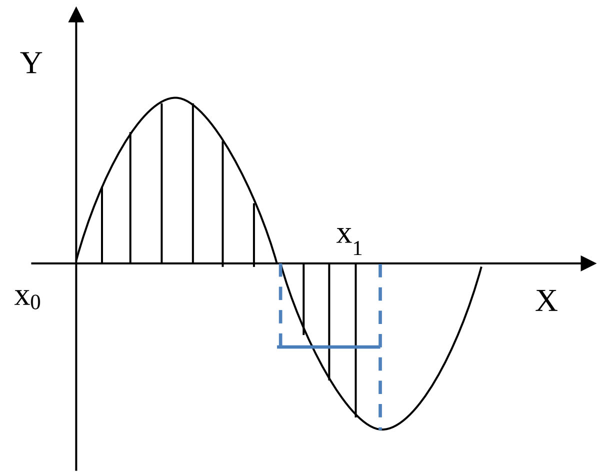

Figure 54 Linear Integration of Sine wave

Then the accuracy of approximation is evaluated. We will obtain the shaded area using approximation method and accurate integration method on interval [x_0, x_1] respectively. Set x_0 to zero and make x_1 increase from 0 to p. Assume p equals to 1 and Figure 55 is plotted to show the integration result with two methods as x coordinate increases. It is noticed that the accurate integration is varying around the approximation value. Then we use approximation value to divide accurate integration value as y axis. In this way, both axis are independent of pitch value. As is shown in Figure 56, when coordinate x is larger than 0.2 times pitch, the error is already within 10%. As x coordinate keeps increasing, the error by using linear approximation drops rapidly. Since the accurate value keeps varying above and below the approximation, this undulation helps offset some error.

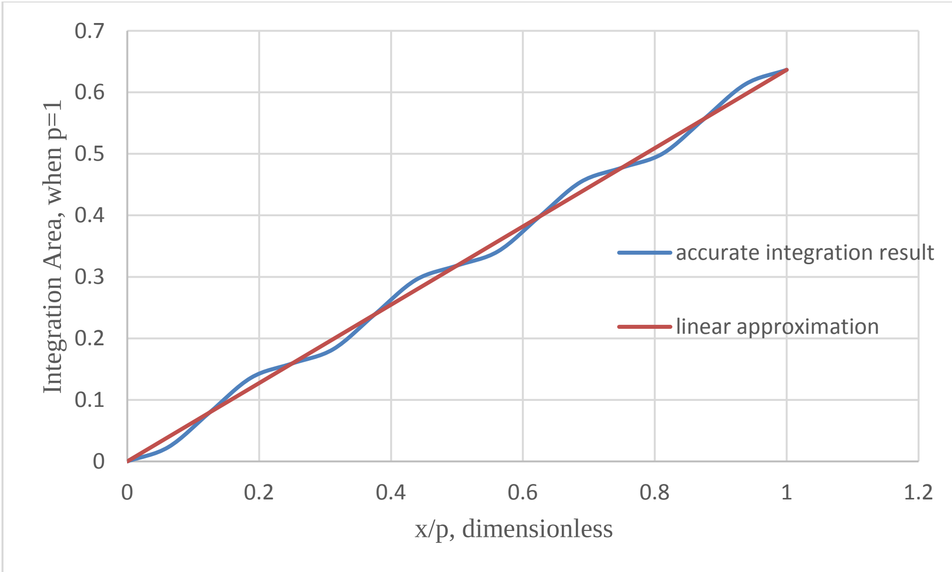

Figure 55 Approximation result and accurate integration result comparison

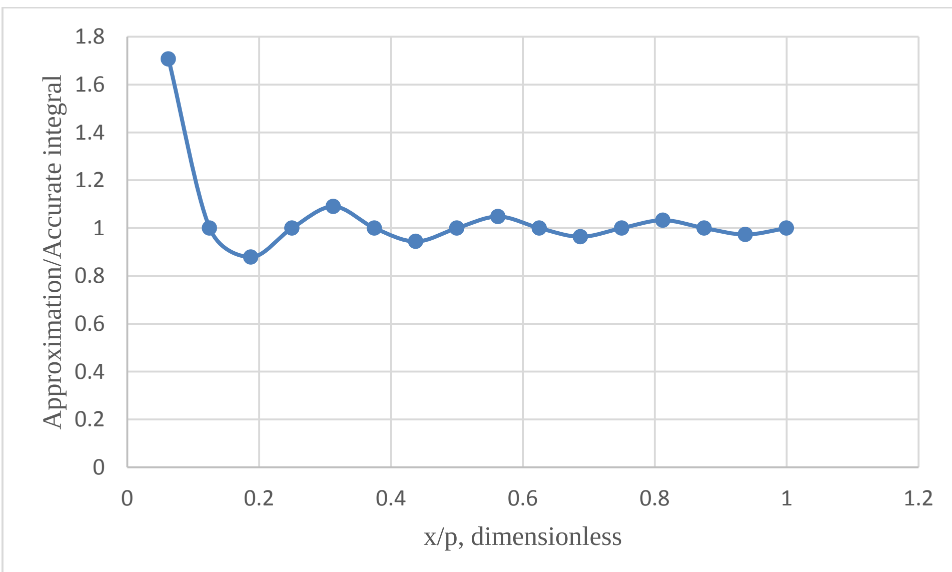

Figure 56 Ratio of approximation result and accurate integration result comparison

APPENDIX D

Geometrical Information:

Table 11 Tubular Dimension Data in Lubinski' Example Verification

r_w	4.250 in.
r_{ce}	3.500 in.
r_{ci}	3.047 in.
E	2.9×10^7 psi
I	50.16 in.^4
r_{cc}	0.75 in.
w_c	2.371 lbf/in.

Table 12 Drill Collar Dimension Data in Lubinski' Example Verification

Mud Weight	12ppg.
r_{ce}	3.125 in.
r_{ci}	1.125 in.
E	2.9×10^7 psi
I	50.16 in.^4
w	7.556 lbf/in.

Table 13 Casing Data in Lubinski' Example

r_{ce}	3.500 in.
r_{ci}	3.047 in.
E	3×10^7 psi
I_2	50.16 in.^4
r_{cc}	0.75 in.
w_c	2.371 lbf/in.

Table 14 Tubing Data in Lubinski' Example

r_{te}	1.438 in.
r_{ti}	1.221 in.
E	3×10^7 psi
I_1	1.61 in.^4
r_{tc}	1.61 in.
w_t	0.542 lbf/in.

Table 15 Tubing Data in Case 7 and Case 8

r_{te}	2.25 in.
r_{ti}	1.979 in.
E	3×10^7 psi
I_1	8.08 in.^4
r_{tc}	0.797 in.
w_t	1.0625 lbf/in.